Investigation of the symbiosis between filarial nematodes and their *Wolbachia* bacteria: analysing genes that are differentially expressed after loss of *Wolbachia*

Dissertation

zur
Erlangung des Doktorgrades (Dr. rer. nat.)
der
Mathematisch-Naturwissenschaftlichen Fakultät
der
Rheinischen Friedrich-Wilhelms-Universität Bonn

vorgelegt von

Uta Strübing

aus
Dresden

Bonn 2012

Angefertigt mit Genehmigung der Mathematisch-Naturwissenschaftlichen Fakultät
der Rheinischen Friedrich-Wilhelms-Universität Bonn.

1. Gutachter: Prof. Dr. Achim Hörauf
2. Gutachter: Prof. Dr. Hans-Georg Sahl

Tag der Promotion: 05.10.2012

Erscheinungsjahr: 2012

Contents

Abbreviations

5-ALA	5-aminolevulinic acid
ALAD	aminolevulinic acid dehydratase
APOC	African Programme for Onchocerciasis Control
Av	*Acanthocheilonema viteae*
Bm	*Brugia malayi*
bp	base pair
cDNA	complementary desoxyribonucleic acid
CI	cytoplasmatic incompatibility
DEC	diethylcarbamazine
DNA	deoxyribonucleic acid
DNase	deoxyribonuclease
dNTP	desoxy nucleotide triphosphate
EtOH	ethanol
FAD	flavin adenin dinucleotide
FC	ferrochelatase
FCS	fetal calf serum
gDNA	genomic deoxyribonucleic acid
GPELF	Global Programme to Eliminate Lymphatic Filariasis
GST	glutatione S-transferase
h	hour
IL	interleukin
i.p.	intraperitoneally
IVM	ivermectin
kb	kilo base
ko	knockout
L	larval stage
Ls	*Litomosoides sigmodontis*
LF	lymphatic filariasis
LPS	lipopolysaccharide
M	molar

µ	micro
Mb	mega base
MDA	mass drug administration
Mf	microfilariae (= the first stage larvae L1)
min	minutes
ml	milliliter
mRNA	messenger ribonucleic acid
mtDNA	mitochondrial DNA
NAD	nicotinamide adenine dinucleotide
OCP	Onchocerciasis Control Programme
OD	optical density
OEPA	Onchocerciasis Elimination Program for the Americas
PAL	peptidoglycan-associated lipoprotein
PCR	polymerase chain reaction
PBS	phosphate buffered saline
p.i.	post infection
qPCR	quantitative polymerase chain reaction
RNA	ribonucleic acid
RNase	ribonuclease
rpm	rotations per minute
RT	room temperature
s	seconds
SA	succinylacetone
SAM	Significance Analysis of Microarrays
Tet	tetracycline
TLR	Toll-like receptor
VEGF	vascular endothelial growth factor
WHO	World health organization
WSP	*Wolbachia* surface protein
*w*Bm	*Wolbachia* of *Brugia malayi*
*w*Mel	*Wolbachia* of *Drosophila melanogaster*
w/v	weight per volume

1. Introduction

1.1. Filarial nematodes

Filarial nematodes belong to the phylum Nematoda (round worms), which comprises the largest number of parasites that cause disease and damage to humans, animals and plants. Within the nematodes the family of the Onchocercidae comprises the filarial parasites. These thread-like worms infest various tissues of their primary hosts (but never the intestine), have a distinct gender dimorphism and give birth to larvae which occupy different parts of the body than the adults (Hiepe et al., 2006). Three out of the eight filarial parasites which infect humans are responsible for most of the disease caused by their infection: *Wuchereria bancrofti* and *Brugia malayi* are the major agents that cause lymphatic filariasis and *Onchocerca volvulus* causes onchocerciasis. They are not only responsible for enormous health problems and disability, but also, as a consequence, bear a great socio-economic burden (Addiss and Brady, 2007; Basanez et al., 2006). The successful activity of several anti-filarial control programmes diminished the number of affected people, nevertheless, many million people still suffer from these diseases, which are far from being eliminated (Hoerauf, 2010; WHO, 2010b).

1.1.1. Biology and epidemiology

1.1.1.1. *Wuchereria bancrofti* and *Brugia* spp.

Lymphatic filariasis, caused by *W. bancrofti*, *B. malayi* and *B. timori*, is the second largest cause for long term disability in the world. More than 1.3 billion people live at risk of infection and 120 million in 83 countries are affected. 90 % of these cases are due to infection by *W. bancrofti*, which is widely distributed in sub-Saharan Africa, India, Southeast Asia, some parts of South America, the Caribbean and the South Pacific. *B. malayi* is found in Southeast Asia and *B. timori* is restricted to minor foci in South Eastern Indonesia. 40 million people suffer from the disease and are not only disfigured but also excluded from social life and normal working which increases the risk of living in poverty. The adult female and male worms live in the

lymphatic vessels, mostly of the extremities and male genitals, where they cause inflammation leading to lymphoedema and hydrocele, respectively. They can be reproductively active for 5-8 years, in this time they produce millions of microfilariae (L1 larvae) which circulate in the blood. Different mosquito species, depending on the geographical location, act as intermediate host and ensure transmission of the disease between humans. They take up microfilariae by blood feeding and enable the development of the L1 larvae to the third stage larvae. The peak concentrations of the microfilariae in the peripheral blood match to the feeding activities of the insect vector, ensuring effective transmission of larvae. Infective L3 larvae are transmitted by another blood feeding from the mosquito to humans, where they develop after two other moults into adult worms. *Culex* is distributed in urban and semi-urban areas, whereas *Anopheles* transmits the disease mainly in rural areas and *Aedes* mainly in the Pacific (Addiss and Brady, 2007; Pfarr et al., 2009; Taylor et al., 2010; WHO, 2010b) (Figure 1.1).

1.1.1.2. *Onchocerca volvulus*

Nearly 37 million people in 34 countries are affected by onchocerciasis caused by infection with *O. volvulus* (Taylor et al., 2010). The disease is most abundant in Africa where > 100 million people in 19 endemic countries are living at high risk of infection (WHO, 2010a). Smaller foci with prevalence of *O. volvulus* are also in Southern and Central America. The transmission of the infective agent to humans occurs by black flies of the family *Simulium*. The most important vector is *S. damnosum*, widely distributed in Africa and Yemen, which breeds in fast-flowing oxygenated rivers and streams (Boatin and Richards, 2006). Onchocerciasis is commonly named river blindness, as people living or working nearby the breeding habitats are at highest risk of getting bitten by black flies and suffering from the disease. Furthermore, people often are forced to leave the river valleys in order to avoid infections and high blindness rates make these fertile countries economically non-viable. (Hoerauf, 2011). During a blood meal the black fly takes up microfilariae from the skin and after two moults within the insect the L3 larvae develops. This infective larvae is transmitted during another blood meal from the intermediate to the human host. Within one year, after another two moults, the mature adult worms develop. The females reside in subcutaneous nodules (Onchocercomata) which are located near the biting sites of the black flies, whereas the male worms can move freely from one nodule to an other. The adults are long-lived and can reach an age of 12-15 years, in this time producing millions of microfilariae which migrate through the skin and the eye. Microfilariae can live up to 2 years and their death

causes inflammation leading to dermatitis and eye lesions (Boatin and Richards, 2006; Udall, 2007; Taylor et al., 2010).

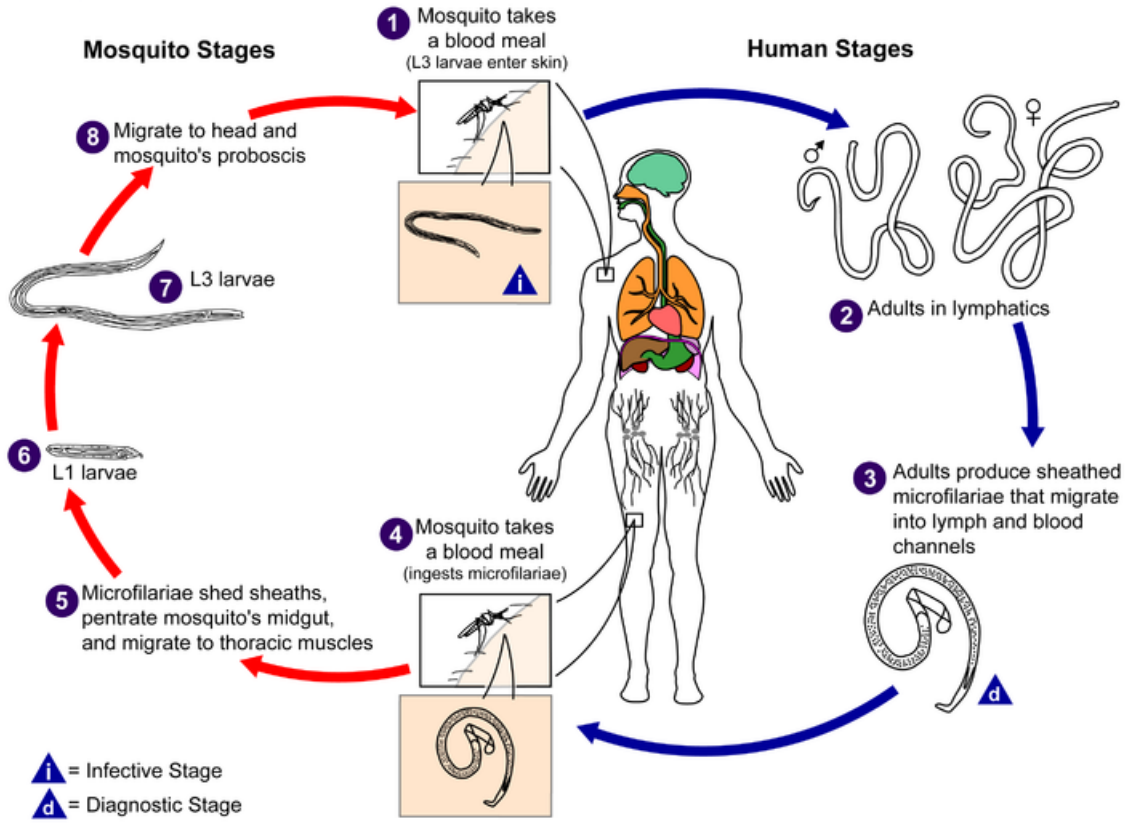

Figure 1.1.: Life cycle of *Wuchereria bancrofti*. The infective 3rd stage larvae enters the human host during a blood meal of the insect vector in different species of *Culex*, *Anopheles*, *Aedes* and *Mansonia* (1). After two moults the infective larvae develop into female and male adults, which reside in the lymphatics, commonly of the limbs and males genitals (2). There they produce thousands of microfilariae, which migrate through the blood and lymphatic vessels with nocturnal periodicity which coincides with the biting activity of the mosquitoes (3). During another blood meal microfilariae are taken up (4) and migrate from the mosquito midgut to the thoracic muscles (5). There they again moult twice from the L1 (6) to the infective L3 larvae (7). After migrating to the proboscis (8) the infective larvae can be transmitted to a human host, thereby closing the cycle (1). Source: Centers of Disease Control and Prevention, `http://www.dpd.cdc.gov/dpdx`

1.1.2. Pathogenesis and disease

1.1.2.1. Lymphatic Filariasis

One third of the infected people develop clinical disease of lymphatic filariasis. The remaining have asymptomatic infections, characterized by high worm loads and microfilaraemia. The worms actively down-regulate the host immune responses and

thereby ensure their survival (Hoerauf et al., 2005). On the other hand, patients that develop lymphoedema or hydrocele have only few or no parasites but vigorous specific immune reactions. Frequency of infections and genetic predisposition seem to play a role in the outcome of the disease (Debrah et al., 2006). In the non-permissive form, inflammatory responses to dying worms in the lymphatic vessels lead to lymphadenitis and filarial fever and temporal immobilisation can occur. Antigenic stimulation promotes the up-regulation of vascular endothelial growth factors (VEGFs), which mediate lymphangiogenesis and dilation of lymphatic vessels. Antigens of the endosymbiotic *Wolbachia* (Chapter 1.2.4) greatly contribute to the pro-inflammatory stimulation. Then the damaged and enlarged lymph vessels are no longer capable of efficiently transporting lymph fluids, making them susceptible for secondary infections. This further promotes lymphangiogenesis, resulting in fluid extravasation and lymphoedema. The severest outcome, elephantiasis, is characterized by a painful massive swelling of the legs with thickened and fissured skin (Figure 1.2 A). Lymphoedema can also occur in breast and arms. A second clinical manifestation of LF in men is hydrocele, the accumulation of lymph fluid in the scrotum (Pfarr et al., 2009; Taylor et al., 2010).

1.1.2.2. Onchocerciasis

Onchocerciasis mainly presents as dermatitis and keratitis due to host inflammatory reactions provoked by the death of microfilariae. The manifestation of the disease starts a year after infection, the time when adult female worms start producing microfilariae (Boatin and Richards, 2006). Severity of symptoms differs greatly between individuals, depending on infection intensity and predisposition of the host with associated immune responsiveness. Patients with generalized onchocerciasis have many parasites and a high microfilarial load, but they develop only weak dermatitis due to down-regulated host pro-inflammatory responses. Death of skin microfilariae causes skin irritations with intense itching (Figure 1.2 B). The dermal lesions range from papular dermatitis and degeneration of skin (atrophy) to severer outcomes with depigmentation and edema of the limb (Sowda). The latter is a form of hyperreactive onchocerciasis dominated by strong pro-inflammatory immune responses. Microfilariae also migrate through the eye conjuntiva, where, upon chronic exposure, stimulation of immune responses leads to sclerosing keratitis causing visual impairment that may eventually result in blindness (Figure 1.2 C). As in lymphatic filariasis *Wolbachia* bacteria play a role in this clinical outcome (Chapter 1.2.4) (Taylor et al., 2010; Hoerauf, 2011).

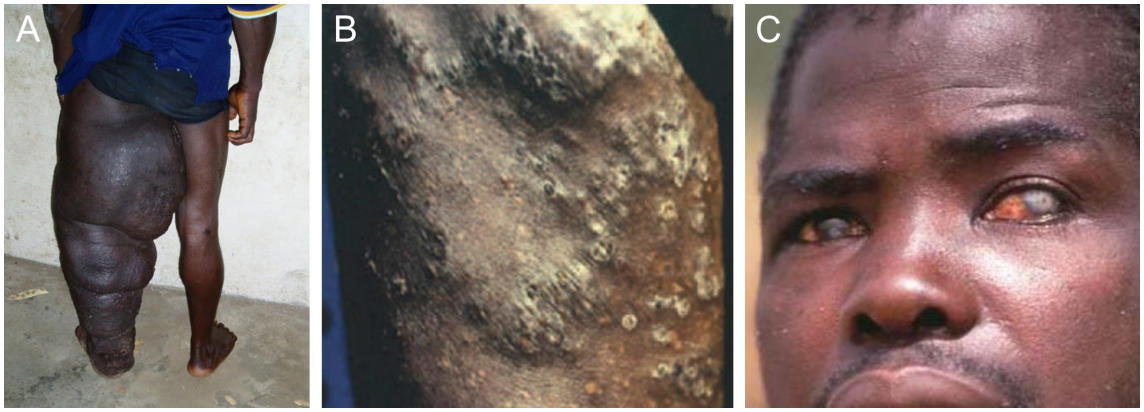

Figure 1.2.: Examples of pathological outcomes of lymphatic filariasis and onchocerciasis. (A) Patient with elephantiasis, the severest form of lymphoedema. Image taken from Debrah et al. (2006). (B) Lichenified onchodermatitis. Image taken from Hoerauf (2011). (C) Patient with ocular lesions due to *O. volvulus* infection. Image courtesy of WHO/TDR/Mark Edwards.

1.1.3. Anti-filarial treatment

The basis for the WHO control programmes to eliminate filariasis is mass drug administration (MDA) using the three drugs ivermectin (IVM), albendazole and diethylcarbamizine (DEC). The Global Programme to Eliminate Lymphatic Filariasis (GPELF) has the goal to eliminate LF by 2020 by breaking transmission. Fiftyone of the 81 endemic countries have launched the programme and annually distribute either 200-400 µg/kg IVM + 400 mg albendazole or, in countries without co-endemicity with *O. volvulus*, 600 µg/kg DEC + 400 mg albendazole. Since 2000 1.9 million treatments have been provided by the GPELF, thereby preventing 32 million disability-adjusted life years. China and Korea became the first countries declared to have eliminated LF in 2008 due to MDA programmes and in many countries the microfilariae rates have been reduced to less than 1 % (Taylor et al., 2010; WHO, 2008).

Several control programmes improved onchocerciasis in the Americas and Africa. The Onchocerciasis Elimination Program for the Americas (OEPA) uses twice yearly mass treatment with IVM and thereby covers 85 % of the affected communities. Early strategies to combat onchocerciasis in Africa, carried out by the Onchocerciasis Control Programme (OCP), relied on extensive vector control using aerial larviciding (Boatin and Richards, 2006; Hoerauf, 2010). The OCP success is continued by the African Programme for Onchocerciasis Control (APOC) that relies on community-directed treatment of 150 µg/kg IVM given annually to break transmission of the disease in African endemic countries by 2015. This programme intends to cover $>$ 90 million people with treatment (WHO, 2010a). DEC is contraindicated for

onchocerciasis due to side effects induced by killing of microfilariae in the eye. IVM, on the other hand, does not cause ocular damage. The drug blocks postsynaptic glutamate-gated chloride channels and thereby paralyses the worm, the immobilized microfilariae are transported to other parts of the body and are not killed within the eye. Slight skin irritations and fever occur only at high microfilarial loads or higher doses of IVM (Hoerauf, 2011). Although IVM as well as DEC and albendazole kill microfilariae and late embryonic stages, they only have a little macrofilaricidal effect. Because the adult female worms are only temporally sterilized, microfilariae reappear in the skin after ca. 6 month. Repeated treatments for the worm's life span are therefore necessary to break transmission (Udall, 2007). Other drugs considered for anti-filarial treatment include moxidectin and suramin. Moxidectin has shown to be very efficient in reducing microfilariae numbers, but also does not have macrofilaricidal properties. Suramin is a macrofilaricidal drug, but the delivery mode (injections for several weeks) is inconvenient and it has immense side effects, making it unsuitable for MDA and also very unpopular for individual treatment (Hoerauf, 2008; Udall, 2007).

The control programmes of the recent years had a great success in preventing many cases of disease and greatly reduced transmission in several countries (Ottesen et al., 2008; WHO, 2010a). Sustaining and further promoting these achievements is important. Thus, reports of IVM resistance are a great concern, as IVM is the sole drug available for MDA against onchocerciasis. An introduction of a new drug, which is suitable for MDA, is therefore urgently needed prior to resistant strains spreading (Bourguinat et al., 2007; Osei-Atweneboana et al., 2007; Bourguinat et al., 2008). An ideal drug against onchocerciasis would be macrofilaricidal or have a long term sterilizing effect. For treatment of LF, a macrofilaricidal effect should not lead to rapid death of the adult worms, which would cause adverse reactions. Ideally, symptoms of lymphoedema and hydrocele would be reversed. A new promising anti-filarial strategy that uses doxycycline to target the endosymbiont *Wolbachia* has proven to show many of these features of an ideal drug (Hoerauf, 2008). The principle is introduced in detail in Chapter 1.2.5.

1.2. *Wolbachia*

Wolbachia bacteria were first discovered by Hertig and Wolbach (1924), who described them as *Rickettsia*-like bacteria in *Culex pipiens*. The establishment of the genus *Wolbachia* followed a few years later (Hertig, 1936). In the 1970s unusual bodies within microfilariae and developmental stages of filarial nematodes have been

identified as bacteria by electron microscopy (Kozek, 1977; Kozek and Marroquin, 1977; McLaren et al., 1975). Unaware of the importance of these bacteria for the filarial biology they were forgotten for the next 20 years until the rediscovery of bacterial sequences in filaria in the 1990s in the course of filarial genome sequencing projects. The sequences were first considered as contaminants but quickly shown to derive from *Wolbachia* bacteria. Sironi et al. (1995) first described *Wolbachia* as the endosymbiont of the filaria nematode *Dirofilaria immitis*.

1.2.1. Distribution and Phylogeny

Wolbachia are gram-negative α-Proteobacteria of the order Rickettsiales. Close relatives are *Anaplasma*, *Ehrlichia* and *Rickettsia* (O'Neill et al., 1992). They are found in an estimated number of 66 % of insect species (Hilgenboecker et al., 2008) and in other arthropods like spiders, butterflies, scorpions and termites (Baldo et al., 2007; Bordenstein and Rosengaus, 2005; Hiroki et al., 2004; Rowley et al., 2004) where they are commonly known as reproductive parasites. *Wolbachia* are an extremely abundant bacterial group, considering the great diversity of insect species and more than 1 million of them harbouring *Wolbachia* (Werren and Windsor, 2000). Furthermore, *Wolbachia* are found in 90 % of filarial nematodes, where they are mutualistic symbionts (in contrast to their lifestyle in arthropods). Filarial species containing *Wolbachia* include the medical important species *B. malayi*, *B. timori*, *Wuchereria bancrofti*, *Onchocerca volvulus*, *Mansonella* sp. and *Dirofilaria immitis*. Notable exceptions are *Loa Loa*, *Acanthocheilonema viteae*, *O. flexuosa* and *Setaria spp.* (Bandi et al., 1998; Taylor and Hoerauf, 1999; Büttner et al., 2003; Keiser et al., 2008).

Phylogenetic analysis based on *Wolbachia* 16S rRNA, *ftsZ*, *groEL*, *gltA*, *dnaA*, *ftsZ* and *Wolbachia* surface protein (*wsp*) sequences, divides *Wolbachia* into eight supergroups A-H, with supergroup G tentative. Supergroups C and D are comprised of *Wolbachia* that are found in filarial nematodes. The other supergroups comprise *Wolbachia* from arthropods with supergroup A and B the most abundant ones. Supergroup F includes *Wolbachia* from arthropods and filariae (Casiraghi et al., 2005; Lo et al., 2007; Werren et al., 2008) (Figure 1.3). Interestingly, the phylogeny of the filarial nematodes is in concordance with the phylogeny of the *Wolbachia* they harbour, suggesting a co-evolution of the filarial host with its endosymbiont. In contrast, phylogeny of the arthropod host is not in concordance with their *Wolbachia*, indicating horizontal transmission of *Wolbachia* between arthropod species. Due to the close association filarial larvae have with the intracellular environment of their insect vectors, a transmission of *Wolbachia* from insects to nematodes, or

vice versa, after the separation of nematodes and arthropods has been suggested. Nevertheless, data are missing to resolve the ancestry of parasitic and mutualistic *Wolbachia* (Bandi et al., 1998; Bordenstein et al., 2009).

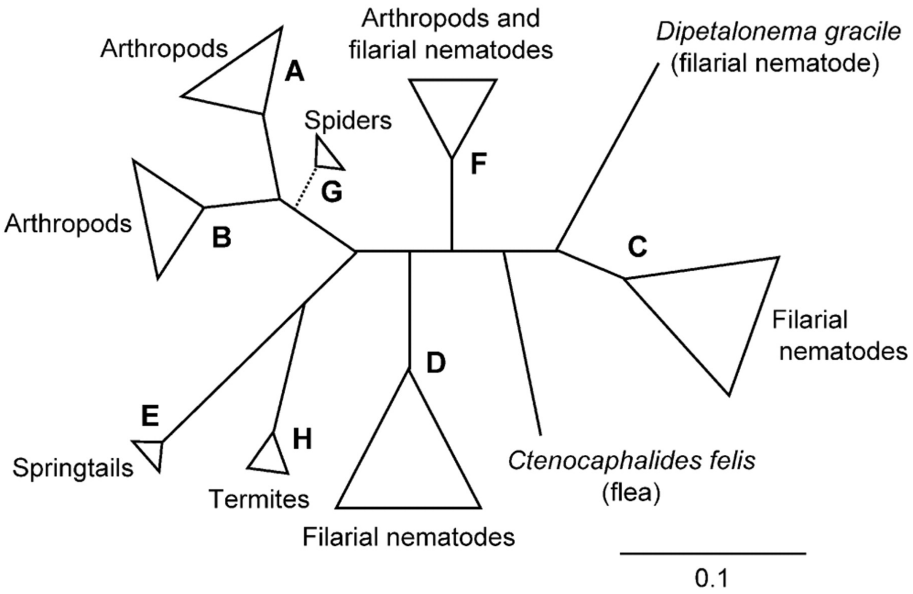

Figure 1.3.: The phylogenetic tree of *Wolbachia*. Various phylogenetic studies divided *Wolbachia* into 8 clades, named supergroups A-H. Figure taken from Lo et al. (2007).

1.2.2. Morphology and Localisation

Wolbachia are rod shaped bacteria with a length of around 1 µm. They are obligate intracellularly and live in various tissues of different arthropod species, but notably are found in their female reproductive organs. In filarial nematodes *Wolbachia* are located in the ovaries, oocytes, embryos and microfilariae, but they are absent from the male reproductive organs. Additionally, they are found in varying amounts in the lateral hypodermal chords of both female and male worms. On electron microscopic photos 3 membranes can be distinguished by which *Wolbachia* are surrounded: the two inner layers are thought to be the inner and outer bacterial membrane, whereas the third outermost layer represents an vacuole with membrane derived from the host (Taylor and Hoerauf, 1999) (Figure 1.4). It is yet not clear which organelle contributes to forming this vacuole. One study describes a *Wolbachia* strain in association with the endoplasmatic reticulum (Serbus et al., 2008; Voronin et al., 2004).

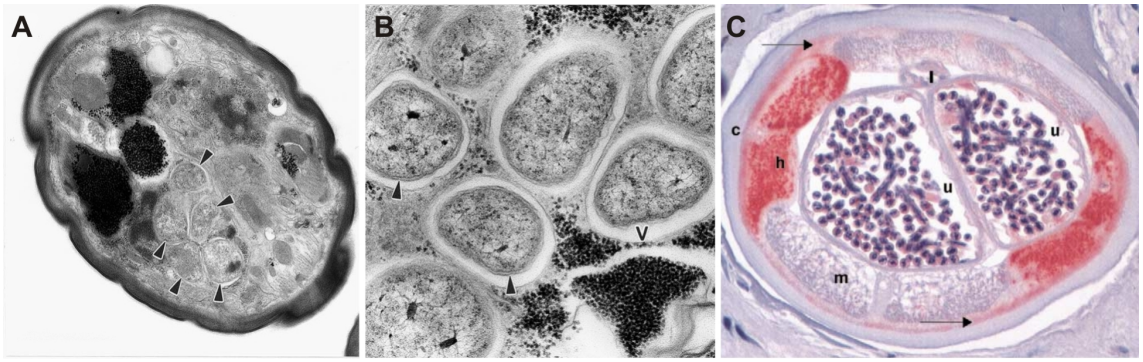

Figure 1.4.: Cross-sections of filarial nematodes showing endosymbiotic *Wolbachia* bacteria. Electron micrograph of *Wuchereria bancrofti*, with a cluster of 5 bacteria (arrows) (A). *Wolbachia* with the characteristic double membrane (arrow) within a vacuole (v) in the lateral chord of an adult female *Brugia malayi* (B). Cross-section of a female adult *Onchocerca volvulus* filaria with a staining against bacterial hsp60 (red). *Wolbachia* are seen in the hypodermis (h) but not in the cuticle (c), the musculature (m), the intestine (i), and the uterus epithelium (u). Arrows indicate unspecific hsp-60 staining, possibly against nematode hsp60 (C). Figures A and B are taken from Taylor and Hoerauf (1999) and Figure C from Hoerauf et al. (2000).

1.2.3. Role of *Wolbachia* in arthropods

Reproductive alterations In arthropods *Wolbachia* mostly behave as parasitic endosymbionts, causing a range of reproductive phenotypes which all enhance the production or survival of female offspring. As *Wolbachia* are transmitted vertically via the maternal germline these alterations increase the number of infected females with a reproductive advantage and promote spreading of *Wolbachia* into insect populations (Serbus et al., 2008).

The most common effect *Wolbachia* induces in insects is cytoplasmatic incompatibility (CI). Here, *Wolbachia*-infected females can mate with infected (with the same *Wolbachia* supergroup) and uninfected males, but crosses between uninfected females with infected males are incompatible and do not produce any offspring. The cytological mechanisms underlying this phenotype are defects in the embryonic mitosis: male and female pronuclei have an asynchronous development, which is due to a delayed nuclear envelope breakdown and chromosome condensation of the male pronuclei. This again can be explained by a delayed activity of Cdk1 kinase and associated failure of histone deposition to the male pronucleus (Landmann et al., 2009).

Other phenotypes that are induced by *Wolbachia* and promote female offspring, although not as common as CI, are parthenogenesis (females instead of males develop from unfertilized eggs), feminization (genetic males develop as females) and male

killing, which results in increased food supply for the surviving female offspring (Werren et al., 2008).

Transmission strategies The success of *Wolbachia* in arthropods can, besides these reproductive alterations, also be explained by highly efficient transmission strategies. Transmission rates are 97 % in the wild and even 100 % in the laboratory. *Wolbachia* have evolved mechanisms which guarantee their incorporation into the germline stem cells during embryogenesis. This involves specific localisation patterns of *Wolbachia* in the oocyte, which seems to be achieved by dynein and kinesin dependent transport along microtubuli (Ferree et al., 2005; Serbus and Sullivan, 2007). Little is known about how *Wolbachia* is able to interact with the host's cytoskeleton, but the annotated genome of *Wolbachia* from *Drosophila melanogaster* (*w*Mel) allows one to make some assumptions, like a role for the many Ankyrin repeat domain proteins encoded by *w*Mel in these processes (Fenn and Blaxter, 2006; Iturbe-Ormaetxe et al., 2005; Walker et al., 2007).

Fitness benefits for insects Recent research led to the assumption that the highly efficient invasion of *Wolbachia* into insect populations can not only be explained by their reproductive parasitism, as some *Wolbachia* strains do not induce CI, yet they are able to invade the host population. A role of *Wolbachia* for iron metabolism and tolerance of oxidative stress indicates that the endosymbiont can function as a nutrional mutualist in insects. Besides altering reproductive mechanisms, fitness benefits provided by *Wolbachia* to their insect host might be a second basis for establishment of infection (Brennan et al., 2008; Brownlie et al., 2009; Kremer et al., 2009).

***Wolbachia*-mediated pest control** Another beneficial effect of *Wolbachia* for insects is the induction of resistance to infection by several viruses (Hedges et al., 2008; Teixeira et al., 2008; Frentiu et al., 2010). This offers a great potential for new pest control strategies. Additionally, *Wolbachia* has a life shortening effect in *Aedes aeygypti*, the vector of dengue virus. An invasion of this *Wolbachia* strain into *Aedes* mosquitoes could be an efficient approach to control dengue (McMeniman et al., 2009).

Although *Wolbachia* of arthropods have a different lifestyle than the nematode *Wolbachia*, many of the host-endobacteria interactions may be based on a similar machinery, e.g. the strategies of transmission via the maternal germline (Landmann

et al., 2010). Thus, knowledge of the mechanisms of the insect-*Wolbachia* association and the genes and pathways involved might also provide information to better understand the molecular mechanisms of the nematode-*Wolbachia* symbiosis, which is yet not well understood.

1.2.4. Role of *Wolbachia* in filarial nematodes

Role for filarial biology The rediscovery of *Wolbachia* bacteria in filarial nematodes in the 1990s awoke a great interest, as this provided a new approach in filarial research to control filarial infections. *Wolbachia* were until then known as reproductive manipulators in arthropods and one could assume that they somehow might influence the filarial biology as well. Subsequent *in vitro* and *in vivo* studies as well as human trials proved that *Wolbachia* not only influence the development and survival, but are essential for their filarial host (in contrast to the insect-*Wolbachia*). Treatment of filaria with anti-rickettsial antibiotics like doxycycline leads to depletion of the bacteria and results in embryonic blockade, degenerate embryos and larval moulting defects. *Wolbachia* depletion also leads to sterility and finally to the death of adult worms (Hoerauf et al., 2000, 2001b, 2008; Langworthy et al., 2000; Taylor et al., 2005). These observations are a direct consequence of *Wolbachia* depletion, as treatment of the *Wolbachia*-free filarial nematode *A. viteae* with the same antibiotics does not alter worm development or survival (Hoerauf et al., 1999). This indicates that *Wolbachia* provides its host with essential nutrients and functions and that the filaria-*Wolbachia* symbiosis is of obligatory mutualistic nature. *Wolbachia* are transmitted vertically via the maternal germline, as shown by crossing experiments with *B. malayi* and *B. pahangi* (Taylor et al., 1999). Recent microscopic studies by Landmann et al. (2010) brought the understanding of the mechanism forward: similar to the transmission in insects, *Wolbachia* have a posterior concentration in the *Brugia* oocyte and show an asymmetric segregation pattern in embryogenesis which guarantees their incorporation into the female germline.

Role for pathology *Wolbachia* bacteria play an important role for the pathology of filarial infections. *Wolbachia*-associated products, such as *Wolbachia* Surface Protein (WSP) are inducers of pro-inflammatory cytokines (Brattig et al., 2004; Taylor et al., 2000) which can also regulate the expression of VEGF-A and VEGF-C (Asano-Kato et al., 2005; Ristimäki et al., 1998). Up-regulation of VEGFs then can lead to lymph vessel growth and thereby mediates lymphatic pathology (Debrah et al., 2006). A direct connection between *Wolbachia* products and pathological outcome has also been shown in onchocerciasis. In an experimental model of keratitis, filarial

antigen induces the infiltration of neutrophils into the eye and this is not seen with *Wolbachia*-free filarial antigen (Gillette-Ferguson et al., 2004; v Saint Andre et al., 2002). Toll-like receptor 2 (TLR-2) has been shown to mediate *Wolbachia*-antigen recognition (Daehnel et al., 2007; Hise et al., 2007). Specifically, the Diacyl *Wolbachia* lipoprotein (WoLP) induces innate and adaptive inflammatory responses in a TLR2 and 6 dependent manner (Turner et al., 2009). The host immune system is exposed to *Wolbachia* immunogenic materials e.g. during the uptake of degenerate larvae or dead worms by macrophages. In the event of a rapid death of microfilariae, e.g. upon treatment with DEC, the immune system is confronted with high amounts of *Wolbachia* antigens leading to adverse reactions (Pfarr et al., 2009).

1.2.5. *Wolbachia* as a target for filariasis control

The essential function of *Wolbachia* for filarial development and survival as well as their impact on the pathological outcome of filarial infections makes them potential targets for treating filariasis. A new anti-filarial chemotherapy using doxycycline or rifampicin to clear *Wolbachia* from worms has been proven to be successful in several clinical trials (Debrah et al., 2011; Hoerauf et al., 2000, 2001b; Supali et al., 2008; Taylor et al., 2005). A 4-6 week course of 200 mg doxycycline/day depleted *Wolbachia* from *W. bancrofti* and led to clearance of microfilariae from blood, to a long-term sterilization of females and eventually to the death of the adult worms. Equally, onchocerciasis treatment for 4-6 weeks with 100-200 mg doxycycline per day has both micro- and macrofilaricidal effects. With the 6-week course of 200 mg/day, 60 % of female worms were dead at the end of the observation period. The slow killing of the worms prevents the sudden release of great amounts of *Wolbachia* and thereby also the adverse reactions seen, e.g. with DEC. This makes doxycycline the only macrofilaricidal drug without major side effects. Furthermore, doxycycline has been shown to improve disease symptoms in lymphatic filariasis, which is another great advantage over the currently used anti-filarial drugs. Severity of lymphoedema and hydrocele can be reversed, which is thought to be due to the *Wolbachia* clearing and associated decrease in pro-inflammatory stimuli. Indeed, the decrease of plasma VEGF levels after *Wolbachia* depletion precedes the amelioration of the disease (Debrah et al., 2006; Mand et al., 2009).

Doxycycline is suitable for individual therapy and is being considered for "endgame" control efforts in foci where transmission has stopped, but where a few individuals are still infected. However, it is not suitable for MDA due to the long period of administration and the contraindications for children under 9 years, and breastfeeding and pregnant women (Hoerauf, 2008; Taylor et al., 2010).

Targeting *Wolbachia* fulfils many of the requirements for a new anti-filarial drug and as there is a greater genetic divergence of the bacteria from the human host than that of the nematodes, chances are increased to specifically target the endosymbiont without interfering with human functions. Therefore, a great effort is made by the Anti-*Wolbachia* Consortium (A-WOL) (`http://A-WOL.com`) to identify potential endosymbiont genes for a new anti-*Wolbachia* chemotherapy which is compatible with the MDA programmes (Slatko et al., 2010).

1.3. Insights from the decoding and annotation of the filarial and *Wolbachia* genome

The sequencing of the genome of *B. malayi*, initiated by the Filarial Genome Project, was undertaken to further research on the parasitic life style and the interactions with the host. *B. malayi* was chosen as representative for a human filarial parasite because a sufficient supply of material is available and the nematode can be maintained in a rodent as well as *ex vivo*. The sequencing of its endosymbiont *Wolbachia* facilitated research on the molecular dependencies of the symbiosis by revealing metabolic gaps in both genomes (Foster et al., 2005; Ghedin et al., 2004).

1.3.1. The genome of *B. malayi*

The genome of *B. malayi* is 95 Mb and is encoded on 5 chromosomes, including an XY sex determination pair. Additionally, the nematode contains a 14 kb mitochondrial genome and the 1 Mb endosymbiont genome. The *Brugia* genome has been sequenced at 9-fold coverage with 90 % of the genome being assembled. Closing the gaps between scaffolds is complicated by the many repetitive elements, which make up 14 % of the genome. *B. malayi* is estimated to have 14.500 -17.800 protein coding genes which is a lower number than reported for the free-living non-parasitic nematode *C. elegans*. The comparative analysis with the genome of *C. elegans* is informative for finding genes relevant for the parasitic life style (adaption to the mosquito and mammalian environment) and for symbiotic mechanisms with the endosymbiont *Wolbachia*. Whereas genes and genome structures that are shared by both organisms indicate common core elements for nematodes, dissimilarities might guide to specific adaptations which have evolved under the pressure of parasitism and the presence of *Wolbachia*. The two nematode genomes are more distinct than previously thought. Although linkage of genes has been conserved, the gene order within linked genes differs between *B. malayi* and *C. elegans*. Furthermore, *C. el-*

egans seems to have lost many genes which have been retained in *Brugia*; these genes might encode proteins needed for the parasitic life style. Approximately 50 % of the *Brugia* genes have orthologs in *C. elegans*, and 20 % of the predicted genes are specific to *B. malayi* because they have no identities in any database (Ghedin et al., 2007).

While the sequencing of the genome gives information about filaria specific genes and pathways, which are likely targets for intervention (for example genes involved in moulting and cuticle formation, neuronal signalling and reproductive biology), it also reveals metabolic gaps in the genome which might be the basis for the mutualistic symbiosis with *Wolbachia*: 9 of 10 genes needed for de novo purine synthesis are missing, only one gene needed to synthesise heme and no genes for riboflavin synthesis are found in the genome (Ghedin et al., 2007; Scott and Ghedin, 2009).

1.3.2. The genome of *Wolbachia* of *B. malayi*

The genome of *Wolbachia* from *B. malayi* (*w*Bm) was the first sequenced *Wolbachia* genome of a parasitic nematode (Foster et al., 2005) (Figure 1.5) and had been published shortly after the genome of *Wolbachia* from *Drosophila melanogaster* (*w*Mel) (Wu et al., 2004). Beside these, the genomes of *w*Pip, the endosymbiont of *Culex pipientis* (Klasson et al., 2008) as well as parts of the *Wolbachia* genomes from several *Drosophila* hosts and filarial nematodes have been sequenced (Salzberg et al., 2005; Scott et al., 2011). Thus, comparative analysis of the genomes of the different *Wolbachia* strains is possible and can help to unravel the genomic basis of mutualistic and parasitic symbiosis (Fenn and Blaxter, 2006).

The circular genome of *w*Bm has a size of 1.1 Mb (Foster et al., 2005) and thus is smaller than the genomes of free-living α-Proteobacteria (> 3 Mb). Reduced genomes and gene losses are a common characteristic of obligate intracellular bacteria and reflect the adaption to the host (Moran, 2003; Sun et al., 2001). 806 protein coding genes were identified and one copy for each ribosomal RNA. The amount of repetitive DNA in the *w*Bm genome is much lower (5.4 %) than in the *w*Mel genome (14 %). Furthermore, in contrast to the *w*Mel genome, *w*Bm does not contain prophages (Foster et al., 2005; Wu et al., 2004). The large amount of repetitive DNA and prophages in the insect *Wolbachia* genomes are suggested to reflect a genome plasticity and the ability to adapt to the cellular environment of novel host species, which is not necessary in the strictly vertically transmitted *Wolbachia* from nematodes. Frequent genome rearrangements in arthropod *Wolbachia* would also explain the missing colinearity between the *w*Mel and *w*Bm genomes (Brownlie and O'Neill, 2005; Foster et al., 2005).

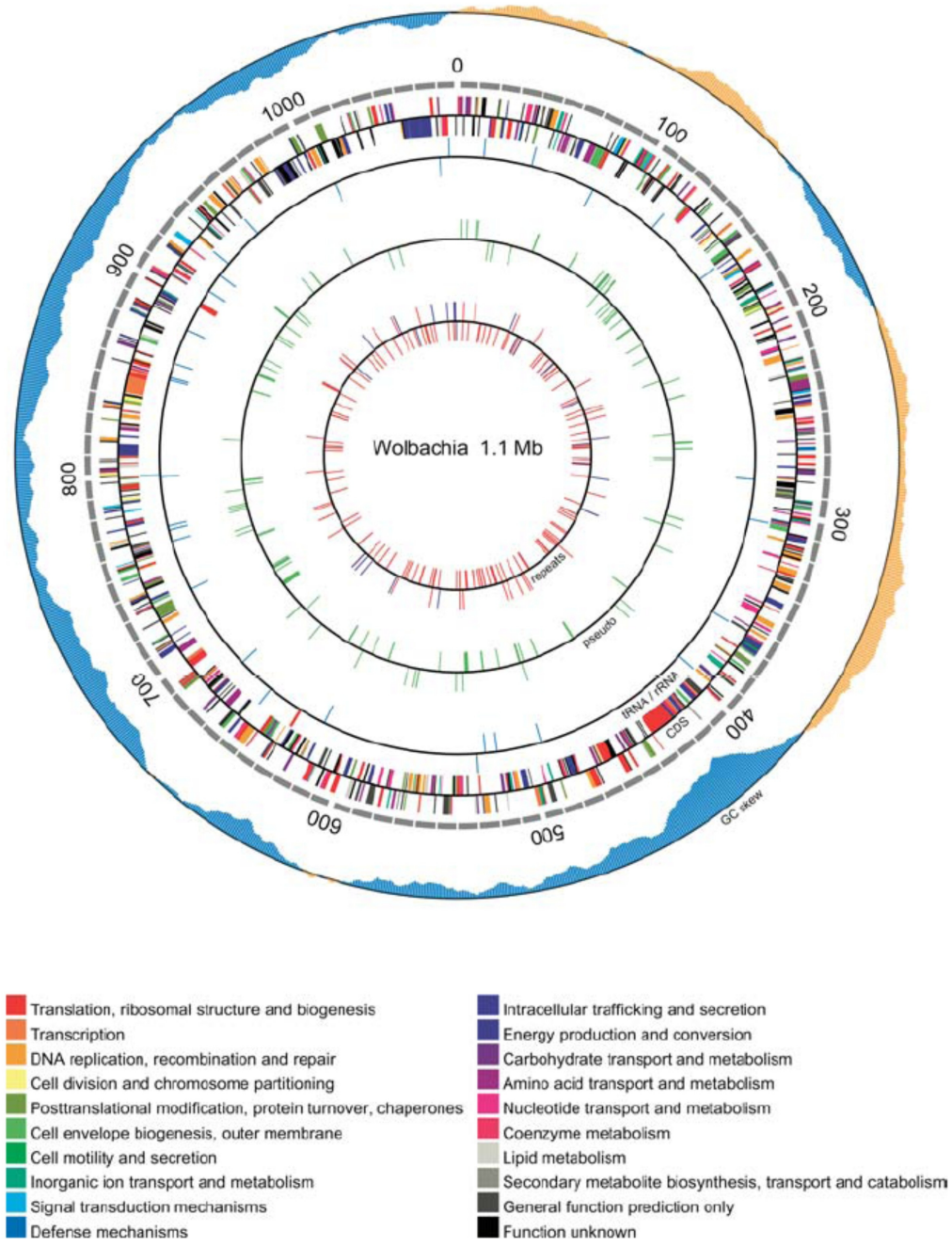

Figure 1.5.: The genome of *Wolbachia* from *B. malayi*. Figure taken from Foster et al. (2005).

The *Wolbachia* genome encodes proteins for translational processes, the biogenesis of cytochrome c oxidase and c-type chromosomes, most genes for DNA replication and repair, as well as genes for protection from oxidative damage. The enzymatic machinery to counter deleterious effects may reflect the adaptation of the bacteria to the intracellular environment of the host. The retention of enzymes for translational processes together with the DNA repair systems could also reflect mechanisms

to reduce deleterious mutations due to repeated bottlenecking during transmission of *Wolbachia*. Most of the signal transduction machinery has been lost from the genome, except some genes for stress response and cell-cycle regulation. Furthermore, transcriptional regulators are not retained in the genome, indicating that *Wolbachia* genes are constitutively expressed (Brownlie et al., 2007; Foster et al., 2005; Slatko et al., 2010). *Wolbachia* has lost several genes for peptidoglycan synthesis, likely because a cell wall is not needed for osmotic stabilization in the host vesicle. Nevertheless, the precursor lipid II can be synthesised and is functional. The role of lipid II in a cell wall-less bacteria is not yet clear but might play a vital role for cell division (Foster et al., 2005; Henrichfreise et al., 2009). As evidenced by the genome information, LPS cannot be synthesised by *w*Bm, despite immunological data indicate an LPS-like molecule to be important in the immune responses in filarial infections. Besides the stimulation of the immune system by WSP (Brattig et al., 2004), a lipoprotein associated with the unusual peptidoglycan structure of *w*Bm (PAL) contributes to the inflammatory responses against *Wolbachia* (Turner et al., 2009).

1.3.2.1. Metabolic capacities that indicate *Wolbachia*-host dependencies

Wolbachia has reduced metabolic pathways, which likely makes them dependent upon their host. *w*Bm is incapable of synthesising many cofactors and vitamins. Pathways for de novo synthesis of Coenzyme A, NAD, biotin, lipoic acid, ubiquinone, folate and pyridoxal phosphate are missing. Strikingly, *w*Bm has lost genes for the synthesis of all amino acids, except *meso*-diaminopimelate.

Metabolic pathways that have been retained in the *w*Bm genome are especially interesting, since they may indicate mechanisms which make filarial nematodes dependent upon their endosymbionts. Since *Wolbachia* is capable of de novo synthesis of purines and pyrimidines, the bacteria might supply the filarial host with additional nucleotides in periods of high DNA requirements (e.g embryogenesis). This is highly likely, since the *B. malayi* genome indicates that the worms have incomplete purine and pyrimidine biosynthetic pathways encoded in the nematode genome (Ghedin et al., 2007). Furthermore, the pathways for biosynthesis of isoprenoids, fatty acids and phospholipids are retained in the *w*Bm genome. The presence of the complete pathway for riboflavin biosynthesis is interesting, as *B. malayi* lacks the enzymes for its synthesis, therefore *Wolbachia* could be an important source for this essential cofactor. The *Wolbachia* genome encodes enzymes for the biosynthesis of glutathione, which either might be used for oxidative stress reduction in the *Wolbachia* vesicle or is provided to the host. Glycolytic enzymes are found in *w*Bm with

only two enzymes missing for glycolysis. Nevertheless, the reverse reaction, gluconeogenenis, using the enzymes fructose-1,6-biphosphatase and pyruvate phosphate dikinase (PPDK) may occur in *Wolbachia*. Intermediates for the citric acid cycle, which is present in *Wolbachia*, might serve as growth substrates, because they might be easily obtained by the proteolysis of host proteins. Pyruvate, which is abundant in the worm, is also a likely substrate for *Wolbachia* as it can be metabolised via the gluconeogenetic pathway. The final product, fructose-6-phosphate, can enter the pentose phosphate pathway, thereby producing the substrates for the biosynthesis of nucleotides, riboflavin and FAD (Brownlie et al., 2007; Fenn and Blaxter, 2006; Foster et al., 2005; Slatko et al., 2010).

Heme biosynthesis One pathway of special interest encoded by *Wolbachia* bacteria is the heme biosynthesis pathway. Heme is an essential cofactor needed in catalases, hemoglobins, cytochromes and peroxidases and is involved in important biological processes like oxidative phosphorylation and electron transport.

Wolbachia encode all but one enzyme to synthesise the cofactor heme. The missing gene is protoporphyrinogen oxidase, a gene that is absent in many alphaproteobacteria, but very likely complemented by another gene (Narita et al., 1999). *B. malayi*, on the other hand, lacks most of the genes needed to produce heme (Foster et al., 2005). The only gene that is encoded by the *B. malayi* genome is ferrochelatase, which catalyses the last step of heme synthesis, the conversion of protoporphyrin IX into heme. Therefore *B. malayi* either takes up heme from the environment or is provided by its *Wolbachia* endosymbiont (Slatko et al., 2010). Recent findings by Wu et al. (2009) indicate that the latter case might be true: the inhibition of heme biosynthesis performed in an *ex vivo* study led to immobility and degenerate tissue of *B. malayi* worms, although hemin was provided in the culture medium. One phenotype observed after depletion of *Wolbachia* from filarial nematodes is the inability of larval moulting, which could be a consequence of heme deprivation. Ecdysteroid-like hormones are important for moulting and reproduction and ecdysone signalling is required in *Brugia malayi* (Tzertzinis et al., 2010). These hormones are synthesised in *Drosophila*, in part, by cytochrome P450 mono-oxygenases (Petryk et al., 2003). A loss of function of these heme dependent enzymes after *Wolbachia* depletion may therefore account for the impairment of developmental processes in the worm (Negri et al., 2010).

1.3.2.2. Further predicted *Wolbachia*-host interactions

Secretion and transport machineries are important for the communication of intracellular bacteria with their host and bacterial persistence within the host cell. Both the arthropod *Wolbachia* and *w*Bm contain a complete gene set to form a functional type IV secretion system (T4SS). This secretion system has been shown to deliver effector proteins, DNA and virulence factors via the bacterial membrane (Masui et al., 2000; Foster et al., 2005; Pichon et al., 2009). It is unknown which molecules are secreted by *Wolbachia* but the Ankyrin domain proteins might be a candidate (Rikihisa and Lin, 2010). Five ANK proteins are found in *w*Bm and 23 in *w*Mel. In eukaryonts ankyrins mediate protein-protein interactions, e.g. to the cytoskeleton (Mosavi et al., 2004). In *Anaplasma phagocytophilum* an Ank protein is secreted and binds to host chromatin (Caturegli et al., 2000; Foster et al., 2005; Iturbe-Ormaetxe et al., 2005). *Wolbachia* Ank proteins might therefore interact with the host cell cytoskeleton or play a role in regulation of host cell cycle and gene expression (Fenn and Blaxter, 2006).

1.4. *Litomosoides sigmodontis* - an animal model for filariasis

In order to study immunology and genetics of filarial infections, Petit et al. (1992) introduced the *L. sigmodontis* experimental model. They identified the BALB/c mouse strain as fully permissive to *L. sigmodontis*, making it the only filarial worm that can complete its life cycle and that develops a patent microfilaremia in an inbred mouse strain. *L. sigmodontis* is closely related to the human filaria *Brugia* spp., *O. volvulus*, and *W. bancrofti* and is therefore widely used to study filariasis (Allen et al., 2000; Hoerauf et al., 2001a; Allen et al., 2008). Like most filarial species, *L. sigmodontis* harbours *Wolbachia* bacteria and depletion of bacteria with tetracycline leads to a block in embryogenesis (Hoerauf et al., 1999), making this filarid a suitable model to study symbiosis (Heider et al., 2006).

1.4.1. The life cycle of *L. sigmodontis*

The natural host of *L. sigmodontis* is the cotton rat *Sigmodon hispidus*. The adults reside in the pleural cavity and at high infection rates also in the coelomic cavity. Mature female worms release microfilariae, the L1 larvae, which circulate in the peripheral blood, where they can be taken up during a blood meal of the intermediate host, the tropical rat mite *Ornithonyssus bacoti*. Within 10-12 days the L1 larvae

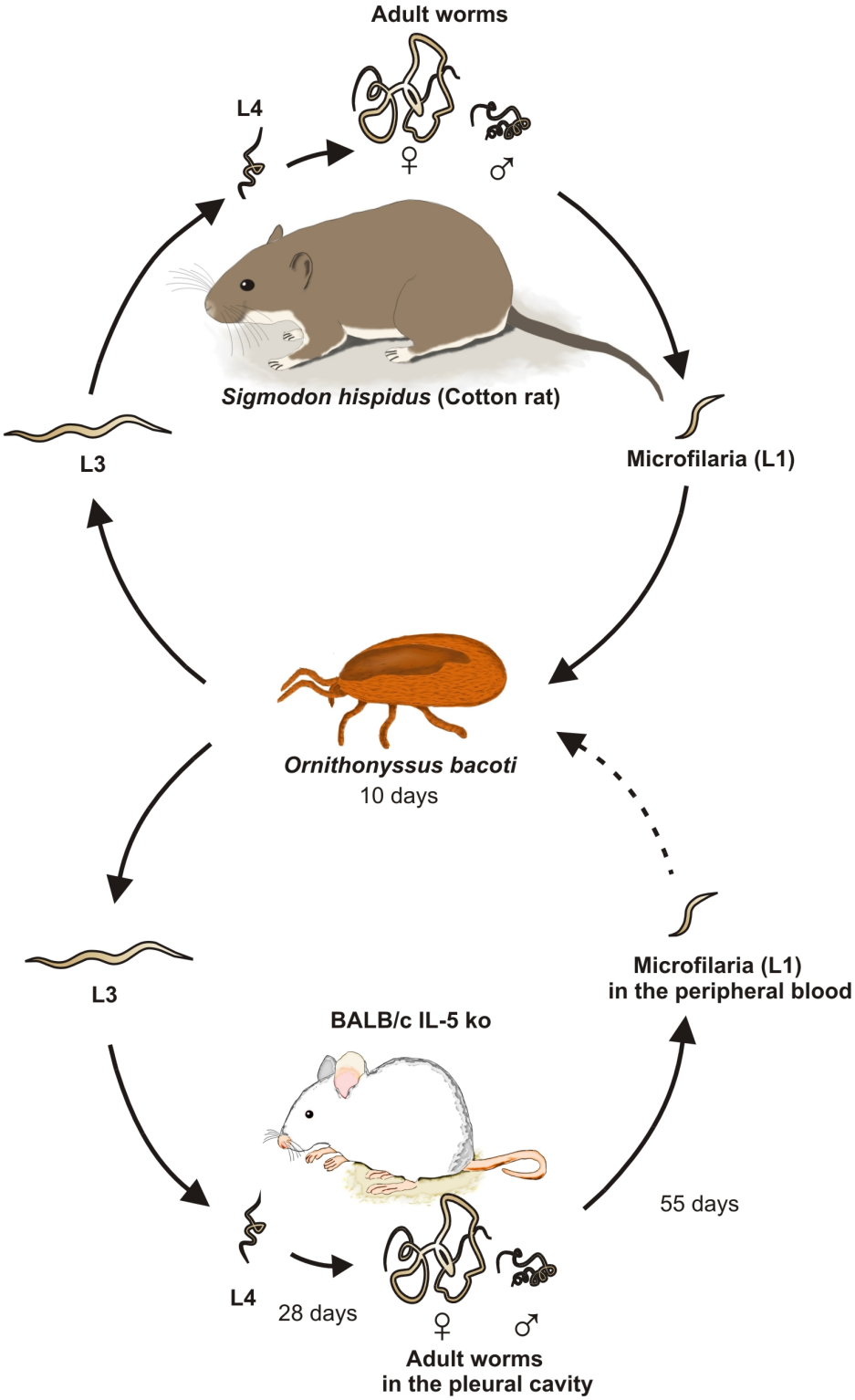

Figure 1.6.: Life cycle of *L. sigmodontis*. During a blood meal, mites take up microfilariae from the peripheral blood of the cotton rat *Sigmodon hispidus*. The larvae molt twice, resulting in the infective L3 larvae. These are used to either infect new cotton rats or BALB/c IL-5 ko mice, which were used for performing experiments in this study.

undergoes two moults into the infective third stage larvae (L3) which is transmitted by another blood feeding from the mite to the definite host, the cotton rat. Within 22-28 days the L3 larvae undergoes two other moults resulting in the juvenile adult worms, which at this time have migrated to the pleural cavity. At this final destination they mate and produce microfilariae which can be detected in the blood around day 55 p.i. (Hoffmann et al., 2000). Female adult worms have a length of up to 13 cm whereas male worms are only around 3 cm in length and can therefore easily be distinguished from each other. The laboratory life cycle is maintained in the cotton rat, as microfilariae concentrations are higher and adult worms live longer in the natural host compared to mice. In order to perform experiments the infective larvae can then be transmitted to BALB/c mice (Figure 1.6).

Th2 immune responses help to control filarial infections. The interleukin (IL) 5 cytokine influences development and number of *L. sigmodontis* in the mice (Saeftel et al., 2003; Volkmann et al., 2003). IL-5 knock out (ko) mice have higher worm burdens and a prolonged patency, which is especially important when treating mice harbouring adult worms over a long period of time, as carried out in this study. An additional advantage of using BALB/c IL-5 ko mice is the reduced formation of inflammatory nodules around the worms.

1.5. Tools for analysing the host-*Wolbachia* interactions

The first experiments that revealed the importance of *Wolbachia* endosymbionts for their filarial host came from assessing the worm phenotype after depletion of the bacteria with antibiotics (Bandi et al., 1999). The *Wolbachia*-free filaria *A. viteae* is used as a control for unspecific effects of the antibiotics or drugs (Heider et al., 2006; Hoerauf et al., 1999).

Research of *Wolbachia* is greatly hindered by the fact that the bacteria cannot be maintained outside their filarial host or insects cells, respectively, which makes classic genetic manipulation tools impossible. Attempts to culture *W. pipientis* in cell-free media showed that the bacteria can survive in amino acid-rich media for at least one week and that they were still able to re-infect the insect cells. If the exact molecular composition can be defined, i.e. molecules needed for *Wolbachia* to replicate, transformation of *Wolbachia* and deletion of specific genes might be possible in the near future (Rasgon et al., 2006). This would greatly ease the way to analyse the role of specific genes for symbiosis. Nevertheless, infection of *Wolbachia*-cured filaria with a genetically manipulated *Wolbachia* will be difficult, as curing of the

worm of the endosymbiont results in developmental defects. Such attempts would therefore be restricted to investigations on insect-*Wolbachia*. However, *Wolbachia* from insects contain a similar set of genes like filarial *Wolbachia* and many symbiotic strategies might work on a similar basis. Investigating the (mostly) parasitic symbiosis of *Wolbachia* from arthropods might therefore also shed light on the mechanism of the mutualistic filaria-*Wolbachia* symbiosis. The cultivation of *Wolbachia* in an insect cell culture inables easy testing of susceptibilities to antibiotics, which can be preselected before moving them into *in vivo* studies (Fenollar et al., 2003). Furthermore, *Wolbachia* from insect cell cultures can be used as a source for *Wolbachia* membranes and proteins and verification of their functionality by using *in vitro* activity assays (Henrichfreise et al., 2009). Functioning of specific *Wolbachia* proteins can also be confirmed by complementation assays in mutant *E. coli* strains (Wu et al., 2009). Microscopic techniques greatly help in investigating *Wolbachia* interactions with host cell structures, *Wolbachia* localisation patterns or identification of up-regulation of proteins (Ferree et al., 2005; Fischer et al., 2011; Landmann et al., 2009; Pfarr et al., 2008; Serbus and Sullivan, 2007). Other techniques that can help to understand the basis of the *Wolbachia*-host symbiosis include the analysis of differentially expressed genes upon anti-*Wolbachia* treatment (Heider et al., 2006), filarial *ex vivo* culture to asses worm phenotypes upon drug treatment or inhibition of specific pathways (Johnston et al., 2010; Townson et al., 2006; Wu et al., 2009) and the proteomic analysis of the secretome or different developmental stages of *Brugia* (Bennuru et al., 2011; Hewitson et al., 2008). Upcoming studies that are going to use GST-tagged *Wolbachia* proteins to identify interactors from *B. malayi* proteins extracts in a pull-down assay have a great potential to identify molecules important for symbiosis (Slatko et al., 2010).

A powerful tool to reveal molecular mechanisms of the *Wolbachia*-filaria relationship is provided by the genome information of *B. malayi* and *w*Bm. It enables the prediction of symbiotic dependencies by comparing presence and absence of genes for metabolic pathways (Foster et al., 2005). Genome information also enables comparison of the *Brugia* genome with the genome of *Wolbachia*-free filarial species to eventually identify essential genes for filarial biology which have been lost in *Brugia* due to their compensation by *Wolbachia* or have been transferred to *Wolbachia*-free filaria, in case they were infected by *Wolbachia* earlier in evolution (McNulty et al., 2010). The sequencing and annotation of the *Brugia* genome has facilitated the development of a filarial microarray, which offers a great potential for filarial research. It has for example been used for identification of gender regulated genes and genes that are important for the infectivity of the third stage larvae (Li et al., 2005, 2009)

and is now another tool for analysing molecular mechanisms of the filaria-*Wolbachia* symbiosis (Figure 1.7).

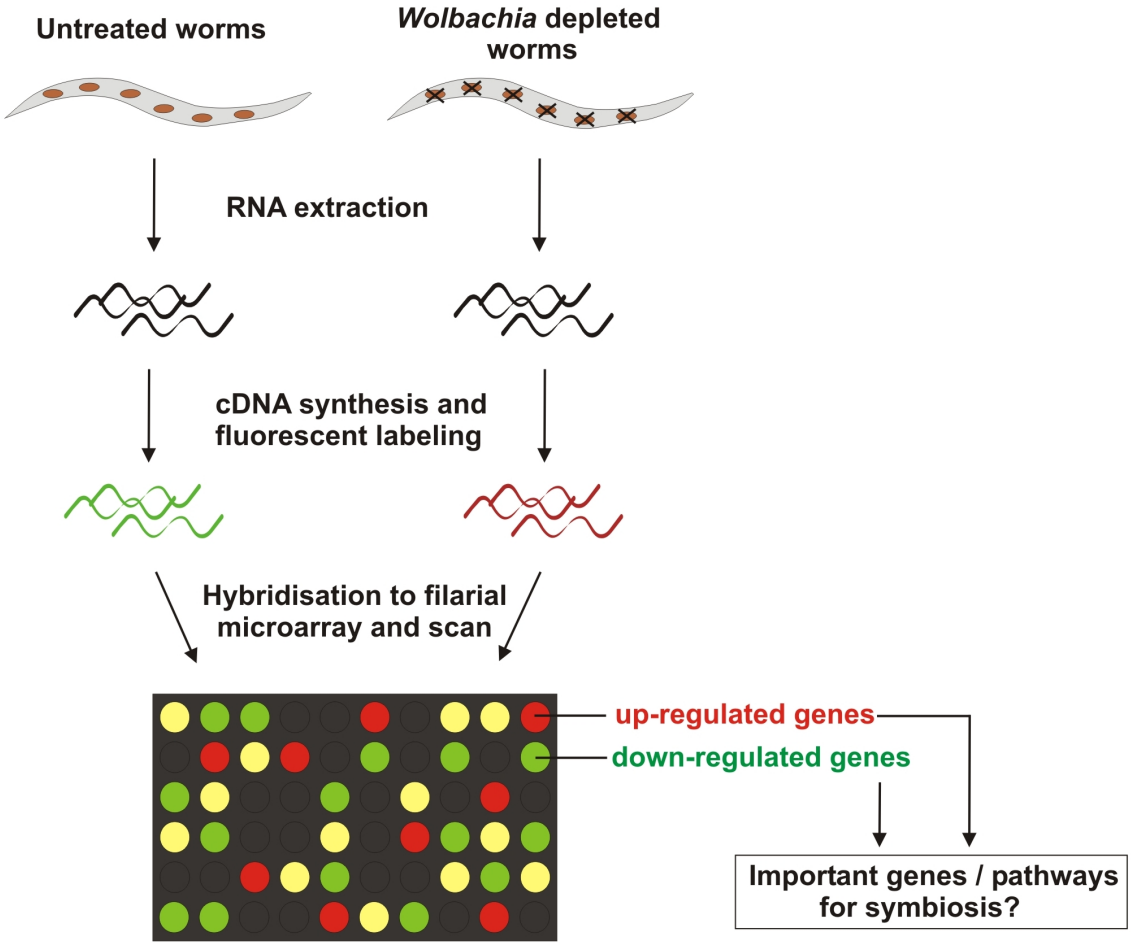

Figure 1.7.: Microarray experiment to identify differential expressed genes after depletion of *Wolbachia* endosymbionts from filaria.

1.6. Objectives

Lymphatic filariasis and onchocerciasis are the second leading causes for disability in the world and lead to enormous health and socio-economic problems in the developing countries. Mass drug treatments for many years have averted many cases of infections and in some countries a stop of transmission of the disease has been announced. Nevertheless, as the currently used drugs only have a microfilaricidal effect, they have to be given over many years to stop transmission. There is a strong need for the development of a new drug against filarial infections before resistance against ivermectin (the most widely used drug by anti-filarial programmes) spreads, which could revert the success of the control programmes. The endosymbiotic mutualistic bacteria *Wolbachia* are excellent targets for filariasis control, as *Wolbachia* depletion with antibiotics results in embryogenic blockade, sterility and death of the worms. Furthermore, worms are killed slowly which prevents adverse effects evoked by a sudden release of worm and *Wolbachia* antigens. However, the most active antibiotic, doxycyline, has to be given over many weeks and cannot be administered to young children and pregnant women and is therefore not suitable for MDA. A well-directed development of new drugs would be possible with the knowledge of the molecular mechanisms of the filaria-*Wolbachia* symbiosis, as blocking the symbiotic interactions should lead to the same detrimental effects for the worm, as seen after depleting the bacteria. The genomic information of the genome of *B. malayi* and *w*Bm together with a well-established and widely used model organism for filariasis provides the basis to address the questions of the molecular interactions between *Wolbachia* and filarial nematodes and to promote target identification for drugs against filariasis. The following goals were therefore addressed in the present study:

1. Identification of differentially expressed genes in *L. sigmodontis* after *Wolbachia* depletion using cross-hybridisation to the *Brugia* microarray to ascertain genes and pathways important for symbiosis.

2. Establishment of an *ex vivo* culture for the model filarial *L. sigmodontis* to enable testing of drugs and inhibition of specific pathways and evaluation of function of genes important for the *Wolbachia*-filaria symbiosis.

2. Materials and Methods

2.1. Materials

Chemicals and molecular biology reagents used in this study are listed. Specific instruments or commercial kits which are not specified here will be mentioned in the corresponding sections.

Chemicals

Agarose	Fermentas, St. Leon-Rot, Germany
5-aminolevulinic acid	Sigma-Aldrich, Munich, Germany
Ampicillin	Sigma-Aldrich, Munich, Germany
1-bromo-3-chloro-propane	Sigma-Aldrich, Munich, Germany
Boric acid	Sigma-Aldrich, Munich, Germany
Disodium hydrogen phosphate	Merck, Darmstadt, Germany
Dimethyl Sulfoxide (DMSO)	Roche, Mannheim, Germany
3-(4,5-dimethylthiazol-2-yl)-2,5-diphenyltetrazolium bromide (MTT)	Roth, Karlsruhe, Germany
Ethanol	Merck, Darmstadt, Germany
Ethidium bromide	Biomol, Hamburg, Germany
EDTA, Disodium Salt, Dihydrate	Sigma-Aldrich, Munich, Germany
HEPES	Merck, Darmstadt, Germany
Hydrochloric acid	Sigma-Aldrich, Munich, Germany
IPTG	Sigma-Aldrich, Munich, Germany
Isoforene	Abbot, Wiesbaden, Germany
Isopropanol	Merck, Darmstadt, Germany
Ketanest	Parke-Davis, Berlin, Germany
LB Agar	Sigma-Aldrich, Munich, Germany
Sodium Chloride	Roth, Karlsruhe, Germany
Sodium Hydroxide	Merck, Darmstadt, Germany
Potassium dihydrogen phosphate	Merck, Darmstadt, Germany

Potassium chloride	Merck, Darmstadt, Germany
RedSafe^{TM}	Chembio, Hertfordshire, United Kingdom
Rompun	Bayer, Leverkusen, Germany
SOC medium	Invitrogen, Karlsruhe, Germany
Succinylacetone	Sigma-Aldrich, Munich, Germany
Tris	Roth, Karlsruhe, Germany
Trizol	Invitrogen, Karlsruhe, Germany
wALADin1 (*Wolbachia* aminolevulinic acid inhibitor 1)	ChemBridge, San Diego, USA
X-Gal	Roth, Karlsruhe, Germany

Molecular biology reagents

Custom Primers	Invitrogen, Darmstadt, Germany Biomers, Ulm, Germany
DNA ladders	New England Biolabs, Ipswich, USA Invitrogen, Darmstadt, Germany
10 x DNase I buffer	Applied Biosystems, Foster City, USA
dNTPs (40 mM)	Qiagen, Hilden , Germany
HotStar Taq Polymerase	Qiagen, Hilden , Germany
Linear acrylamid	Applied Biosystems, Foster City, USA
$MgCl_2$	Qiagen, Hilden , Germany
Oligo-dT primer	Qiagen, Hilden, Germany
10 x PCR buffer	Qiagen, Hilden , Germany
RNase free DNase I	Applied Biosystems, Foster City, USA
RNase Inhibitor	Peqlab, Erlangen, Germany Invitrogen, Karlsruhe, Germany
Sybr Green	Roche, Mannheim, Germany
Taqman Hybridisation Probe	Operon Biotechnologies, Cologne, Germany
10 x Yellow Sub^{TM}	Geneo BioTechProducts, Hamburg, Germany

Cell culture reagents

Fetal Calf Serum	PAA, Pasching, Austria
L-glutamin	PAA, Pasching, Austria
Minimum essential medium with earls salts (MEM)	PAA, Pasching, Austria
PBS for cell culture	PAA, Pasching, Austria
Penicillin/Streptomycin	PAA, Pasching, Austria
RPMI-1640	PAA, Pasching, Austria
Trypsin/EDTA 10 x	PAA, Pasching, Austria

2.2. Animals and parasitological methods

2.2.1. Maintenance of animals

Cotton rats (*Sigmodon hispidus*) and jirds (*Meriones unguiculatis*) were maintained at the animal facilities of the Institute for Medical Microbiology, Immunology and Parasitology (IMMIP), University Clinic Bonn, Germany. IL-5 deficient BALB/c mice were bred at the Haus für Experimentelle Therapie (HET) and afterwards maintained under Specific Pathogen Free (SPF) conditions in the IMMIP. Ethical clearance for animal handling was approved by the regional authority in Cologne, Germany (AZ 50.203.2-BN15,40/04).

2.2.2. Animal model

The natural host of *L. sigmodontis*, the cotton rat *S. hispidus*, was used to maintain the life cycle of *L. sigmodontis* as described in Chapter 1.4.1. For the experiments described in this study we used BALB/c mice which are deficient for the Th2 cytokine IL-5 (BALB/c IL-5 ko mice).

2.2.3. Infection cycle of *L. sigmodontis*

The life cyle of *L. sigmodontis* was maintained in our lab by passages of the parasite through the cotton rat and the intermediate mite vector. Mites were maintained on bedding material in glass flasks at a temperature of 26-28°C and air humidity of 80-90 %. To allow mites to have a blood meal on infected microfilariae positive animals, the cotton rats were placed into wire cages and then placed over night onto bedding material containing the mites. To avoid contamination of the rooms with

mites, the cages were placed onto trays with detergent containing water, therefore all mites were either kept in the cages or died in the water. The infected mites in the bedding material were collected into Erlenmeyer flasks covered with a mesh screen and then incubated for 10-14 days, until L1 larvae developed into the infective L3 larvae, used for infection of cotton rats or experimental mice. Mice were anaesthetised with Rompun/Ketanest and placed onto bedding material containing the mites. Anaesthetising the mice prevents them trying to get rid of the mites and therefore increases the infection efficiency. Mites were allowed to have a blood meal on the mice over night, the next day the mice were decontaminated from remaining mites by placing the cages onto water with detergent over night. All materials that came into contact with mites during the infection processes were either dunked into water containing detergent or frozen at -20°C to kill any mites.

Rompun/Ketanest long term anesthetic

Rompun (20 mg/ml)	100 µl + 200 µl PBS
Ketanest (10 mg/ml)	200 µl
	500 µl

50 µl of the Rompun/Ketanest mixture was injected intramuscularly per mouse.

PBS

20 x PBS:	160 g NaCl
	23 g Na_2HPO_4
	4 g KH_2PO_4
	4 g KCl
	ad 1000 ml nanopure water
	pH adjusted to 7.4

2.2.4. Infection cycle of *Acanthocheilonema viteae*

The life cycle of *A. viteae* was maintained at the Department of Molecular Parasitology, Humboldt University, Berlin by passages through jirds (*Meriones unguiculatus*) and ticks (*Ornithodorus moubata*). Infected ticks containing the L3 larvae and *A. viteae*-infected jirds, respectively, were kindly provided by Prof. Richard Lucius, Humboldt University, Berlin. The infected ticks can be kept for several month in a humid environment. Infection of jirds with *A. viteae* was carried out as described by Lucius and Textor (1995). Briefly, ticks containing the L3 larvae were disrupted in

RPMI medium, so larvae could move out of the body of the ticks into the medium. Jirds were then injected subcutanously with 80 L3 larvae. Treatment of jirds started when microfilariae were detectable in the blood.

2.2.5. Evaluation of microfilariae release

Mice For microfilariae count in *L. sigmodontis*-infected mice, blood was taken from the tail by cutting the tip and collected into a capillary. The blood was then blown out onto a microscope slide and 10 µl blood were immediately pipetted into 300 µl of Hinkelmann solution on ice. The mixture was then incubated for 5 min at RT. The Hinkelmann solution lyses the erythrocytes and also stains the microfilariae. After centrifugation for 5 min at 2000 rpm at RT the supernatant was removed except for 10 µl sediment. The complete sediment was analysed under a microscope (Leica Microsystems GmbH, Wetzlar, Germany) and the microfilariae were counted. Values were given as number of microfilariae/µl of blood.

Jirds To obtain blood from jirds containing *A. viteae* microfilariae, animals were shortly anaesthetised with isoforene and bled from the retro-orbital sinus using a glass capillary tube. Blood was collected in EDTA tubes and 2 µl of EDTA blood was mixed with 300 µl Hinkelmann solution and stained and analysed as described above for *L. sigmodontis* blood microfilariae.

Hinkelmann's solution

0.5 % w/v eosin Y (2.5 g)
0.5 % v/v phenol (2.5 ml)
0.185 % v/v formaldehyde (0.925 ml)
ad 500 ml with distilled water

2.2.6. Tetracycline treatment

Tetracycline (Tet) treatment of *L. sigmodontis*-infected BALB/c IL-5 ko mice started around day 60 after infection, when mice had a patent infection and blood microfilariae were detectable. Mice were treated daily for 36 days with intraperitoneal (i.p.) injections of 1 mg tetracycline in 200 µl PBS (50 mg Tet/kg/day).

Tet treatment of *A. viteae*-infected jirds also started ∼3 months after infection when microfilariae were seen in blood. Animals were treated orally with tetracycline (0.5 % w/v) in drinking water for 6 weeks. The water was changed daily.

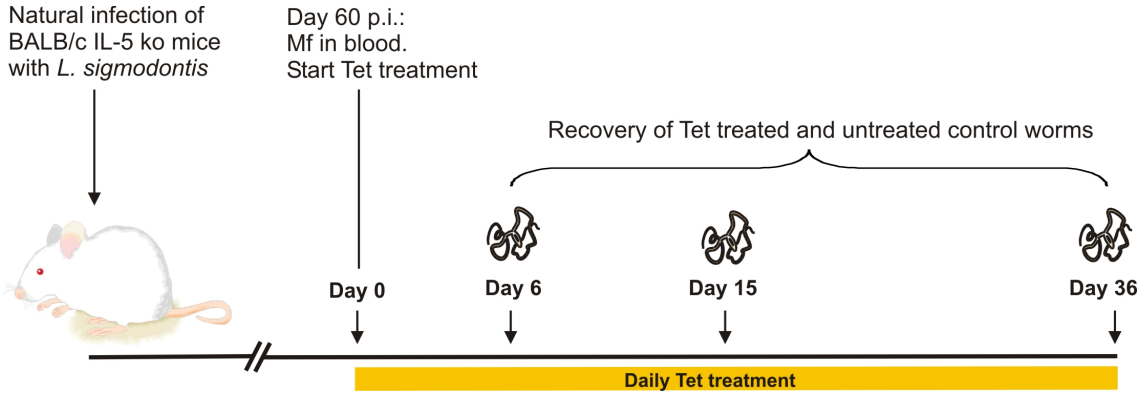

Figure 2.1.: Tet treatment scheme of *L. sigmodontis*-infected BALB/c IL-5 ko mice. Tet = tetracycline, Mf = microfilariae. Treatment of mice started when mice had a patent infection and Mf were detected in the blood. Mice were treated daily with i.p. injections of tetracycline. At days 6, 15 and 36 worms were recovered from Tet treated and untreated mice for use in microarray and qPCR expression studies.

2.2.7. Worm recovery

L. sigmodontis worms were recovered from the thoracic cavity at days 6, 15 and 36 of Tet treated and untreated BALB/c IL-5 ko mice by flushing the pleural cavity with PBS and carefully removing worms with a pipette or forceps. Nematodes were washed in PBS and separated by sex. Tubes containing 3 female worms were shock frozen in liquid nitrogen and stored at -80°C for subsequent RNA and DNA isolation.

A. viteae nematodes were recovered from jirds after 6 weeks of Tet treatment and from untreated animals, respectively. Jirds were anaesthetised with isoforene and bled from the retro-orbital sinus to reduce bleeding during dissection. Adult worms were recovered from subcutaneous and intramuscular tissues and the visceral cavity. Worms were washed in PBS, separated by sex and 2 female worms per tube were shock frozen in liquid nitrogen and stored at -80°C.

2.3. Molecular biology methods

2.3.1. RNA extraction

Total RNA was isolated from 2-3 (quantitative PCR) or 5-10 (microarray) female *L. sigmodontis* worms per tube using the Trizol extraction method, following the manufacturer's protocol with some modifications. Briefly, nematodes in 800 µl Trizol reagent were transferred to 2 ml tubes containing 0.5 mm glass beads and homogenised in a Precellys 24 homogeniser (Peqlab, Erlangen, Germany) 4 x 10 s at 5000 rpm. Instead of chloroform, 80 µl of 1-brom-3-chloro-propane was used to separate the homogenate into RNA-containing aqueous and DNA containing organic

phases. For precipitation of RNA, linear acrylamide was used as co-precipitant with a final concentration of 9 µg/ml and 1 volume isopropanol. RNA was treated with RNase-free DNase I for 1 h at 37°C, followed by clean-up and concentration of the RNA with the RNeasy Minelute kit (Qiagen) as per the manufacturer's protocol. Extraction of total RNA from 2 female *A. viteae* worms was carried out as described above, but with the modification that 1 ml Trizol, 100 µl 1-brom-3-chloro-propane and a homogenisation programme of 2 x 30 s at 6800 rpm were used to accommodate the larger size of *A. viteae* worms.

2.3.1.1. RNA concentration and quality

The concentration, purity and integrity of RNA was analysed prior to reverse transcription into cDNA. Concentration of RNA[1] and the 260/280 ratio[2] of the RNA was measured spectrometrically using a NanoVue (GE Healthcare, Chalfont St Giles, UK). The ratio measured for RNA extracted in this study was around 2, which indicates clean RNA without protein contamination. Furthermore, integrity of RNA was analysed using the Experion automated gel electrophoresis system (Bio-Rad, Munich, Germany) following the manufacturer's instructions. Here, electrophoresis is conducted on channels of a microchip and peaks of a fluorophore bound to very small amounts of RNA can be measured and an electropherogram with peaks of RNA is produced. Two distinctive peaks corresponding to 28S and 18S ribosomal RNA indicate undegraded RNA (Figure 2.2 A). The electropherograms of the RNA samples can be transformed into a picture of a virtual agarose gel, visualising the bands of the ribosomal RNAs compared to an RNA ladder (Figure 2.2 B) (Fleige and Pfaffl, 2006).

2.3.2. Reverse transcription

Depending on the concentrations after isolation, 100-500 ng of total RNA were reverse transcribed into cDNA with oligo-dT primers using the Omniscript Reverse transcription kit (Qiagen). For reverse transcription of mitochondrial encoded genes, gene specific primers at a concentration of 0.5 µM were used. The reaction was incubated for 75 min at 37°C and then stored at -20°C.

[1] Depending on worm size and extraction efficiency amount of RNA extracted from 3 female *L. sigmodontis* ranged from 300 ng - 2 µg.

[2] The 260/280 ratio is used to assess purity of nucleic acid solutions. Pure DNA is indicated by a ratio of ca 1.8 and pure RNA by a ratio of ca 2.0.

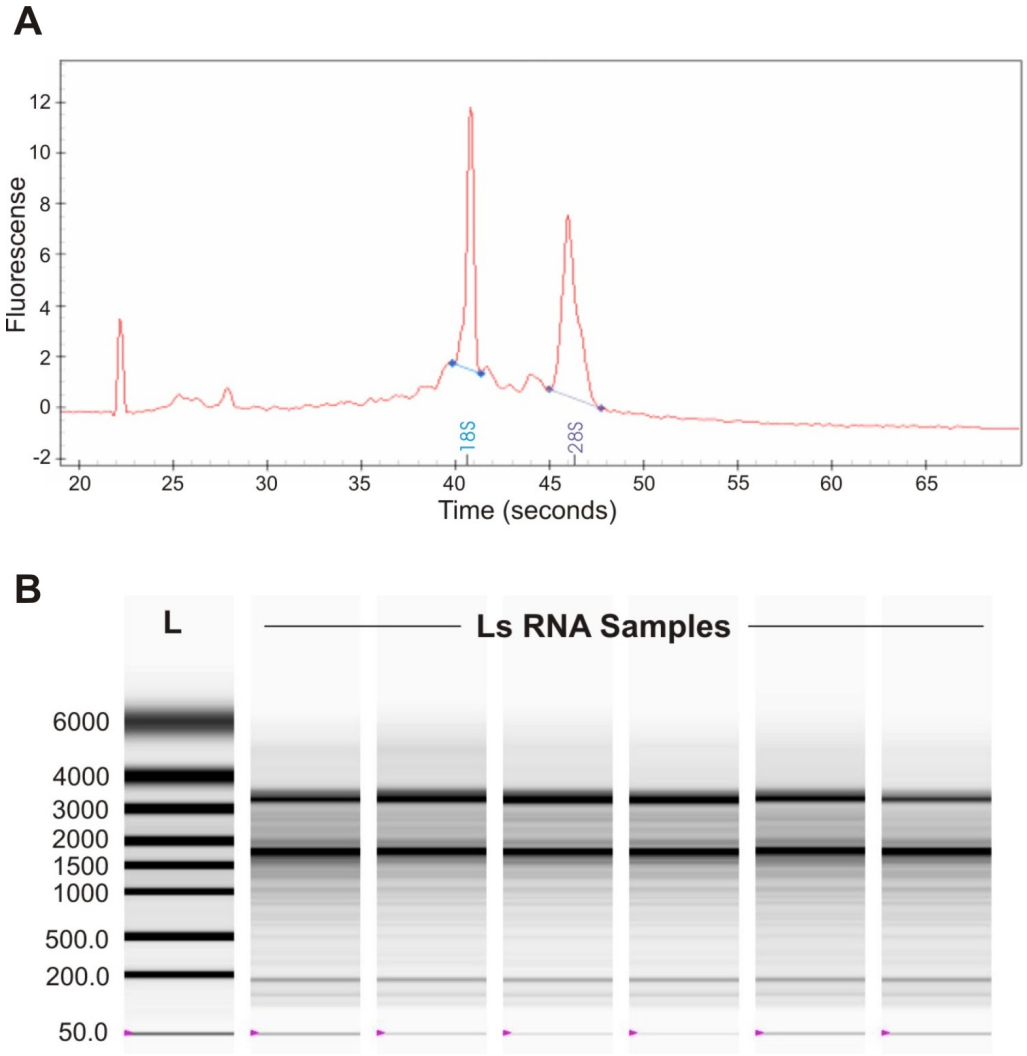

Figure 2.2.: Quality control of RNA extracted from female *L. sigmodontis* worms. L = RNA ladder, Ls = *L. sigmodontis*, 18S/28S = ribosomal 18S/28S RNA. Two distinct peaks for 18S and 28S ribosomal RNAs indicate undegraded RNA in this sample (A). Virtual agarose gel showing bands corresponding to ribosomal RNAs (B).

Reverse transcription reaction

	1 reaction
100-500 ng RNA in nuclease free water	13.67 µl
10 x reaction buffer	2 µl
oligo-dT Primer	1 µl
dNTPs	2 µl
Reverse Transcriptase	1 µl
RNase Inhibitor (30 U/µl)	0.33 µl
	20 µl

2.3.3. DNA extraction

DNA from *L. sigmodontis* worms was precipitated from the organic phase obtained by the Trizol extraction method described in Chapter 2.3.1 following the manufacturer's instructions. Briefly, DNA was precipitated by adding 100 % ethanol. The pellet was washed two times with 0.1 M Sodium citrate in 10 % ethanol and one time with 75 % ethanol. Afterwards the pellet was dissolved in 100-200 µl 8 mM NaOH. Insoluble material was removed by centrifugation at 12,000 g for 10 min. The supernatant containing the DNA was adjusted to a pH 7.5 by adding 16 µl 0.1 M HEPES per 100 µl DNA.

0.1 M Sodium Citrate, 10 % EtOH
5.88 g Sodium Citrate
add nuclease free water up to 180 ml
add 20 ml 100 % EtOH

8 mM NaOH
400 µl 1 M NaOH
add nuclease free water up to 50 ml

0.1 M HEPES
2.38 g HEPES
add nuclease free water up to 100 ml

In case no RNA was needed from the worms, the QIAamp DNA Mini Kit (Qiagen) was used for DNA extraction. Worms were homogenised with small scissors in buffer AL and incubated with proteinase K at 56°C over night. The manufacturer's tissue protocol was followed and DNA was eluted with 100-200 µl buffer AE.

2.3.4. Cloning of *L. sigmodontis* and *A. viteae* sequences

2.3.4.1. Primer design

Primers were designed using the software "Primer3" (`http://frodo.wi.mit.edu/primer3/`). Parameters for quantitative PCR (qPCR) primers included a PCR product size range of 100-130 bp, optimal primer length of 21 bp, maximum poly-X of 3 and an optimal primer melting temperature of 60°C. Unwanted hairpins and self dimerisation was checked using the "Oligonucleotide Properties Calculator" (`http://www.basic.northwestern.edu/biotools/oligocalc.html`). As se-

quence information for many *L. sigmodontis* genes that were analysed in this study were not available in public databases, sequences were amplified using primers designed on the basis of the corresponding *B. malayi* sequences. Depending on sequence availability, cDNA sequences of *B. malayi* were aligned to *Ascaris suum*, *O. volvulus*, *W. bancrofti* or *C. elegans* sequences and primers matching to conserved parts of the gene with high sequence similarity were designed. In some cases degenerate primers were designed with a maximum of 5 degenerate bases per primer. *L. sigmodontis* sequences were than used to design *L. sigmodontis* specific qPCR primer. The sequence editor software GENtle (`http://gentle.magnusmanske.de/`) was used for sequence storage and management, checking primer positions and identifying sequences by alignment. New nucleotide sequence data for *L. sigmodontis* genes obtained in this study are available in the GenBank™ database under the Accession No.: GU971360, GU971361, GU971362, GU971363, GU971364, GU971365, GU971366, GU971367, GU971368, GU971369, GU971370, GU971371, GU971372 and GU971373.

2.3.4.2. Conventional PCR

For establishment of qPCR the 100-130 bp gene specific sequence to be amplified in qPCR had to be cloned from *L. sigmodontis* cDNA. Sequences that were not available from public databases were amplified from *L. sigmodontis* and *A. viteae* cDNA samples using *B. malayi* or degenerate *B. malayi* primers (Chapter 2.3.4.1). *L. sigmodontis* gene sequences corresponding to *B. malayi* succinyl-CoA ligase (Bm1_00840), Mif-1 (Bm1_28435), Protein kinase domain containing protein (Bm1_37575), Lipoic acid synthetase (Bm1_23910), Biopterin dependant aromatic amino acid hydroxylase (Bm1_46865) and DNA/pantothenate metabolism flavoprotein (Bm1_45070) were kindly provided by Prof. Mark Blaxter, University of Edinburgh, Scotland. Conventional PCRs were performed in a 20 µl reaction with the reagents concentrations shown in Table 2.2 and primers listed in Table 2.3. The following cycling conditions were used: denaturing step of 95°C for 15 min followed by 35 cycles of 94°C for 30 s, annealing at 55°C for 30 s and elongation at 72°C for 30 s[3]. A final elongation step at 72°C for 10 min followed. PCR products were stored at 4°C until further use. If PCRs didn't yield the expected product with these conditions annealing temperatures were lowered or $MgCl_2$ concentrations were changed or if this was not successful new primers were designed.

[3]Elongation times were extended for longer product lengths; aproximately 1 min for 1000 bp.

Table 2.2.: Protocol for conventional PCR

	1 reaction	final concentrations
10 x PCR buffer with 15 mM $MgCl_2$	2	1 x buffer, 1.5 mM $MgCl_2$
10 x Yellow Sub^{TM} [a]	2 µl	1 x
dNTPs (40 mM)	0.1 µl	0.2 mM
Forward Primer (10 µM)	2 µl	1 µM
Reverse Primer (10 µM)	2 µl	1 µM
cDNA or gDNA	2 µl	
Hot Star Taq	0.1 µl	0.25 U
nuclease free water	9.8 µl	

[a] Increases yield and specificity of PCR reaction and contains loading buffer and dye, therefore PCR mix can be applied directly to an agarose gel.

Table 2.3.: Primer for cloning *A. viteae* and *L. sigmodontis* sequences

Gene target	**Primer name**	**Primer sequence 5′ - 3′**
Av cytochrome B	Bmc-cytB FW	GGATTGCTTTTACTGGTTATGTT
	Bm-cytB RV	CTAGACCTAGAACCAGTAAAATG
Ls hypothetical gene	Bm-30045 F1	CATTTCTGTAGTATGTATTTCTTCGCT
	Bm-30045 deg[a]R1	TTCAAGGTYCTCCAYGCAGT
Ls acetyl-CoA hydrolase/	Bm-aCoA deg F1	GGAATCCAYACWGAAATGTTCTCAG
transferase	Bm-aCoA deg R1	GWGCAATAATGGKCTTTCCR
Ls abc transporter	Bm-abc deg F1	TTGTWCCWCAGGATTCMGTWCTTT
	Bm-abc deg R1	AATYGTMGCYARACGATGTGCA
Ls retinoblastoma-binding	Bm-rbp4 deg F1	GTACSCAYACWTCRGATGAACARAATC
protein	Bm-rbp4 deg R1	CATCYTCKACMACYGCATTAT
Ls diphosphomevalonate	Bm-mvd deg F2	GMTCWGGAAGTGCMTGYCG
decarboxylase	Bm-mvd deg R2	ATTCGGACCRGCRTCAAAY
Ls rab5	Bm-rab5 deg F2	GGWTTCTACGGKACMCCRCAATG
	Bm-rab5 deg R2	ACTYTCCTTWAGYGCCTCRAARAT
Ls actin	Ov-act FW	GACGCAAATCATGTTCGAGA
	Ov-act RV	CGGATGTCAATATCACACTTCA

[a] degenerate primer

2.3.4.3. Gel electrophoresis

An agarose gel was run to determine the length of DNA[4] amplified in PCR. Depending on the expected length of the PCR product, a 1-2 % gel was prepared by dissolving and heating the agarose in 0.5 % TBE buffer. Initial gels were stained with ethidium bromide, but later gels were stained with RedSafe (being biologically safer than ethidium bromide). After polymerisation of the gel, samples were applied into the slots of the gel and run at 120 Volt in 0.5 % TBE buffer. DNA bands were made visible under UV light. The length of the DNA molecules was estimated by comparing the DNA bands to a DNA size marker run on the same gel.

Tris-borate-EDTA (TBE)

10 x stock solution:	108 g Tris
	55 g boric acid
	9.3 g $Na_2EDTA\ 2H_2O$
	ad 1000 ml nanopure H_2O
Working solution:	0.5 x stock solution

2.3.4.4. TOPO-TA cloning

PCR products were cloned into the TOPO-TA vector (Invitrogen) for sequencing and to generate standard plasmids to be used in qPCR. Taq Polymerase amplified PCR products can directly be cloned into this vector as Taq Polymerase adds single deoxyadenosine to the 3′ ends of PCR products and the linearised vector has overhanging 3′-deoxythymidine residues. The Topoisomerase I enzyme catalyses the ligation reaction.

TOPO-TA cloning reaction

1 µl vector
1-3 µl PCR product (depending on amount of PCR product)
1 µl salt solution
nuclease free water up to 6 µl

The reaction was incubated for 5-30 min at RT. 2 µl of the cloning reaction were then added to 50 µl of One Shot Chemically Competent *E.coli* (Invitrogen), gently

[4]DNA molecules can be separated by size in an electric field due to the negative charge of nucleic acids. Shorther molecules move faster through the agarose matrix and therefore farther than longer molecules.

mixed and incubated for 30 min on ice. A 30 s heat shock in a 42°C waterbath followed and cells were immediately transferred to ice. 250 µl SOC medium was added and the cells were incubated for 1 h on a shaker at 37°C. 10 and 50 µl of transformed bacteria were plated onto LB-Agar plates containing ampicillin (100 µg/ml), IPTG (0.5 mM) and X-Gal (40 µg/ml), and incubated at 37°C overnight.

2.3.4.5. Colony PCR

Colony PCR was performed to identify clones with the expected size of insert cloned into the TOPO-TA vector. Reactions were performed in 20 µl and consisted of 1 x PCR buffer, 1 x YellowSub, 1.5 mM $MgCl_2$, 0.2 mM dNTPs, 0.1 mM M13 forward primer, 0.1 mM M13 reverse primer and 0.25 U HotStar Taq Polymerase. A small amount of colony material was disolved into the PCR reaction mix using a pipet tip. 10 white clones[5] were chosen for analysis. Cycling conditions were as described in section (conventional PCR) for conventional PCR. As M13 Primer bind to the vector, 200 bp of the vector sequence are amplified and have to be added to the insert length to identify the expected PCR product length on the agarose gel.

M13 Primer sequences
M13 Forward (-20) Primer: 5′-GTAAAACGACGGCCAG-3′
M13 Reverse Primer: 5′-CAGGAAACAGCTATGAC-3′

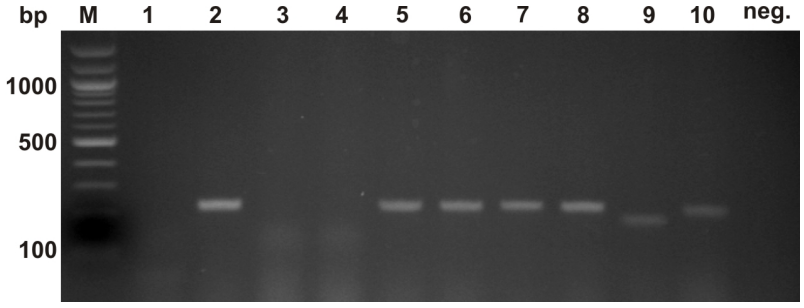

Figure 2.3.: Example for products of a Colony PCR run on an agarose gel. bp = basepair, 1-10 = clones 1-10, neg.= negative (water) control. Clones 2, 5, 6, 7, 8 and 10 show a DNA band at the expected size.

[5]White colour of clones indicates insertion of DNA into the multiple cloning site of the vector. In this case the *lacZ* gene is disrupted, no functional β-galactosidase enzyme can be formed and X-Gal cannot be hydrolised into the otherwise blue colour.

2.3.4.6. Plasmid purification

For purification of plasmids, *E. coli* were grown in 5 ml LB medium with 50 µg/ml ampicillin overnight in a shaker at 37°C and 250 rpm. Bacteria were centrifuged at 600 rpm for 10 min and the plasmids were purified from the pellet using the DNA MiniPrep kit (Qiagen) following the manufacturer's protocol. The plasmid purification kit was either applied by hand or by using the automated plasmid purification system (QiaCube, Qiagen). The concentration and purity of the plasmids was assessed spectrometrically with a nanodrop. Part of the plasmid solution was used for sequence confirmation by sequencing (Seqlab, Göttingen, Germany) and the remaining stored at -20°C until further use as a plasmid standard in qPCR.

2.3.5. Quantitative PCR

QPCR was performed in a 20 µl volume for most genes except for *Av-act* and *Ls-act* gDNA, which was performed in a 10 µl volume. Reactions consisted of 1 x PCR buffer, 0.2 mM dNTPs, 0.25 U Hotstar Taq Polymerase, 1/10 volume of Sybr Green (1:1000 dilution of stock in DMSO) and 2 µl DNA. QPCR for *Ls-ftsZ* was conducted using 5 µM of the Taqman Hybridisation Probe 6-FAM-CAGGGATGGGTGGT-GGTACTGGAA-TAMRA instead of Sybr Green. Primer sequences, optimised $MgCl_2$ and primer concentrations are listed in Table 2.4. QPCR reactions were performed in triplicate on a Rotorgene 3000 (Corbett Research, Sydney, Australia) with the following cycling conditions: denaturing step of 95°C for 15 min followed by 35 cycles of 94°C for 10 s, annealing for 20 s (see Table 2.4 for temperatures) and 72°C for 20 s. Fluorescence was acquired at the end of the 72°C step on the Fam channel. After amplification, a melting curve was measured using a temperature gradient from 62 to 99°C to confirm specific amplification (Figure 2.4 C). For all genes, no non-specific products were measurable. Copy numbers were calculated by comparing crossing point data for the test samples to a standard curve obtained from serial dilutions of the plasmid containing the specific gene (Figure 2.4 A,B). The signal for the actin gene was used to normalise each sample to correct for differences in the amount of starting material and efficiency of RNA extraction. A regulated gene was confirmed if the fold change as measured by qPCR was $\geq$ 1.3-fold. All PCRs presented here, except the PCRs for *Ls-act* gDNA, *Ls-hsp60* (Heider et al., 2006) and *Ls-ftsZ* (Arumugam et al., 2008), were established within the scope of this study.

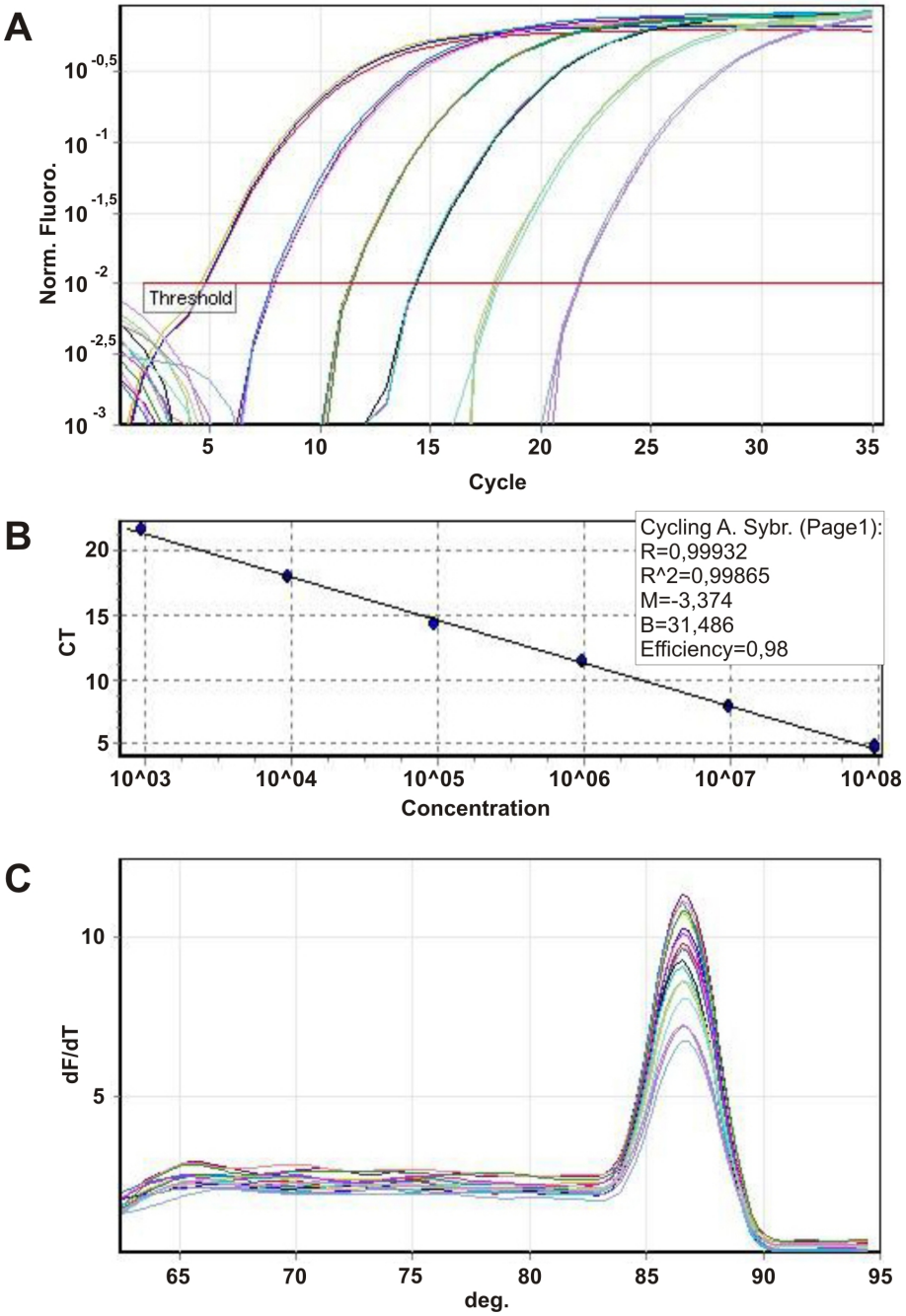

Figure 2.4.: Example for a gene specific standard (A, B) and melt curve (C) in qPCR, CT = threshold cycle, dF/dT = rate of change in fluorescence.

Table 2.4.: Cycling conditions for quantitative PCR

Gene target	**corresponding *B.malayi* accession number**	**Primer name**	**$MgCl_2$ concentration**	**Primer concentration**	**Annealing temperature**
Av cytochrome c oxidase subunit 1	AF538716	Av-cox1 F1/R1	2 mM	300 nM	57°C
Av cytochrome b	AF538716	Av-cytB F2	3 mM	400 nM	57°C
Ls abc transporter	Bm1_30435	Ls-abc F1/R1	3.5 mM	500 nM	57°C
Ls acetyl-CoA hydrolase/transferase	Bm1_42975	Ls-acCoA F1/R1	3 mM	400 nM	57°C
Ls actin (only cDNA)	Bm1_34930	Ls-act FW2/RV2	3 mM	500 nM	57°C
Ls actin (gDNA) / Av actin	Bm1_34930	Ov-act F1/R1	3.5 mM	900 nM	52°C
Ls biopterin dependant aromatic amino acid hydroxylase,	Bm1_46865	Ls-cat2 F1/R1	4 mM	500 nM	57°C
Ls cytochrome b	AF538716	Ls-cytB F1/R1	2.5 mM	400 nM	57°C
Ls cytochrome c oxidase subunit 1	AF538716	Ls-cox1 F1/R1	4 mM	500 nM	57°C
Ls cytochrome c oxidase subunit 2	AF538716	Ls-cox2 F1/R1	4.5 mM	200 nM	57°C
Ls diphosphomevalonate decarboxylase,	Bm1_42945	Ls-mvd F1/R1	3 mM	500 nM	57°C
Ls DNA/panthotenate metabolism flavoprotein	Bm1_45070	Ls-DFP F2/R2	3.5 mM	500 nM	57°C
Ls EF hand family protein, Troponin c	Bm1_48810	Ls-tropC F1/R1	2.5 mM	500 nM	57°C
Ls globin family protein	Bm1_50430	Ls-globin F1/R1	3 mM	500 nM	57°C
Ls heat shock protein 60	Bm1_56580	LsHspLC F2/R2	4.5 mM	300 nM	58°C
Ls hypothetical gene	Bm1_04280	Ls_04280 F1/R1	3.5 mM	500 nM	53°C
Ls hypothetical gene	Bm1_30045	Ls-30045 F1/R1	3.5 mM	500 nM	57°C
Ls juvenile protein p120	Bm1_19955 / Bm1_00865	Ls-juvp120 F1/R1	4.5 mM	400 nM	57°C
Ls lipoic acid synthetase	Bm1_23910	Ls-lias F1/R1	4 mM	500 nM	57°C
Ls macrophage migration inhibitory factor-1	Bm1_28435	Ls-mif1 F1/R1	3.5 mM	500 nM	57°C
Ls *med7* transcription factor	Bm1_23975	Ls-med7 F1/R1	3.5 mM	400 nM	57°C
Ls NADH dehydrogenase 4	AF538716	Ls-ND4 F1/R1	4 mM	500 nM	57°C
Ls NADH dehydrogenase 5	AF538716	Ls-ND5 F1/R1	3 mM	400 nM	57°C
Ls protein kinase domain containing protein	Bm1_37575	Ls-c-met F1/R1	3.5 mM	500 nM	57°C
Ls *rab5*	Bm1_29925	Ls-rab5 F1/R1	2.5 mM	300 nM	57°C
Ls retinoblastoma-binding protein, putative	Bm1_15930	Ls-rbp4 F1/R1	4 mM	500 nM	57°C
Ls 60S ribosomal protein L3, putative	Bm1_13895	Ls-60SL3 F1/R1	2 mM	500 nM	57°C
Ls RNA-binding protein	Bm1_37780	Ls-rbp F1/R1	2.5 mM	500 nM	55°C
Ls succinyl-CoA ligase	Bm1_00840	Ls-sucCoA F1/R1	3.5 mM	500 nM	57°C
Ls troponin T, putative	Bm1_55000	Ls-tropT F1/R1	2 mM	300 nM	57°C
Wolbachia of Ls *ftsZ*	AY583309 (*w*Bm)	Ls-ftsZ F1/R1	5 mM	200 nM	58°C

Table 2.5.: Primer sequences used for qPCR

Gene name	Primer name	Primer sequence 5′ - 3′
Av cytochrome c oxidase subunit 1	Av-cox1 F1	CGTTCCACTGCGGTTACTTT
	Av-cox1 R1	AAGAACCAGCCAAAACAGGA
Av cytochrome b	Av-cytB F2	TTGAGGGCAAATGAGGTATTG
	Av-cytB R2	ACTACCTCAAATTCACCAAACCA
Ls abc transporter	Ls-abc F1	AAATCCGACTGCAACTGAAGA
	Ls-abc R1	TTCAAACCTCTTTCACCAACAA
Ls acetyl-CoA hydrolase/transferase	Ls-acCoA F1	CCGAAAGTAGTCGATGTCCAA
	Ls-acCoA R1	TGTTGCTTGGGTAAATGATCC
Ls actin (only cDNA)	Ls-act FW2	ACCGATTTACGAAGGTTACGC
	Ls-act RV2	TCACGTACAATTTCACGTTCG
Ls actin (gDNA) / Av actin	Ov-act F1	GTGCTACGTTGCTTTGGACT
	Ov-act R1	GTAATCACTTGGCCATCAGG
Ls biopterin dependant aromatic amino	Ls-cat2 F1	TCGCAACAAATTGGACTTCTC
acid hydroxylase	Ls-cat2 R1	TCACGACACAAACCAAATTCA
Ls cytochrome b	Ls-cytB F1	TCGTTTGACTAATGTTTGATTGG
	Ls-cytB R1	ACCGCAGCCCAATAGCTC
Ls cytochrome c oxidase subunit 1	Ls-cox1 F1	GGTAGTTGGTCAACCGGAAT
	Ls-cox1 R1	AATGTAACCGCCCTACAACG
Ls cytochrome c oxidase subunit 2	Ls-cox2 F1	GTTGTGTTTTGCCGGTAGGT
	Ls-cox2 R1	AACAAACCATTTAGCACATCCA
Ls DNA/panthotenate metabolism flavoprotein	Ls-DFP F2	TGCCAGGTTTAGTAGAAGCTTTG
	Ls-DFP R2	ATGCAGGCAAATCATTTCAAG
Ls diphosphomevalonate decarboxylase,	Ls-mvd F1	TGCATTGGAAAGCTGGTATTT
	Ls-mvd R1	TGCATCATGTGAGGTTACCAA
Ls EF hand family protein, Troponin c	Ls-tropC F1	AGGGCAACGGCTACATATCTC
	Ls-tropC R1	TCAATCTTTCCAGAACCATCC
Ls globin family protein	Ls-globin F1	TATGCTCGTGAAACGGTCAA
	Ls-globin R1	TCCATCTATTGCAGTGTGTTCC
Ls heat shock protein 60	LsHspLC F2	TACGTGAGCCAATCATGACA
	LsHspLC R2	ATCATATCCAAACGCCAACTC
Ls hypothetical gene	Ls-04280 F1	CGGCCTATTGGCTAAGATCA
	Ls-04280 R1	AAACCCTCCAGAGTCCCAAA
Ls hypothetical gene	Ls-30045 F1	TCGCTATCAGCGAAAATGC
	Ls-30045 R1	CTCCATGCAGTCATCAAACG
Ls juvenile protein p120	Ls-juvp120 F1	TCAACAATTCCAAGAACAGCA
	Ls-juvp120 R1	GATGTGGTTGCTGAAGCATTT
Ls lipoic acid synthetase	Ls-lias F1	AGACATCACGTAAGCCACCTC
	Ls-lias R1	CGCCATCTTCAATATCGTCTC
Ls macrophage migration inhibitory factor-1	Ls-mif1 F1	AAGTACGGATCCATGTGCTGT
	Ls-mif1 R1	AGCCAACAGCGTGTACAATTT
Ls *med7* transcription factor	Ls-med7 F1	GGTCACGAAGCATTAAACCAA
	Ls-med7 R1	GCTCCACCAACTCATTGTCAT
Ls NADH dehydrogenase 4	Ls-ND4 F1	TTGGCTCATGGCTATACTTCTG
	Ls-ND4 R1	AACATTGAAATAACCCCGAAAA
Ls NADH dehydrogenase 5	Ls-ND5 F1	GGGGGTTTCATTATTTGTCTTA
	Ls-ND5 R1	CCTGCTGCCCAAAATTAAAA
Ls protein kinase domain containing protein	Ls-c-met F1	AGGTTATGCGTGCTGACCTCT
	Ls-c-met R1	TCACTGCCGTTGCATACATTA
Ls *rab5*	Ls-rab5 F1	TGGATGACCTCTCTGGTATGG
	Ls-rab5 R1	TACTGCTCCACTTCTGCCATT
Ls retinoblastoma-binding protein, putative	Ls-rbp4 F1	CCTACCGATGATGCACAGTTT
	Ls-rbp4 R1	CTCACCTTCGTGGTTCATCTT
Ls 60S ribosomal protein L3, putative	Ls-60SL3 F1	GATTCATCTTACCGCGTTCAT
	Ls-60SL3 R1	AAACTGTTACCGCTTCGACAA
Ls RNA-binding protein	Ls-rbp F1	AGGAAGATGTGGCGAATTTCT
	Ls-rbp R1	CCGCTGCTTCTGTTTCAAAT
Ls succinyl-CoA ligase [ADP-forming]	Ls-sucCoA F1	TGGTGAATGGAGCTGGATTAG
beta-chain, mitochondrial	Ls-sucCoA R1	CCGAAAGGACTCAGACACTTG
Ls troponin T, putative	Ls-tropT F1	GTAGGACCGGAGGTAATCCAG
	Ls-tropT R1	TTCTTTGTTGTTGGTGGTGGT
Wolbachia of Ls *ftsZ*	Ls-ftsZ F1	CGATGAGATTATGGAACATATAA
	Ls-ftsZ R1	TTGCAATTACTGGTGCTGC

2.3.5.1. Calculation of plasmid copy numbers

The copy numbers / µl of the gene specific plasmids used for generating standard curves can be estimated as shown in the following example:

Length of plasmid:	3956 bp (TOPO-vector) + 116 bp (insert) = 4072 bp
Molecular mass:	4072 bp x 660 Da/bp = $2.69 \cdot 10^6$ g/mol
DNA concentration:	222 ng/µl

Copy numbers can now be calculated with:

$(222 \cdot 10^{-9}\,\text{g/µl} \text{ x } 6 \cdot 10^{23}\,\text{copies/mol}) \text{ / } (2.69 \cdot 10^6\,\text{g/mol}) = \mathbf{4.95 \cdot 10^{10}\,copies/µl}$

The same calculation is done by the dsDNA copy number calculator available at `http://www.uri.edu/research/gsc/resources/cndna.html`.

2.4. Microarray

Our microrarray experiment compared gene expression profiles from Tet treated female *L. sigmodontis* to the expression of untreated age-matched control worms. The experiment was performed for three different timepoints: day 6, 15 and 36 of Tet treatment. RNA quality control, cDNA synthesis, hybridisation of cDNA to the *B. malayi* microarray chip, image analysis and normalisation of data was performed at the core Microarray facility of Washington University School of Medicine, St. Louis, MO and we kindly thank Dr. Michael Heinz for his support and advice.

2.4.1. Microarray fabrication

Our studies used the second-generation filarial microarray (BmV2array) developed by the Filarial Microarray Consortium, of which our lab is a partner (`http://www.filariasiscenter.org/molecular-resources/research-materials`). The array contains 65mer oligonucleotides corresponding to 15,455 ESTs and ORFs from *B. malayi*, 1,016 from *O. volvulus*, 878 from *W. bancrofti* and 804 from *Wolbachia* of *B. malayi* (*w*Bm). The number of different oligos corresponding to one gene varies from 1 to more than 20. Information about the number of protein domain matches is reported by Li et al. (2009) in a supplemental file (Summary of protein domain matches for BmV2array elements).

2.4.2. cDNA synthesis

First strand cDNA was generated by oligo-dT primed reverse transcription (Superscript II, Invitrogen) utilising the 3DNA Array 900 kit (Genisphere) with Cy3 or Cy5 specific oligo sequences attached to the oligo-dT Primer. One µl of fluorophore specific oligo-dT primer was added to 2 µg of total RNA and the solution was incubated at 80°C for 5 min and then cooled on ice for 2 min. 0.5 µl RNase inhibitor (Superase-In, Ambion), 2 µl 5 x first strand buffer, 0.5 µl dNTP mix (10 mM each dATP, dCTP, dGTP and dTTP), 1 µl 0.1 M DTT and 0.5 µl Superscript II RNase H - Reverse Transcriptase were added to each sample. Reverse transcription was carried out at 42°C for 2 h. The reaction was terminated by adding 1 µl of 1 M NaOH/100 mM EDTA and incubation at 65°C for 10 min followed by neutralisation with 1.2 µl of 2 M Tris-HCL, pH 7.5.

2.4.3. Hybridisation

Each microarray slide for the 3 different time points was hybridised with differentially labelled cDNA from tetracycline and control worms. Dye-flip replicates were performed to exclude an impact through preferentially labelling of one fluorophore.

Each sample pair ($\sim$ 24 µl) was resuspended in formamide-based hybridisation buffer (vial 7-Genisphere) (26 µl) and Array 50dT blocker (Genisphere) (2 µl). Two hybridisations were carried out in a sequential manner. The primary hybridisation was performed by adding 48 µl of sample to the microarray under a supported glass coverslip (Erie Scientific) at 43°C for 16-20 h at high humidity in the dark. Prior to the secondary hybridisation, slides were gently submerged into 2 x SSC, 0.2 % SDS (at 43°C) for 11 min, transferred to 2 x SSC (at RT) for 11 min, transferred to 0.2 x SSC (at RT for 11 min) and then spun dry by centrifugation. Secondary hybridisation was carried out using the complimentary capture reagents provided in the 3DNA Array 900 kit (Genisphere). For each reaction, the following were added: 3DNA capture reagent with Cy3 (2.5 µl), 3DNA capture reagent with Cy5 (2.5 µl), SDS-based hybridisation buffer (vial 6-Genisphere) (26 µl), and nuclease free water (21 µl). The secondary hybridisation solution was incubated in the dark at 80°C for 10 min, then 50°C for 15 min. Hybridisation was performed by adding 48 µl secondary hybridisation solution to the slide under a supported glass coverslip at 65°C for 4 h at high humidity in the dark. At hybridisation termination, arrays were gently submerged into 2 x SSC, 0.2 % SDS (at 65°C) for 11 min, transferred to

2 x SSC (at RT) for 11 min, transferred to 0.2 x SSC (at RT) for 11 min, and then spun dry by centrifugation.

2.4.4. Image analysis

Slides were scanned with a Perkin Elmer ScanArray Express HT scanner to detect Cy3 and Cy5 fluorescence. Laser power was kept constant for Cy3/Cy5 scans and photomultiplier tube (PMT) was varied for each experiment based on optimal signal intensity with lowest possible background fluorescence. A low PMT setting scan was also performed to recover signal from saturated elements. Gridding and analysis of images was performed using ScanArray v3.0 (Perkin Elmer). For determining foreground and background intensities of each spot, the adaptive circle spot-finding algorithm was used.

2.4.5. Data analysis

Spots that passed the criteria of an intensity unit > 200 and signal to background ratio > 2 in one of the two channels were marked as present and were included in further analyses. Normalisation of data was done using Lowess. The log2 transformed values of the normalised and background subtracted ratio of intensities (treated vs. untreated) were used for identification of significant changes in gene expression applying Significance Analysis of Microarrays (SAM, version 3.02). SAM is a statistical method adapted specifically for determining significant changes in very large datasets like microarray expression data. A score is assigned to each gene on the basis of gene expression relative to the standard deviation of repeated measurements. SAM estimates the percentage of genes identified by chance, which is named false discovery rate (FDR) (Tusher et al., 2001). An example for a SAM plot with up- and down-regulated genes is given in Figure 2.5. The one-class response type was used with a FDR $\leq 5\,\%$ (= q-value ≤ 0.05). For each time point two hybridisations (dye-flips) were performed. Since each oligo is spotted two times on the array we had a total of four technical replicates. SAM imputes missing data (K-Nearest Neighbor algorithm); therefore oligos that did not have at least 2 of the 4 technical replicates hybridised were not identified as significantly regulated genes, due to high standard deviations. Finally, the resulting data were filtered for genes having a minimum 2-fold gene expression change. The microarray data of the experiments reported here have been submitted to Gene Expression Omnibus (accession GSE20976).

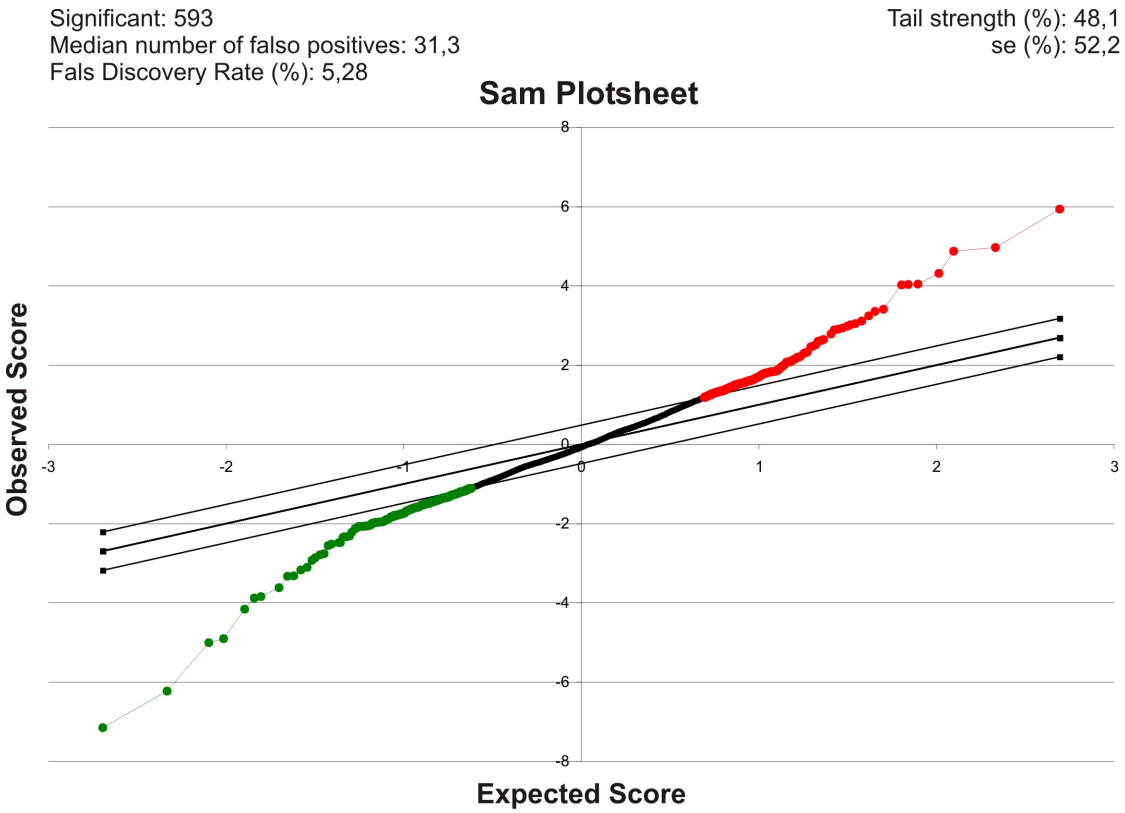

Figure 2.5.: Example for a SAM plotsheet with a false discovery rate of 5.28 %. The observed score indicates the observed relative difference d(i) of gene expression whereas the expected score indicates the expected relative difference $d_E(i)$. The middle of the three lines indicates the line where d(i) is identical to $d_E(i)$. The outer lines represent the delta value which can be adjusted, resulting in larger and smaller sets of significant genes with larger or smaller false discovery rates, respectively. Red datapoints represent up-regulated and green points indicate down-regulated genes.

2.5. *Ex vivo* culture of filarial worms

2.5.1. Maintenance of LLCMK2 cells

We kindly thank Dr. Simon Townson (Northwick Park Institute for Medical Research, Harrow, UK) for providing us with LLCMK2-cells[6]. The cells were maintained in 75 cm^2 cell culture flasks in Minimal essential medium Eagle (MEM), supplemented with L-glutamine, 10 % FCS and 1 % Penicillin/Streptomycin and cultured at 37°C and 5 % CO_2. Medium was exchanged every 3-4 days and cells were sub-cultivated once a week. Cells were washed with PBS and incubated with Trypsin/EDTA (4 ml/flask) for ∼5 min at 37°C. When cells started to detach medium was added, the cells were resuspended and 1/4 of the original flask was transferred to a new one.

[6] monkey kidney cells

For cryopreservation one flask with confluent cells was used for 4 vials of frozen cells. Cells were resuspended in standard medium and an equal volume of ice cold freezing medium (standard medium + 20 % DMSO) was added dropwise to the cells. Cells were frozen in cryotubes at -20°C for 3 h and then transferred to -80°C. Alternatively cells were directly transferred to -80°C using a freezing container (Mr. Frosty, Thermo Scientific - Nalgene, Schwerte, Germany). For re-cultivation, cells were quickly thawed, centrifuged at 1200 rpm for 5 min at 4°C and the medium was replaced with fresh standard medium. One vial of frozen cells was used for a 25 cm^2 cell culture flask.

2.5.2. Feeder cell layer

LLCMK2 cells were used as feeder cells for *ex vivo* culture experiments with filarial worms. 1/4 flask of confluent grown cells was seeded to one 6-well plate (for female worms) or 48-well plate (for male worms) 2 days before adding the worms.

2.5.3. Isolation and selection of worms

L. sigmodontis worms less than 14 months old were isolated from cotton rats with a patent infection. *A. viteae* were isolated from jirds with a patent infection, as described in Chapter 2.2.7. The worms were washed in PBS and single worms were then transferred into cavities of a 12-well plate (female worms) and 48-well plates (male worms), respectively, containing medium. Integrity of the worms was than evaluated under an inverse microscope (Leica Microsystems). Single intact female worms were then transferred to cavities of a 6-well plate with a LLCMK2 feeder cell layer or without cells, respectively. Female worms were cultivated on 6-well plates and male worms on 48-well plates. In the survival assay (Chapter 3.7.1), worms were cultivated in 4 ml medium with half of the medium changed every 3 days. In all other drug treatment experiments the female worms were cultivated in 3 ml medium containing the drug with a complete medium change every 2 days.

2.5.4. Drug treatment

The media containing the drugs were freshly prepared with the standard medium used for cultivation of worms (MEM + 10 % FCS + 1 % Penicillin/Streptomycin) prior to drug treatment. Succinylacetone was either directly dissolved in the medium to a final concentration of 3 mM or prepared as 300 mM stock solution in DMSO and diluted 1:100 in the medium. Stock solutions in DMSO were prepared for wALADin1 (100 mM and 50 mM) and 5-ALA (500 mM) and diluted 1:100 in the

Table 2.6.: Motility score description for *L. sigmodontis* cultured *ex vivo*

Score	Description
0	Worm is stretched, no movement
1	Minor movement observed by eye, alternated by no movement, worm ist stretched
2	Slow movement, worm is stretched
3	Moderate movement, worm is slightly stretched; some worms are completely stretched at one side, but the other side shows active motility
4	Active movement, not as closely knotted as '5'
5	Very active movement, worm is knotted

medium. All media contained a final concentration of 1 % DMSO. Media containing the final concentrations of drugs (3 mM SA, 500 µM wALADin1, 1 mM wALADin1, 5 mM 5-ALA) were then sterile filtered.

2.5.5. Motility scoring

Motility was scored as a measure for viability. We used a scoring system from 0-5, with 5 = best motility and 0 = no motility. Table 2.6 describes the phenotypes observed for each score. Depending on the drugs used in the experiment, worm behaviour might be observed which was different from this scoring scheme and was therefore recorded separately. The worm movement was also documented using a Sony DCR-HC46E video camcorder and video material was edited using Final Cut Pro 6.0 for Macintosh. Examples for *L. sigmodontis* and *A. viteae* motility scoring 0-5 are given on videos 1 and 2 (for overview of videos see appendix Table A.1).

2.5.6. Microfilariae count

Old medium was collected at each day of medium change for microfilariae count. The medium was centrifuged at 1200 rpm for 5 min at 4°C. Medium was discarded and microfilariae were taken up in 200 µl of medium. Microfilariae and early stages were directly counted under a Neubauer counting chamber (LO-Laboroptik GmbH, Friedrichsdorf, Germany). Differentiation between living and dead microfilariae was possible, as larvae can move within the counting chamber.

2.5.7. MTT assay

On the last day of culture, a biochemical evaluation of the worm viability was performed using the MTT[7] assay. As a control for dead worms, worms frozen in liquid nitrogen and heat shocked for 10 min at 70°C were included in the assay. Worms were washed in PBS and then incubated for 30 min in 0.5 mg MTT/ml PBS at 37°C. Afterwards, single worms were transferred to 200 µl DMSO and incubated for 1 h to solubilise the blue formazan product. The plate was gently agitated to disperse the blue colour and the absorption of the formazan was measured at a microplate spectrophotometer (Spectra Max, Molecular Devices, Sunnyvale, USA) at 490 nm. For adsorption values over 1, the samples were diluted in DMSO and measured again.

[7] The yellow compound MTT [3-(4,5-dimethylthiazol-2-yl)-2,5- diphenyltetrazolium bromide] is reduced by the mitochondrial enzyme succinate dehydrogenase of living tissues to produce the blue precipitate MTT formazan. Inhibition of formazan formation is correlated with worm damage or death.

3. Results

3.1. *Wolbachia* are effectively depleted from *L. sigmodontis*

An effective depletion of *Wolbachia* in our experiments was confirmed by qPCR that detects *Wolbachia ftsZ* copies (1 *ftsZ* = 1 *Wolbachia*). At day 6 of Tet treatment *Wolbachia ftsZ* copies were reduced by 99.3 %. On day 36 a further decrease of *Wolbachia* levels was measured, with 99.8 % reduction of bacterial DNA (Figure 3.1).

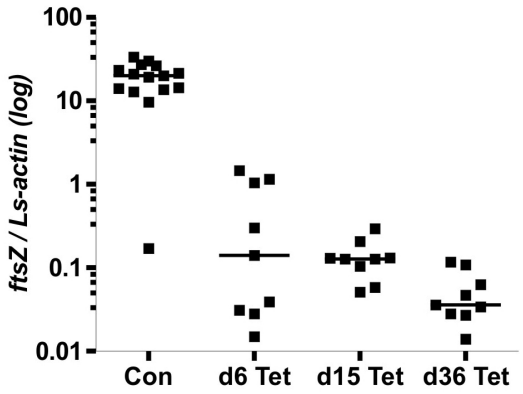

Figure 3.1.: *Wolbachia* are depleted from *L. sigmodontis* after Tet treatment. To confirm the depletion of *Wolbachia* due to Tet treatment *ftsZ* copies were measured by qPCR of gDNA extracted from treated and control worms. PCR reactions were performed in triplicate. Copy numbers were normalised to copies of filarial actin from the same sample. Each square represents gDNA levels from 3 female worms. Lines are median values.

Our microarray experiment aimed to study gene expression changes of *L. sigmodontis* genes in response to depletion of *Wolbachia* rather than of *Wolbachia* genes itself. Therefore oligo-dT primer were used for cDNA synthesis. Nevertheless, some hybridisation of *Wolbachia* oligos was detected, very likely due to binding of the oligo-dT primer to A-rich regions of the *Wolbachia* genes. Microarray analysis revealed significantly down-regulated *Wolbachia* oligos (except 3 up-regulated oligos at day 36) with a much higher fold change (Table 3.1 and 3.2) than most of the filarial down-regulated oligos. Whereas the mean fold change of all *Wolbachia* genes

down-regulated at day 6, 15 and 36 (FDR $\leq 5\,\%$ and minimum 2-fold change) was 8.8, the mean fold change of the significantly down-regulated filarial genes was only 2.9. Thus, successful depletion of *Wolbachia* was also confirmed by the results of the microarray.

Table 3.1.: Regulated *Wolbachia* genes at day 6 and 15 of Tet treatment with fold change ≥ 2 and FDR $\leq 5\,\%$

Oligo ID	FDR %	Fold change	Model name	Annotation
Down-regulated oligos day 6				
BMX14298	2.01	0.21	Wbm0531	Ribosomal protein S16
bm.01655	0.00	0.04	BMC11139	16S ribosomal RNA gene
BMX14105	0.00	0.19	Wbm0338	50S ribosomal protein L2
BMX14468	1.76	0.25	Wbm0700	50S ribosomal protein L27
BMX14524	1.76	0.09	Wbm0756	NifU homolog involved in Fe-S cluster formation
BMX14070	3.35	0.22	Wbm0302	Ribosomal protein L28
BMX14288	1.76	0.26	Wbm0521	Ribosomal protein S21
BMX14110	4.61	0.19	Wbm0343	Translation elongation factor EF-Tu, GTPase
BMX13119	0.00	0.05	TC3121	no match
BMX13089	0.00	0.05	TC3089	no match
bm.00809	0.00	0.06	BMC03273	no match
bm.03319	0.00	0.10	BMC05922	no match
bm.02869	1.76	0.17	BMC03240	no match
BMX12409	1.76	0.18	WB-contig_1624	no match
bm.03228	0.00	0.08	BMC01096	no match
BMX12657	0.00	0.08	WB-contig_453	no match
bm.00929	0.00	0.05	BMC03698	no match
bm.03514	0.00	0.07	BMC12386	no match
bm.01569	0.00	0.06	BMC07973	no match
Down-regulated oligos day 15				
BMX14113	0.00	0.06	Wbm0346	30S ribosomal protein S12
BMX14105	0.00	0.08	Wbm0338	50S ribosomal protein L2
BMX14007	0.00	0.30	Wbm0239	hypothetical protein
BMX14537	0.00	0.10	Wbm0769	Membrane protease subunit, stomatin/prohibitin homolog
BMX13825	0.00	0.11	Wbm0053	Outer membrane protein
BMX14070	0.00	0.12	Wbm0302	Ribosomal protein L28
BMX14288	0.00	0.09	Wbm0521	Ribosomal protein S21
BMX14110	0.00	0.04	Wbm0343	Translation elongation factor EF-Tu, GTPase
bm.03228	0.00	0.04	BMC01096	no match
bm.00929	0.00	0.03	BMC03698	no match
bm.00809	3.47	0.04	BMC03273	no match
BMX12657	0.00	0.07	WB-contig_453	no match
bm.03514	0.00	0.07	BMC12386	no match
BMX12409	0.00	0.15	WB-contig_1624	no match
bm.01569	0.00	0.06	BMC07973	no match
BMX13089	0.00	0.03	TC3089	no match
BMX13119	0.00	0.03	TC3121	no match
bm.03319	0.00	0.07	BMC05922	no match

Table 3.2.: Regulated *Wolbachia* genes at day 36 of Tet treatment with fold change ≥ 2 and FDR $\leq 5\,\%$

Oligo ID	FDR %	Fold change	Model name	Annotation
Up-regulated oligos day 36				
BMX14282	2.79	3.32	Wbm0515	hypothetical protein
BMX14078	2.48	2.01	Wbm0310	Short-chain alcohol dehydrogenase family enzyme
BMX14443	2.79	2.05	Wbm0675	Stress-induced morphogen, BolA
Down-regulated oligos day 36				
BMX14128	1.52	0.13	Wbm0362	Predicted membrane protein
bm.01655	0.00	0.11	BMC11139	16S ribosomal RNA gene
BMX14113	3.13	0.30	Wbm0346	30S ribosomal protein S12
BMX14105	0.00	0.10	Wbm0338	50S ribosomal protein L2
BMX14468	1.52	0.24	Wbm0700	50S ribosomal protein L27
BMX14225	3.13	0.40	Wbm0459	ATP synthase subunit C
BMX14475	1.52	0.12	Wbm0707	Cold shock protein
BMX14415	2.48	0.38	Wbm0647	DNA-directed RNA polymerase beta' chain
BMX14537	0.52	0.11	Wbm0769	Membrane protease subunit, stomatin/prohibitin homolog
BMX14010	1.52	0.26	Wbm0242	NADH dehydrogenase beta subunit
BMX14393	0.52	0.18	Wbm0625	NADH:ubiquinone oxidoreductase chain J
BMX14070	3.13	0.28	Wbm0302	Ribosomal protein L28
BMX14400	0.00	0.05	Wbm0632	Ribosomal protein L36
BMX14103	1.52	0.09	Wbm0336	Ribosomal protein S16
BMX14298	1.52	0.09	Wbm0531	Ribosomal protein S16
BMX14288	0.00	0.16	Wbm0521	Ribosomal protein S21
BMX13917	1.52	0.06	Wbm0147	Thiol-disulfide isomerase, thioredoxin family
BMX14421	1.52	0.13	Wbm0653	Translation elongation factor EF-Tu, GTPase
BMX14110	0.00	0.05	Wbm0343	Translation elongation factor EF-Tu, GTPase
BMX14007	0.00	0.28	Wbm0239	hypothetical protein
BMX13995	0.00	0.09	Wbm0225	hypothetical protein
bm.01569	3.59	0.18	BMC07973	no match
bm.03514	4.28	0.27	BMC12386	no match
bm.00929	3.59	0.19	BMC03698	no match
bm.03319	0.00	0.04	BMC05922	no match
bm.03228	0.00	0.03	BMC01096	no match
BMX12409	0.00	0.02	WB-contig_1624	no match
bm.00809	1.84	0.09	BMC03273	no match
BMX13089	1.52	0.08	TC3089	no match
BMX12657	0.00	0.05	WB-contig_453	no match

3.2. *Hsp60* is not up-regulated after *Wolbachia* depletion

Expression of *L. sigmodontis hsp60* was measured during Tet treatment as an indicator for a possible stress response in the worms due to Tet treatment or depletion of *Wolbachia*. Expression of *hsp60* showed no alteration over the treatment time compared to the control (Figure 3.2).

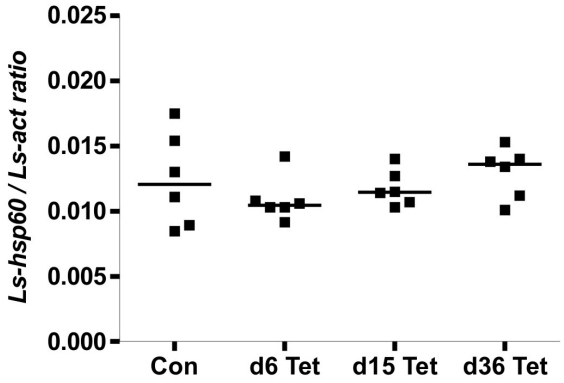

Figure 3.2.: *Hsp60* is not up-regulated in *L. sigmodontis* after *Wolbachia* depletion. To control for a possible stress response during Tet treatment, expression of filarial *hsp60* was measured by qPCR. PCR reactions were performed in triplicate. Copy numbers were normalised to cDNA copy numbers of filarial actin from the same sample. Each square represents cDNA levels from 3 female worms. Lines are median values.

3.3. Differentially expressed *L. sigmodontis* genes after depletion of endosymbiotic *Wolbachia*

The microarray experiment was conducted to identify genes of *L. sigmodontis* that show differential expression upon depletion of intracellular *Wolbachia*. This study represents the first attempt to use the *B. malayi* microarray to study gene expression changes in *L. sigmodontis*. Binding of *L. sigmodontis* cDNA to the oligonucleotides on the chip covered approximately 20 % of the spots (average percentage of all 6 slides, not including oligos derived from *Wolbachia* gene sequences). Within the thresholds of a q-value ≤ 0.05 (= False Discovery Rate $\leq 5\,\%$) and a minimum fold change of 2, we detected most of the oligos corresponding to regulated genes at day 36 of Tet treatment (142 up- and 193 down-regulated). Fewer oligos passed the thresholds at day 6 (1 up- and 57 down-regulated) and the fewest at day 15 (3 up- and 5 down-regulated).

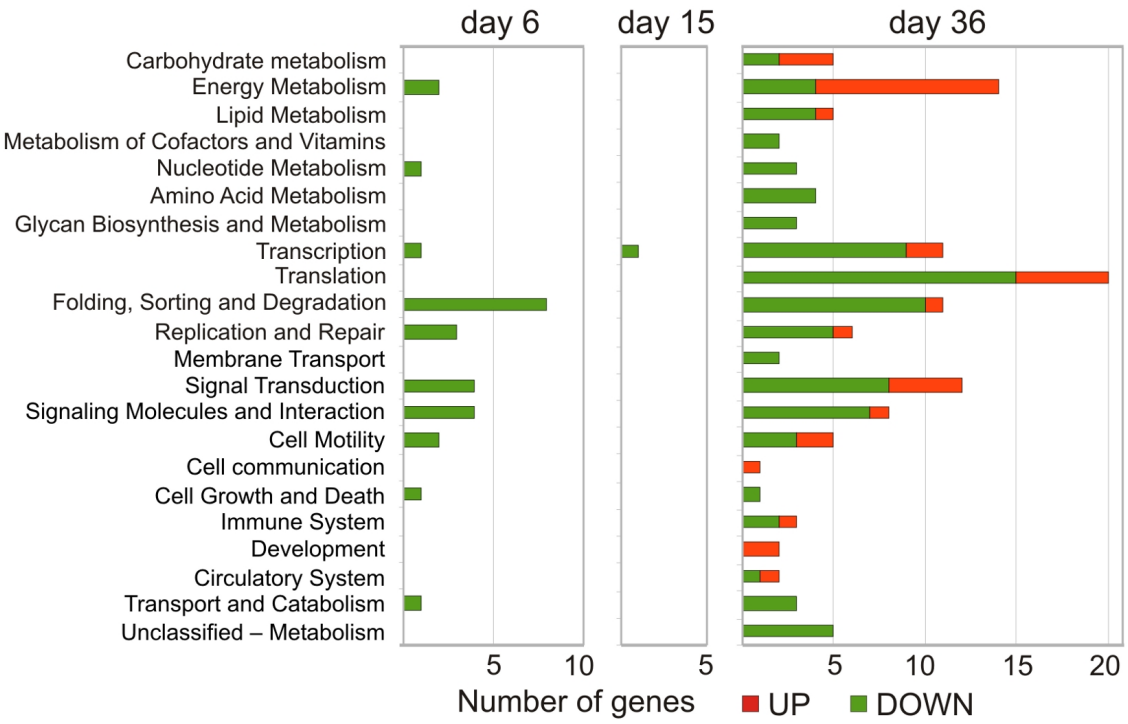

Figure 3.3.: KEGG classification of *L. sigmodontis* genes, that are regulated in response to *Wolbachia* depletion at days 6, 15 and 36 of tetracycline treatment. Numbers of functionally annotated genes with q $\leq$0.05 and fold change $\geq$2 are shown. Red represents up-regulation and green down-regulation.

3.3.1. KEGG analysis

KEGG analysis (Kanehisa and Goto, 2000) classified the differentially regulated genes into functional groups and highlighted pathways that were most affected by the depletion of *Wolbachia*. The regulated oligos included hypothetical and unknown genes and also genes that cannot be assigned a gene ontology term by KEGG. Figure 3.3 comprises the classification of 40 % of the significantly regulated oligos. Detailed information of all regulated genes can be found in the appendix in Tables B.1, B.2 and B.3. Hypothetical and unknown proteins made up over 30 % of the down-regulated and over 40 % of the up-regulated genes at day 36 of Tet treatment, with q $\leq$ 0.05 and fold change $\geq$2.

From the KEGG analysis and genome annotation, genes involved in genetic information processing including translation, transcription and genes coding for proteins involved in folding/sorting and degradation were predominantly down-regulated at day 36 of Tet treatment. Translation proteins included the 60S ribosomal proteins L3, (Bm1_13895), L12 (Bm1_07030), L18a (Bm1_23030), L21 (Bm1_47445), L27 (Bm1_28975), 40S ribosomal protein S7 (Bm1_09900) and 50S ribosomal protein L21 (Bm1_46405). Besides these ribosomal proteins, different translation fac-

tors were down-regulated including EF-1 guanine nucleotide exchange domain containing protein (Bm1_27955), translation elongation factor eEF-2 homolog eft-1 (Bm1_44395), initiation factor 2-associated protein (Bm1_37925), WD40 associated region in TFIID subunit family protein (Bm1_47705) and eukaryotic translation initiation factor 4E type 3 (Bm1_32915). Down-regulated genes involved in protein degradation were also identified: Hsp70 (Bm1_43675) and proteasome A-type and B-type family proteins (Bm1_55200 and Bm1_30555).

Down-regulated genes that play a role in transcription included transcription factor-like GATA zinc finger family protein (Bm1_44270) and other zinc finger family proteins (Bm1_41325, Bm1_55855, Bm1_43055, Bm1_24215), which often play a role in transcription regulation, but can also have other regulatory functions that involve binding to RNA and proteins. Different genes involved in splicing were down-regulated at day 36, such as U2 small nuclear ribonucleoprotein A (Bm1_15860), THO complex subunit 3 (Bm1_12545) and putative splicing factor SF2 (Bm1_45785). In contrast, other genes involved in splicing were up-regulated, like a protein similar to RNA helicase p68 (DDX5; BMC06625), and ATP-dependent RNA helicase DDX5/DBP2 (Bm1_52675).

Several genes belonging to the cytoskeleton were differentially expressed. Up-regulated oligos at day 36 of Tet treatment included genes belonging to thin filaments of musculature: troponin C (Bm1_48810), troponin T (Bm1_55000) and tropomyosin (Bm1_01235). Furthermore, proteins that bind to proteins of the cytoskeleton and that are involved in their regulation were seen to be differentially expressed: a calponin homolog (Bm1_49080) and gelsolin (Bm1_33155) were up-regulated at day 36, whereas a coronin gene (Bm1_03260) and the gex interacting proteins 4 (Bm1_41495) and 10 (Bm1_31280) were down-regulated at day 36. At day 6 of Tet treatment the actin-binding genes profilin family protein (Bm1_21620) and actin-depolymerization factor 1 (Bm1_22990) were found to be down-regulated. Several cuticle collagens were up-regulated at day 36 (Bm1_36555, Bm1_17485, Bm1_13245, Bm1_27595). At day 15 of Tet treatment one collagen gene was up-regulated (Bm1_01465) and another down-regulated (Bm1_17480).

Genes belonging to energy metabolism displayed the most noticeable group of up-regulated genes. This finding is described in detail in Chapter 3.5.

3.4. Validation of a sub-set of regulated genes by qPCR

QPCR was used to confirm the up- and down-regulation trends of a subset of genes found to be differentially expressed in the microarray. 20 genes that had either multiple regulated oligos, a strong fold change, or were interesting in regard to filaria-*Wolbachia* symbiosis were chosen. This selection included genes from different functional classes: structural proteins (Troponin T and C), proteins of metabolic pathways (Succinyl-CoA ligase beta chain, Acetyl-CoA hydrolase/transferase, Lipoic acid synthase, DNA/panthonate metabolism flavoprotein, Diphosphomevalonate decarboxylase, Aromatic aminoacid hydrolase), a transcription factor (Med7 transcription factor), secreted proteins (Mif1, Juv-p120) and proteins involved in transport and trafficking (Globin family protein, ABC transporter, Rab5 GDP/GTP exchange factor). Two hypothetical genes were also included (Bm1_30045, Bm1_04280), since they showed a strong up-regulation in the microarray. From this list, 60 % of the differentially expressed genes were confirmed by qPCR. Expression changes of the up-regulated genes agreed well with the microarray results, whereas only a few of the selected down-regulated genes were validated (Table 3.3).

Table 3.3.: qPCR results to validate expression changes in *L. sigmodontis* after *Wolbachia* depletion

BLAST Match	*B. malayi* locus	Annotation ID	Time	Fold change[a] Microarray	qPCR[b]
Up-regulated genes					
Globin family protein	Bm1_50430	14992.m10859	d36	4.8 (1)[c]	**2.1**[d]
Troponin C	Bm1_48810	TC2796, BMW00285.523, BMC12124, BMW01217.101	d36	2.4 (4)	**1.8**
Troponin T[e]	Bm1_55000	BMC00075	d6	2.4 (1)	**1.3**
		BMC00075, TC2790	d36	2.4 (2)	**1.7**
Mif1	Bm1_28435	BMC00238	d36	2.2 (1)	**1.3**
Hypothetical protein[e]	Bm1_30045	BMC00075	d15	2.7 (1)	**1.3**
		BMC02980,14950.m01825, WB-contig_1411	d36	8.1 (3)	**2.0**
Hypothetical protein	Bm1_04280	12962.m00049, TC3117, WB-contig_256	d36	6.9 (3)	**1.8**
Succinyl-CoA ligase beta chain	Bm1_00840	12498.m00044	d36	4.6 (1)	0.89
Acetyl-CoA hydrolase/transferase	Bm1_42975	14975.m04536	d36	2.1 (1)	**1.4**
ABC transporter	Bm1_30435	14952.m01388	d36	2.0 (1)	0.95
RNA binding protein	Bm1_37780	BMC00185, 14972.m07250	d36	3.0 (2)	**2.0**
Similar to c-met receptor	Bm1_37575	BMC00090	d36	2.1 (1)	1.1
Down-regulated genes					
Med7 transcription factor	Bm1_23975	TC3295, TC3326	d36	0.32 (2)	1
Retinoblastoma binding protein	Bm1_15930	BMC08875, 14224.m00309	d6	0.34 (2)	**0.52**
Secretory protein Juv-p120	Bm1_19955/ Bm1_00865	14478.m00108/14478.m00109	d36	0.43 (2)	**0.53**
Lipoic acid synthase	Bm1_23910	14696.m00211	d36	0.44 (1)	0.94
DNA/panthotenate metabolism flavoprotein	Bm1_45070	BMC03590	d36	0.48 (1)	0.9
Diphosphomevalonate decarboxylase	Bm1_42945	14975.m04530	d36	0.28 (1)	0.84
Aromatic aminoacid hydrolase	Bm1_46865	14981.m02410	d36	0.13 (1)	1.4
60S ribosomal protein L3	Bm1_13895	14039.m00115, WB-contig_530	d36	0.38 (2)	1.3
Rab5 GDP/GTP exchange factor	Bm1_29925	14950.m01801	d36	0.31 (1)	0.88

[a] Fold change: treated versus untreated.
[b] Median of six samples containing three worms.
[c] Indicates the number of oligonucleotides on the microarray that were regulated.
[d] Bold: validated expression changes.
[e] Genes were regulated at two time points in microarray.

3.4.1. Fluorescence intensities among up- and down-regulated genes

As we observed a clear difference of expression validation between up- and down-regulated genes (Table 3.3) we further analysed the microarray data for possible reasons leading to this discrepancy. A comparison of the microarray fluorescence intensities of the spots corresponding to the genes selected for qPCR validation shows significantly higher fluorescence signals for the genes which were validated in qPCR (average of 5181) than those which were not validated (average of 832) ($p = 0.0051$, Mann-Whitney test) (Table 3.4).

Table 3.4.: Microarray fluorescence intensities (FI) of genes measured in qPCR

BLAST match	***B. malayi* locus**	**Time**	**Mean FI**[a]
Up-regulated genes			
Globin family protein	Bm1_50430	d36	**355**[b]
Troponin C	Bm1_48810	d36	**4552**
Troponin T	Bm1_55000	d6	**3486**
		d36	**4552**
Mif1	Bm1_28435	d36	**2394**
Hypothetical protein	Bm1_30045	d15	**4602**
		d36	**3686**
Hypothetical protein	Bm1_04280	d36	**2709**
Succinyl-CoA ligase beta chain	Bm1_00840	d36	402
Acetyl-CoA hydrolase/transferase	Bm1_42975	d36	**628**
ABC transporter	Bm1_30435	d36	1634
RNA binding protein	Bm1_37780	d36	**31744**
Similar to c-met receptor	Bm1_37575	d36	2881
Down-regulated genes			
Med7 transcription factor	Bm1_23975	d36	606
Retinoblastoma binding protein	Bm1_15930	d6	**816**
Secretory protein Juv-p120	Bm1_19955/ Bm1_00865	d36	**2645**
Lipoic acid synthase	Bm1_23910	d36	574
DNA/panthotenate metabolism flavoprotein	Bm1_45070	d36	316
Diphosphomevalonate decarboxylase	Bm1_42945	d36	387
Aromatic aminoacid hydrolase	Bm1_46865	d36	410
60S ribosomal protein L3	Bm1_13895	d36	686
Rab5 GDP/GTP exchange factor	Bm1_29925	d36	428

[a] Mean fluorescence intensities of all spots of the gene on the microarray corresponding to the channel with the higher signal (for down-regulated genes: control, for up-regulated genes: Tet treated).

[b] Bold: Fluorescence intensities of genes with validated expression changes in qPCR, compare Table 3.3.

3.4.2. Expression patterns of validated regulated genes

In this section selected genes with a validated expression change and their expression patterns on days 6, 15 and 36 of Tet treatment are described in more detail.

Globin family protein Globins are heme and oxygen binding proteins which are widely distributed amongst nematode species (Hoogewijs et al., 2008). One of these globin family proteins was up-regulated in *L. sigmodontis* after Tet treatment. In our microarray experiment one oligo (BMX8086) corresponding to the globin Bm1_50430 was 4.8-fold up-regulated and qPCR analysis for 3 time points of Tet treatment revealed that expression of this gene gradually increased with duration of Tet treatment and was 2.1-fold up-regulated at day 36 ($p = 0.0022$) (Figure 3.5 A). The *C. elegans* homolog of this up-regulated globin is the protein ZK637.13, the canonical globin 1 ($E = 3e\text{-}37$). The crystal structure of the *C. elegans* Glb-1 demonstrates the characteristic 3 over 3 alpha helical sandwich structure and the incorporated heme molecules (Figure 3.4).

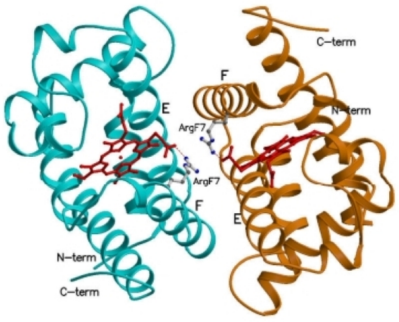

Figure 3.4.: The up-regulated *B. malayi* globin family protein Bm1_50430 is homologous to the *C. elegans* globin 1 gene (ZK637.13), one out of a total of 33 *C. elegans* globin genes. The *C. elegans* Glb-1 molecule consists of two subunits, interacting mainly through the E and F helices (orange and cyan). Heme is shown in red. Figure is taken from Geuens et al. (2010).

RNA binding protein Two oligonucleotides corresponding to the *B. malayi* RNA binding protein Bm1_37780 were 3-fold up-regulated at day 36 of Tet treatment (Table 3.3). This up-regulation has been confirmed using qPCR with *L. sigmodontis* specific primers. The observed fold change at day 36 was 2 ($p = 0.0043$) with the expression already starting to increase at day 6 of treatment (Figure 3.5 B). This gene is one of 15 *B. malayi* RNA binding proteins with an RNA recognition motif (RRM) domain. A BlastP search using the Bm1_37780 aminoacid sequence revealed

the homology to the *Ascaris suum* Cleavage stimulation factor subunit 2 (CstF-2) tau variant (E-value = 7e-43).

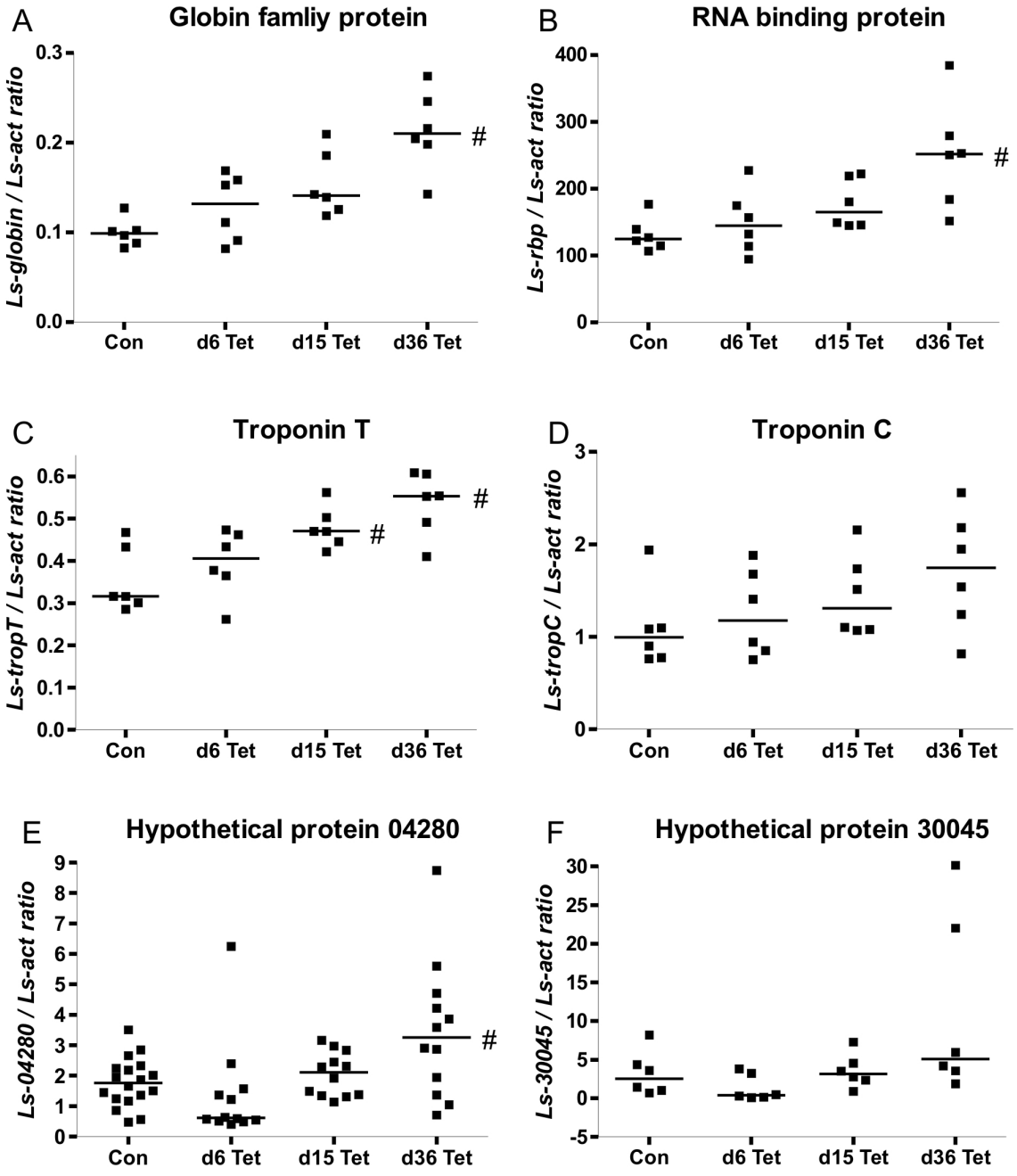

Figure 3.5.: Up-regulated genes after *Wolbachia* depletion. PCR reactions were performed in triplicate. Copy numbers were normalised to cDNA copy numbers of filarial actin from the same sample. Each square represents gene expression from 3 female worms. Lines are median values, # denotes a significant difference of gene expression compared to the control, as determined with Mann-Whitney-U test ($p \leq 0.05$).

Troponin T and C Our microarray experiment revealed subunits of the troponin complex up-regulated after Tet treatment. Troponin is a globular molecule, consisting of the three subunits T, C and I. Troponin T (Bm1_55000) was significantly up-regulated at day 6 (1 oligo) of Tet treatment as evidenced by microarray analysis. This gene was also up-regulated at day 36 (2 oligos) (Table 3.3). QPCR analysis confirmed that expression of Troponin T increased from day 6 to 36 of Tet treatment, with a significant 1.5-fold ($p = 0.0152$) up-regulation at day 15 and 1.7-fold ($p = 0.0087$) up-regulation at day 36 (Figure 3.5 C). Consistent with this result, another subunit of the troponin complex showed increased expression after Tet treatment of *L. sigmodontis*: 4 oligos corresponding to the *B. malayi* troponin C gene (Bm1_48810) were $\sim$2.5-fold up-regulated at day 36 in microarray and 1.7-fold in qPCR analysis, although it was not significant ($p = 0.0649$). Similar to the expression pattern observed for troponin T, expression of troponin C increased with duration of Tet treatment (Figure 3.5 D). The best *C. elegans* blastx match to the *L. sigmodontis* mRNA sequence is the troponin C *pat-10* gene (E-value = 6e-80, 93 % similarity).

Hypothetical proteins 30045 and 04280 Two hypothetical genes were chosen for further validation of the differential expression detected by microarray analysis. Here, multiple oligos corresponding to the genes Bm1_30045 and Bm1_04280 showed that expression increased 8.1 and 6.9-fold, respectively (Table 3.3). An up-regulation of the genes after 36 day of Tet treatment compared to untreated control worms could be confirmed by qPCR, although the expression change was much lower. Expression of Bm1_04280 significantly increased 1.8-fold ($p = 0.0211$) and expression of Bm1_30045 increased 2-fold, although not significantly. The hypothetical protein (Bm1_04280) was identified by BLAST as small nuclear RNA U2-1 (91 % similarity to *A. suum* snRNA U2-1, E = 9e-58).

Juvenile protein p120 (Juv-p120) The protein Juv-p120 is the major excretory-secretory product of juvenile *L. sigmodontis*. In our microarray experiment we found two oligos corresponding to *juv-p120* 2.3-fold down-regulated at day 36 of *Wolbachia* depletion (Table 3.3). This result was confirmed by qPCR analysis with a decrease of 1.9-fold ($p = 0.0411$) after Tet treatment compared to the untreated control. As in the microarray analysis, down-regulation of *juv-p120* was not observed at days 6 and 15 of treatment (Figure 3.6 A).

Retinoblastoma binding protein Two oligos corresponding to the retinoblastoma-binding protein Bm1_15930 were 2.9-fold down-regulated in *L. sigmodontis* at day 6 of Tet treatment, as evidenced by our microarray analysis (Table 3.3). QPCR analysis verified the decrease in expression (1.9-fold) at day 6 of treatment, although it was not significant ($p = 0.0649$). Same as seen in the microarray analysis, expression levels at day 15 and 36 of Tet treatment were the same as in untreated worms (Figure 3.6 B). The *L. sigmodontis* sequence used for qPCR also has a great homology to a second retinoblastoma binding protein (Bm1_57630) encoded by *B. malayi*. One oligo corresponding to this genes was also down-regulated at day 6 of treatment as shown by microarray analysis (Table B.1). Blast searches revealed homology to the highly related mammalian retinoblastoma binding proteins Rbbp4 and Rbbp7, components of a histone deacetylase complex (Nicolas et al., 2000). However, a blastx search with the Ls sequence used for qPCR identified the best homology to *Ascaris suum* Rbbp4 (E = 3e-100, 94 % identity) and the Rbbp4 of several mammalian species (E $\leq$ 3e-76).

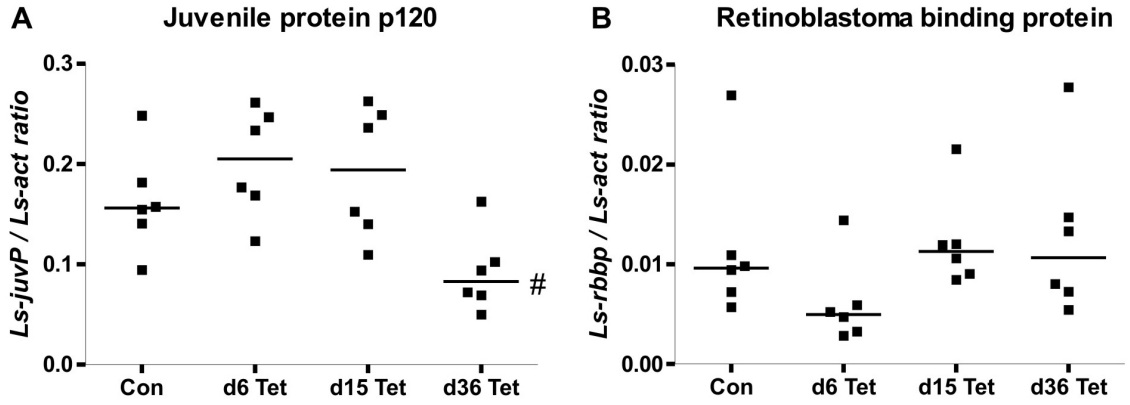

Figure 3.6.: Down-regulated genes after *Wolbachia* depletion. PCR reactions were performed in triplicate. Copy numbers were normalised to cDNA copy numbers of filarial actin from the same sample. Each square represents gene expression from 3 female worms. Lines are median values, # denotes a significant difference of gene expression compared to the control, as determined with Mann-Whitney-U test ($p \leq 0.05$).

3.5. Expression of mitochondrial encoded respiratory chain enzymes

3.5.1. Expression of mitochondrial encoded genes in *L. sigmodontis* after *Wolbachia* depletion

Evident from the microarray results was the fact that mitochondrial encoded genes of the respiratory chain were up-regulated after *Wolbachia* depletion. The *Brugia* mitochondrial genome encodes 12 subunits of the respiratory chain, which belong to the complexes NADH dehydrogenase, cytochrome bc1, cytochrome c oxidase and ATP synthase (Figure 3.7). The microarray analysis resulted in 24 oligos corresponding to 9 mitochondrial encoded subunits of the respiratory chain with a significant up-regulation and a minimum 2-fold change in expression. When oligos with < 2-fold significant change were included, 28 oligos corresponding to 10 of the 12 mitochondrial encoded subunits were found to be up-regulated (Table 3.5).

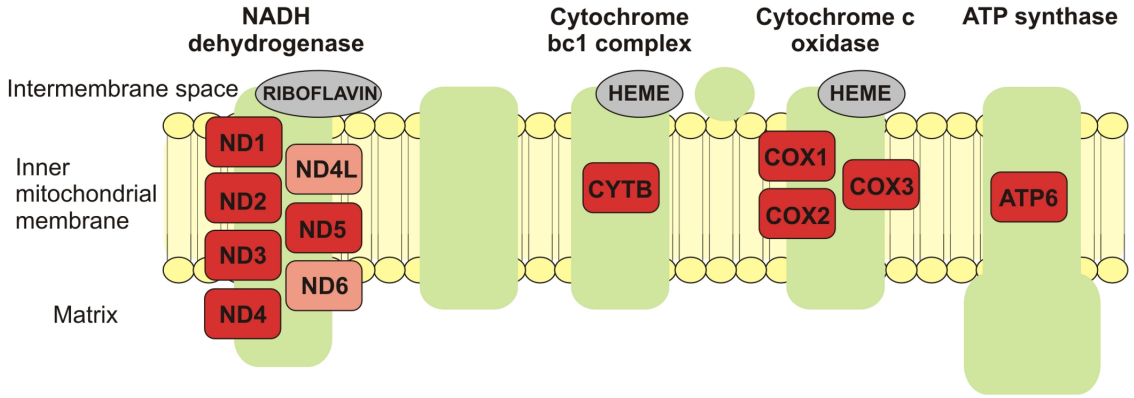

Figure 3.7.: Mitochondrial encoded subunits of the respiratory chain of *Brugia malayi*. Shown are the 12 mitochondrial encoded subunits (red) belonging to 4 of the respiratory chain complexes. Except subunits ND4L and ND6 (light red) all subunits were up-regulated at day 36 of tetracycline treatment in *L. sigmodontis*. Cofactors essential in the respiratory chain complexes are shown in grey.

To validate the differential expression seen in the microarray, qPCR was performed for the respiratory chain subunits cytochrome c oxidase subunit 1 and 2 (cox1 and cox2), cytochrome b (cytB) and NADH dehydrogenase subunit 4 and 5 (ND4 and ND5). The qPCR confirmed an increase in expression at day 36 for these 5 genes. Expression of Ls-cox1 increased 1.6-fold ($p = 0.0008$), Ls-cox2 1.7-fold ($p = 0.001$), Ls-cytB 1.8-fold ($p = 0.0029$), Ls-ND4 1.9-fold ($p = 0.0025$) and Ls-ND5 1.8-fold

(p = 0.0293) compared to expression in untreated control worms (Figure 3.8). As in the microarray, change of expression on days 6 and 15 of Tet treatment was not detected by qPCR.

Table 3.5.: Mitochondrial encoded subunits of the respiratory chain complexes up-regulated at day 36 of tetracycline treatment as evident from microarray analysis

			Fold change microarray[c]	
Annotation[a]	**Annotation ID**	**Oligo ID**[b]	**Oligo**	**Median**[d]
Cytochrome c oxidase subunit 1	TC2778	BMX12792	3,5	2,7
	TC7739	BMX10990	2,89	
	WB-contig_182	BMX12477	2,72	
	BMW00283.860	BMX11370	2,7	
	BMC12170	bm.01757	2,7	
	BMC06165	bm.03325	2,47	
	TC2780	BMX12794	2,32	
	BMC12111	bm.03436	2,22	
Cytochrome c oxidase subunit 2	BMC12116	bm.03438	2,82	2,61
	BMC00030	bm.03171	2,81	
	BMC00071	bm.03174	2,4	
	BMC06256	bm.03082	2,31	
Cytochrome c oxidase subunit 3	BMC01393	bm.00380	27,36	2,37
	BMC00359	bm.03045	3,05	
	BMC12260	bm.03485	1,68	
	BMC00256	bm.03201	1,64	
Cytochrome b	WB-contig_187	BMX12481	2,93	2,22
	BMC11632	bm.03368	2,22	
	WB-contig_207	BMX12492	2	
NADH dehydrogenase subunit 1	TC2803	BMX12812	2,36	2,36
NADH dehydrogenase subunit 2	BMC00485	bm.03545	2,54	2,43
	WB-contig_1474	BMX12282	2,43	
	BMW01358.408	BMX11795	2,2	
NADH dehydrogenase subunit 3	TC3244	BMX13241	2,64	2,24
	BMW00166.284	BMX11305	1,83	
NADH dehydrogenase subunit 4	WB-contig_383	BMX12609	1,94	1,94
NADH dehydrogenase subunit 5	TC3096	BMX13096	2,15	2,15
ATPase subunit 6	TC2809	BMX12816	2,51	2,51

[a] *Brugia malayi* mitochondrion (GenBank Accession No. AF538716).

[b] Significantly regulated oligonucleotides with $q \leq 0.05$.

[c] Treated versus untreated.

[d] For subunits represented by multiple oligos, the median fold-change was calculated.

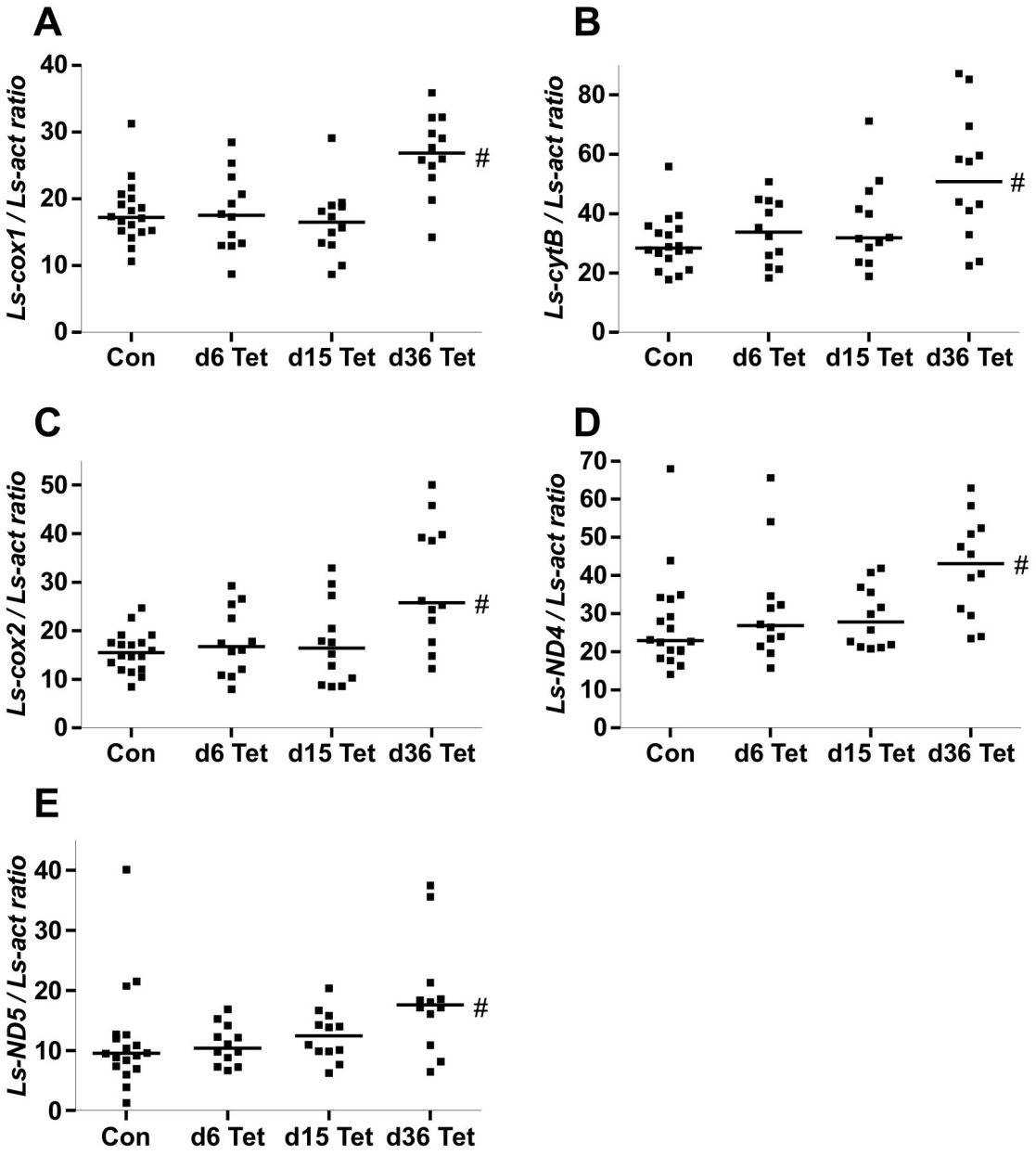

Figure 3.8.: Expression of mitochondrial encoded subunits of the respiratory chain of *L. sigmodontis* increased at day 36 of Tet treatment. To confirm up-regulation of respiratory chain genes qPCR for cytochrome c oxidase subunit 1 (A), cytochrome c oxidase subunit 2 (B), cytochrome b (C), NADH-dehydrogenase subunit 4 (D) and NADH-dehydrogenase subunit 5 (E) was performed for days 6, 15 and 36 of tetracycline treatment. PCR reactions were performed in triplicate. Copy numbers were normalised to cDNA copy numbers of filarial actin from the same sample. Each square represents gene expression from 3 female worms. Lines are median values, # denotes a significant difference of gene expression compared to the control, as determined with Mann-Whitney-U test ($p \leq 0.05$). Graphs are representative of 2 experiments.

3.5.2. Expression of mitochondrial encoded genes in *A. viteae* after Tet treatment

To exclude a direct effect of tetracycline on the worms as the cause of up-regulation of respiratory chain genes, experiments with the *Wolbachia*-free filaria *A. viteae* were performed. Transcript levels of cytochrome c oxidase subunit 1 and cytochrome b from 6 weeks orally Tet treated *A. viteae* were not different to transcript levels of untreated control worms (Figure 3.9). Therefore, under these conditions, tetracycline had no measurable effect directly on the mitochondria.

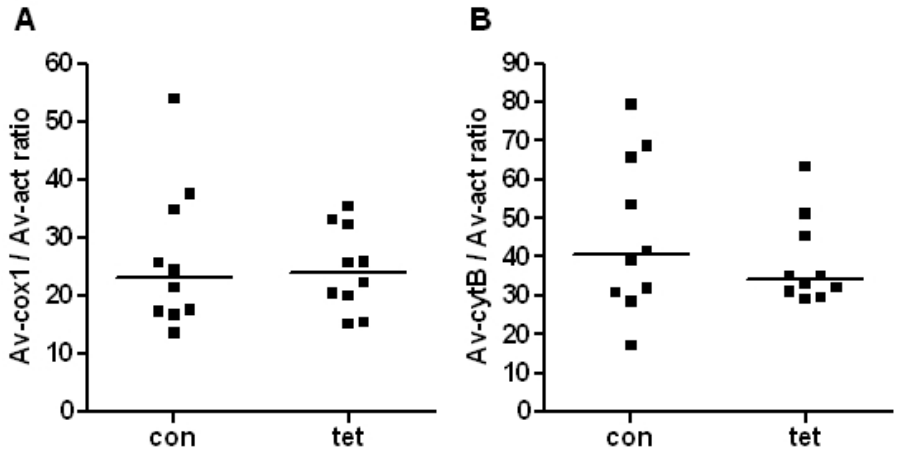

Figure 3.9.: Expression of mitochondrial-encoded subunits of the respiratory chain of *A. viteae* is not altered after Tet treatment. QPCR was performed with cDNA for cytochrome c oxidase subunit 1 (A) and cytochrome b (B) from untreated and 6 weeks orally Tet treated worms. PCR reactions were performed in triplicate. Copy numbers were normalised to copy numbers of *A. viteae* actin from the same sample. Each square represents gene expression from 2 female worms. Lines are median values. Graphs are representative of 2 experiments.

3.6. Mitochondrial DNA (mtDNA) content after Tet treatment in *L. sigmodontis* and *A. viteae*

Mitochondria are dynamic organelles and their number per cell can change for example depending on the energy demands of the cell. To ascertain whether Tet treatment or *Wolbachia* depletion has an impact on mtDNA content we measured the levels of DNA of mitochondrial encoded genes from Tet treated worms and compared them to mtDNA levels of untreated worms. Genomic DNA of the nuclear encoded gene actin was measured to control for the amount of DNA extracted from the worms.

MtDNA levels were significantly elevated in *L. sigmodontis* at day 15 ($p = 0.0236$ (cox1), $p = 0.0013$ (cytB)) and day 36 ($p = 0.0168$ (cox1), $p = 0.0063$ (cytB)) of Tet treatment. The gDNA amount of the nuclear encoded gene actin also increased at day 15 and 36 of Tet treatment, although this increase was not significant. However, the pattern of mt and nuclear gDNA levels during Tet treatment in *L. sigmodontis* are comparable. MtDNA content of Tet treated *A. viteae* was measured to control for possible changes in mitochondrial copy numbers due to a direct effect of tetracycline. MtDNA levels were not elevated after 6 weeks of oral Tet treatment in *A. viteae*, nevertheless actin copy numbers, which were used to control for the total amount of DNA extracted from the worms, showed a 5-fold decrease after Tet treatment ($p = 0.0089$).

One possible reason for the lower actin gDNA copies seen in *A. viteae* worms after Tet treatment could be an impairment in embryogenesis due to Tet treatment. Fewer embryos and microfilariae in the worms could lead to a decrease of actin copy numbers. In a further experiment the microfilariae numbers in blood of *A. viteae*-infected jirds were counted after 6 weeks of oral Tet treatment and compared to untreated *A. viteae*-infected jirds. Additionally, we examined whether uteri from worms that were isolated from Tet treated and untreated jirds were filled with embryonic stages and microfilariae. No decrease of microfilariae numbers in blood was detected after Tet treatment (Figure 3.12). All worms, both the untreated and Tet treated worms, had uteri filled with embryos.

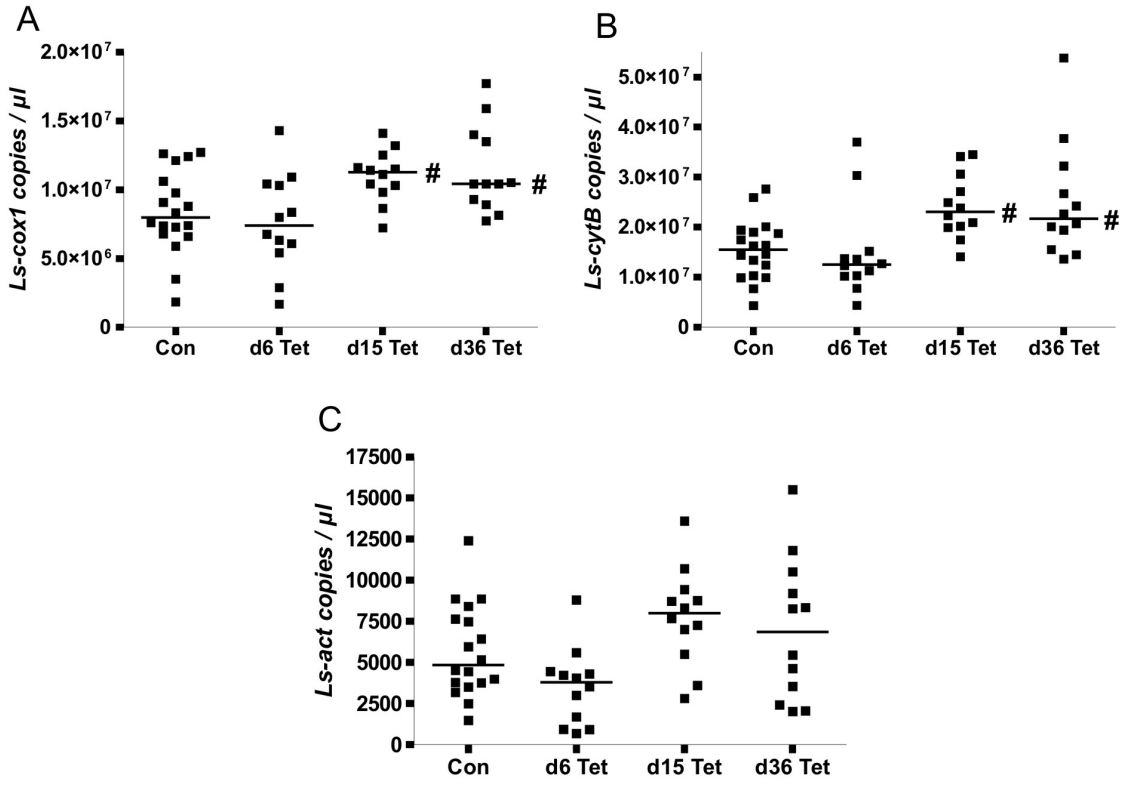

Figure 3.10.: MtDNA content during Tet treatment of *L. sigmodontis*. QPCR was performed with mitochondrial DNA of cytochrome c oxidase subunit 1 (A) and cytochrome b (B) from untreated and 6, 15 and 36 days Tet treated *L. sigmodontis*. Copy numbers were compared to gDNA copies of the nuclear encoded actin gene (C). PCR reactions were performed in triplicate. Each square represents gene expression from 3 female worms. Lines are median values, # denotes a significant difference of gene expression compared to the control, as determined with Mann-Whitney-U test ($p \leq 0.05$).

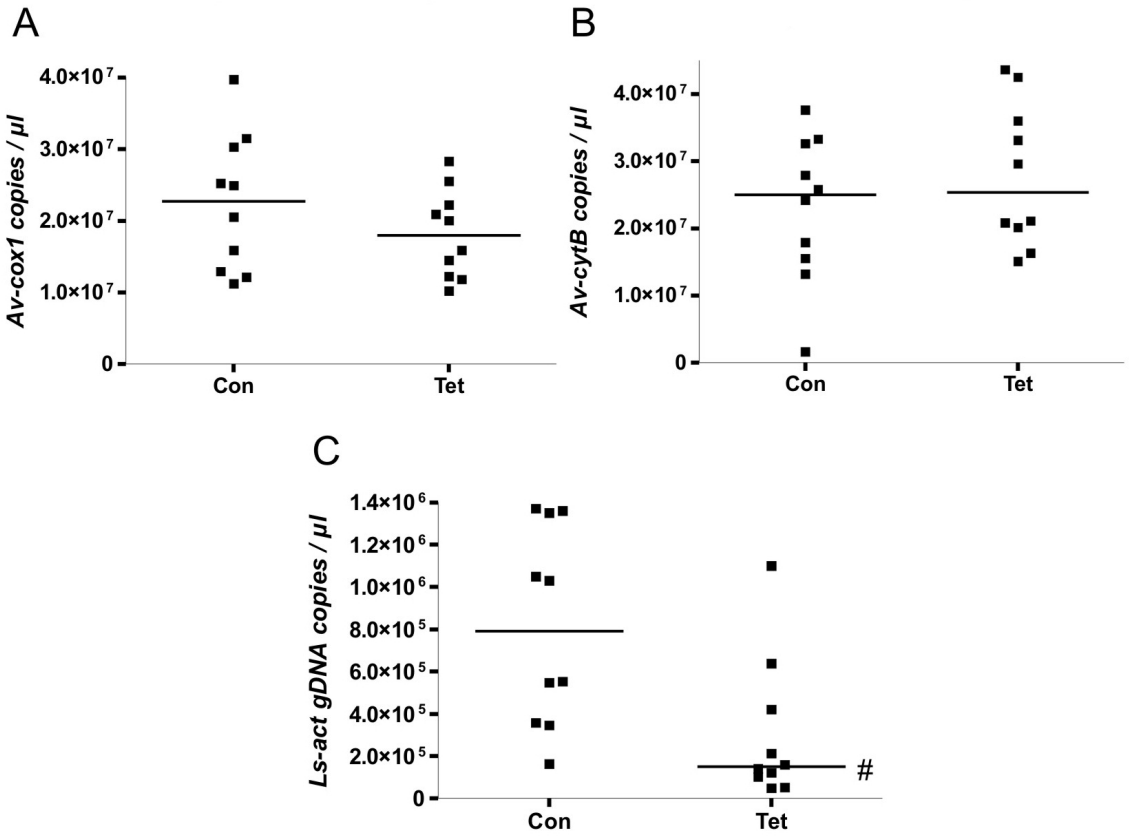

Figure 3.11.: MtDNA content during Tet treatment of *A. viteae*. QPCR was performed with mtDNA of cytochrome c oxidase subunit 1 (A) and cytochrome b (B) from untreated and 6 weeks orally Tet treated *A. viteae*. Copy numbers were compared to gDNA copies of the nuclear encoded actin gene (C). PCR reactions were performed in triplicate. Each square represents gene expression from 2 female worms. Lines are median values, # denotes a significant difference of gene expression compared to the control, as determined with Mann-Whitney-U test ($p \leq 0.05$).

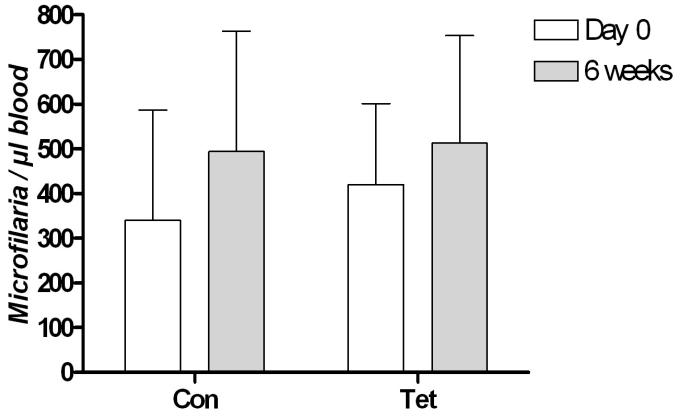

Figure 3.12.: Numbers of microfilariae in blood of *A. viteae*-infected Tet treated jirds. Microfilariae were counted before and after 6 weeks orally Tet treatment and compared to microfilariae numbers in untreated jirds. Columns represent mean and standard deviation of microfilariae numbers from 4 - 6 jirds.

3.7. Inhibition of heme biosynthesis of *Wolbachia* from *L. sigmodontis*

3.7.1. Survival of *L. sigmodontis ex vivo* is enhanced by the presence of feeder cells

To perform experiments with *L. sigmodontis ex vivo* we first established appropriate culture conditions which allowed us to cultivate the worms over a longer period of time. Several publications report the positive effects of feeder cells on filaria cultured *ex vivo* (Townson et al., 1986; Falcone et al., 1995; Townson et al., 2006) Notably, LLCMK2 feeder cells supported the survival of *Onchocerca gutturosa ex vivo*. In order to test the suitability of these cells for cultivation of *L. sigmodontis* we compared the survival of *L. sigmodontis* in the presence of the LLCMK2 feeder cells and without cells, respectively. The motility of the worms was assessed as measurement for viability. The feeder cells clearly improved the survival of *L. sigmodontis* ($p = 0.0392$)(Figure 3.13 A). The median survival of female worms in the presence of cells was 58 days (range 29 - 64) and 26 days without feeder cells (range 8 - 33). The initial drop in motility of *L. sigmodontis* cultured in the presence of feeder cells results from a few worms (6/24) which were apparently damaged during removal from the pleural cavity and separation by sex. Therefore, in further experiments worms were cultured 1-2 days before starting drug treatment in order to sort out unhealthy or damaged worms.

With the conditions established in this experiment *L. sigmodontis* could be cultured for a minimum of 14 days with no obvious impairment of the worms and are therefore suitable for *ex vivo* experiments and testing of long term effects of drugs.

3.7.2. Inhibition of *Wolbachia* ALAD effects the survival and microfilariae release of *L. sigmodontis*

Our previous experiments reported the up-regulation of heme proteins after depleting *Wolbachia* bacteria from *L. sigmodontis*. We now aimed to demonstrate the dependency of filaria on the cofactor heme, which might be delivered by *Wolbachia* to the worms. *L. sigmodontis* were cultured in the presence of succinylacetone (SA), a known inhibitor of ALAD, the second enzyme of the heme biosynthesis pathway (Figure 4.3). Any effects of the drug on the worms were assessed by evaluating the motility of the worms and counting the microfilariae released into the medium.

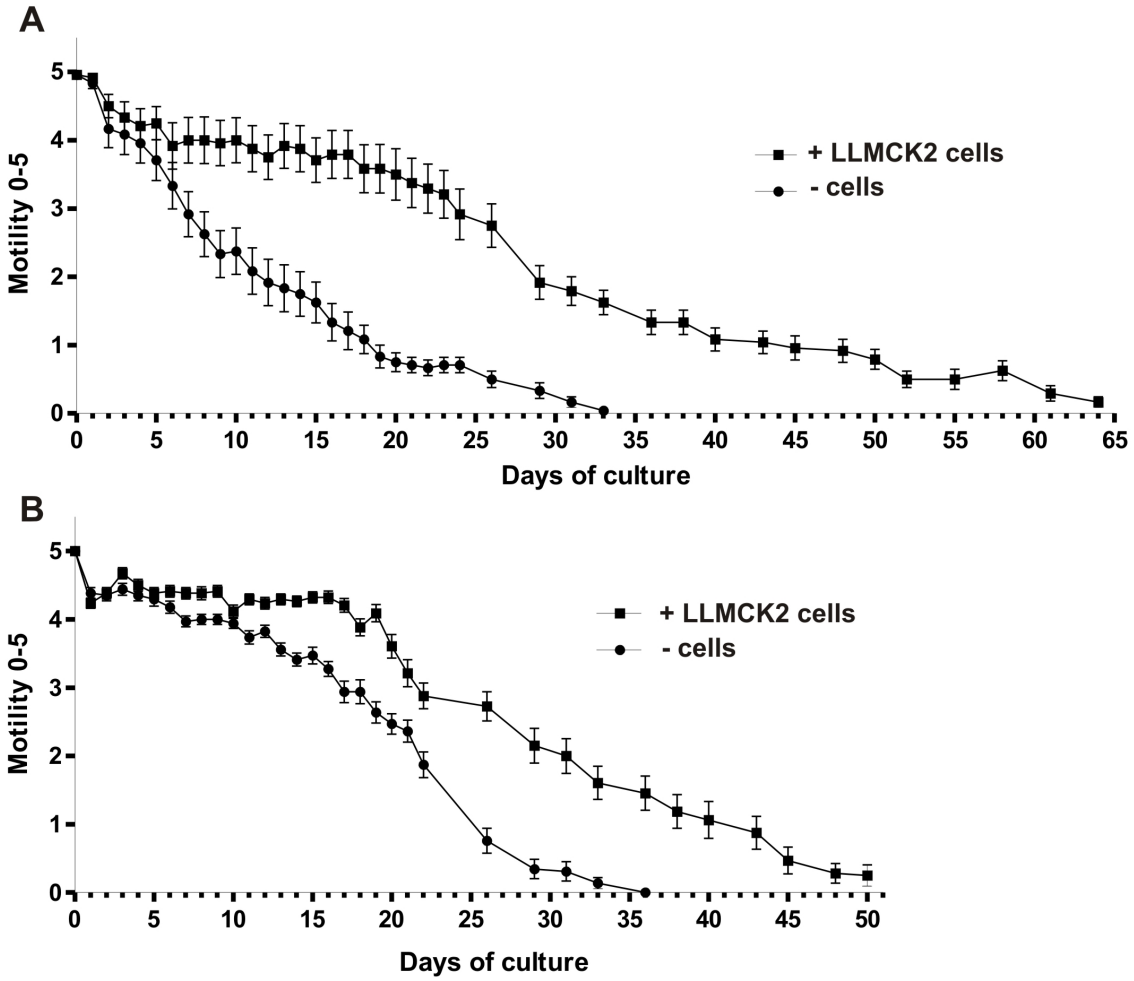

Figure 3.13.: Survival of *L. sigmodontis ex vivo*. *L. sigmodontis* were obtained from a cotton rat with a patent infection. Single female worms were incubated in a cavity of a 6-well plate in 5 ml MEM + 10 % FCS + 1 % Penicillin/Streptomycin either on a feeder cell layer (LLCMK2 cells) or without feeder cells (A). Single male worms were cultivated in a cavity of a 24-well plate in 1.5 ml medium in the presence of or without feeder cells (B). Half of the medium was exchanged every 2 - 3 days and worms were transferred to new plates every 14 days. Motility of worms was assessed using a score from 0 - 5 with 0 = no motility and 5 = best motility (see description of scores in Table 2.6). Error bars represent SEM of 24 worms.

SA significantly effected the motility of the worms. An initial effect was seen at day 3 of treatment and motility gradually worsened until day 14. At this last time point, control worms were still actively moving and knotted (mean motility score 4.6) whereas SA treated worms were stretched and only slowly moving (mean motility score 1.9) (Figure 3.14 A). Additionally, microfilariae numbers of SA treated worms were significantly decreased from day 6 on compared to untreated control worms

(Figure 3.14 B). An impairment of microfilariae motility could already be seen at day 2 of SA treatment.

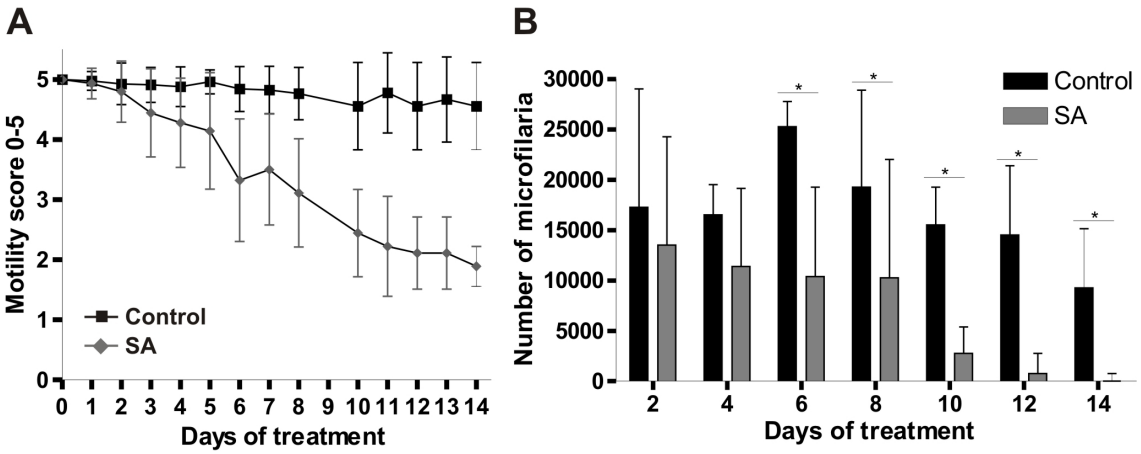

Figure 3.14.: Effect of succinylacetone (SA) on motility and microfilariae release of *L. sigmodontis ex vivo*. Single female worms were cultured on a LLCMK2 cell layer in 3 ml MEM + 10 % FCS + 1 % Penicillin/Streptomycin (control) or in medium containing 3 mM SA. Medium was completely exchanged every 2 days. Motility of worms was assessed daily using a score from 0 - 5 with 0 = no motility and 5 = best motility (see description of scores in Table 2.6) Data points present mean and standard deviation of a minimum of 9 worms (A). Microfilariae in the old medium were counted every two days at the day of medium exchange. Bars represent median and interquartile range of a minimum of 9 worms (B).

SA is a heme biosynthesis inhibitor which not only inhibits the *Wolbachia* ALAD but also the human enzyme. In contrast, the substance wALADin1 specifically inhibits the *Wolbachia* ALAD without interfering with the human enzyme. This substance has been identified by large scale screening of a substance library in order to identify anti-*Wolbachia* drugs (Christian Lentz, unpublished data). Using the *L. sigmodontis ex vivo* culture we assessed the impact of wALADin1 on worm viability. Using a much lower concentration of wALADin1 (500 µM and 1 mM) than of SA (3 mM) the effect of wALADin was much stronger. We observed a drastic effect on the worms at a time point early as 2 hours after start of treatment. The worms treated with wALADin1 showed a characteristic phenotype: they were moving slower but without being stretched, rather having a contracted or cramped appearance. The condition of these worms worsened during the course of treatment, however the contracted/cramped phenotype changed into a stretched appearance. The effect of wALADin1 was dose dependent. With a concentration of 1 mM no motility was observed from day 8 on, whereas worms treated with 500 µM wALADin1 were moving until day 14, the last time point of culture, although very weakly (motility score "1").

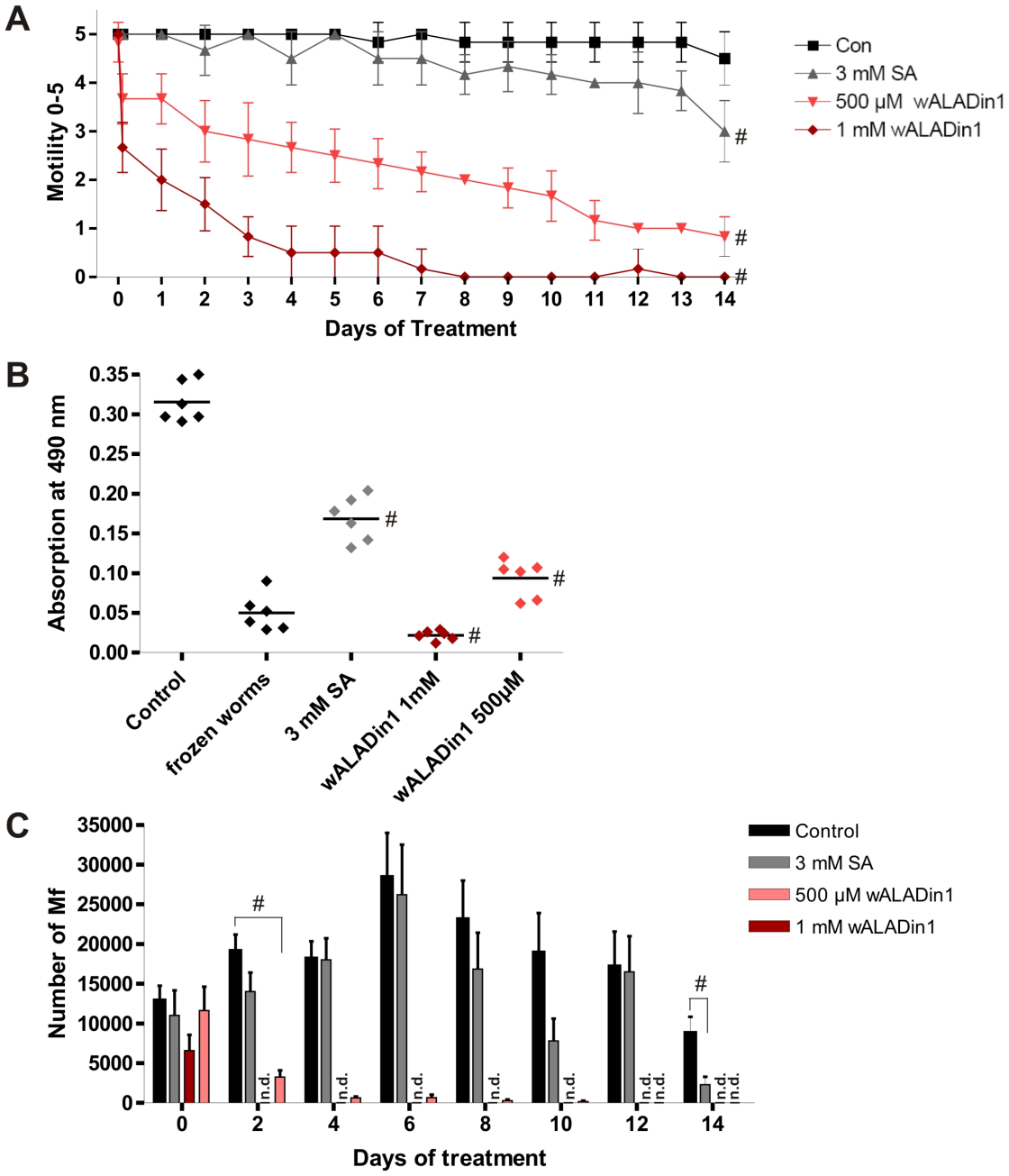

Figure 3.15.: Effect of the ALAD inhibitor wALADin1 on survival and microfilariae release of *L. sigmodontis ex vivo*. Single female worms were cultured on a LLCMK2 cell layer in 3 ml MEM + 10 % FCS + 1 % Penicillin/Streptomycin (control) or in medium containing 3 mM SA, 500 µM and 1 mM wALADin1. All media contained 1% DMSO. Medium was completely exchanged every 2 days. Motility of worms was assessed daily using a score from 0 - 5 with 0 = no motility and 5 = best motility (A). Enzymatic activity of worms was assessed at day 14 using the MTT viability assay (B). Live microfilariae released into the medium were counted every two days at the day of medium exchange, n.d. = not detected (C). Shown are means of 6 worms. # indicates a significant difference compared to the control, as determined with Mann-Whitney-U test ($p \leq 0.05$).

In this experiment the SA treated worms, which served as a positive control for the effect of heme inhibition on the worms, showed impaired motility late in the treatment, compared to what was seen in the previous experiment. At day 14 the worms were still moving with a motility "score 3" (Figure 3.15 A). One parameter that differed was the presence of 1 % DMSO in the medium, which served as solvent for all drugs in this experiment, whereas SA was directly dissolved in the medium in the experiment presented in Figure 3.14 A.

The effect of the drugs on motility of *L. sigmodontis* worms at days 0, 3, 9 and 14 (corresponding to the experiment shown in Figure 3.15 A) is also documented on videos 3 - 6 (for overview of videos see appendix Table A.1).

The biochemical evaluation of worm viability was carried out at day 14, the last time point of treatment. Viability was measured as the ability of the mitochondrial succinate dehydrogenase to reduce the yellow MTT into a blue formazan product. 500 µM wALADin1 reduced the viability of the worms to 30 % of control level, whereas worms treated with 1 mM wALADin1 had no enzyme activity. Viability of SA treated worms was reduced by 50 % compared to the control worms (Figure 3.15 B). These results matched well to the motility states of the worms at day 14.

wALADin1 strongly affected release of motile microfilariae by the worms. At a concentration of 1 mM no motile microfilariae were detectable beginning at day 2. Also, with the lower wALADin1 concentration motile microfilariae numbers were significantly reduced starting at day 2 ($p = 0.022$) and not detectable at day 12 (Figure 3.15 C).

3.7.3. Effects of heme biosynthesis inhibitors on the *Wolbachia*-free filaria *A. viteae*

To exclude unspecific effects of the heme biosynthesis inhibitors SA and wALADin1, we performed inhibition experiments with *A. viteae*. *A. viteae* does not contain *Wolbachia* and (except ferrochelatase) no heme biosynthesis enzymes have been found in the genome. Any effects of SA and wALADin1 on the worms are therefore considered unspecific effects.

We were able to cultivate *A. viteae* in MEM + 10 % FCS + 1% Penicillin / Streptomycin in the presence of LLCMK2 feeder cells for 14 days without an impairment in motility. The addition of 3 mM SA did not effect the motility of the worms (Figure 3.16 A) and viability of worms measured in the MTT assay was not decreased compared to the control worms (Figure 3.16 C). We therefore conclude, that the effects of SA we have seen on *L. sigmodontis* are due to the inhibition of the ALAD enzyme.

On the other hand, the motility of *A. viteae* was impaired by treatment with wALADin1. An initial strong effect could be observed directly after adding medium containing the drug. Worms treated with 1 mM wALADin1 did not recover during the course of treatment, which is also reflected by the results of the MTT viability assay (Figure 3.16 C). Nevertheless, the lower concentration of wALADin1 (500 µM) had an initial effect on the worms, starting at the first day of treatment, but condition of worms did not worsen during the course of treatment as it was seen with treatment of *L. sigmodontis*. Additionally, the MTT assay at day 14 did not detect an impairment of viability of worms treated with 500 µM wALADin (Figure 3.16 A and C). Hence, although there is an unspecific effect of wALADin on the worms, the effect of wALADin on *A. viteae* is a different than on *L. sigmodontis*. Movement of *A. viteae* worms during treatment with wALADin1 and SA at days 0, 3, 9 and 14 (corresponding to the experiment shown in Figure 3.16 A) is also documented on videos 7 - 11 (for overview of videos see appendix Table A.1).

The substrate of ALAD in the heme biosynthesis pathway is 5-aminolevulinic acid (5-ALA). Upon inhibition of the ALAD enzyme a accumulation of 5-ALA is possible and might be a cause for the effect on the worms we observed. We therefore aimed to evaluate the effect of 5-ALA on the worms motility and viability. 5 mM 5-ALA had a very strong initial effect observed directly after addition of the drug. The first addition of the drug at day 0 resulted in a complete paralysis of the worm (motility score "0"). However, this drastic effect was not long lasting and worms were moving with a motility score of 3.5 until day 14 (Figure 3.16 B). The MTT assay did not reveal an effect of 5-ALA on the enzyme activity, it even was above control level (Figure 3.16 C). The effect of 5-ALA on motility of *A. viteae* worms at days 0, 3 and 14 (corresponding to the experiment shown in Figure 3.16 B) is also documented on video 12 (for overview of videos see appendix Table A.1).

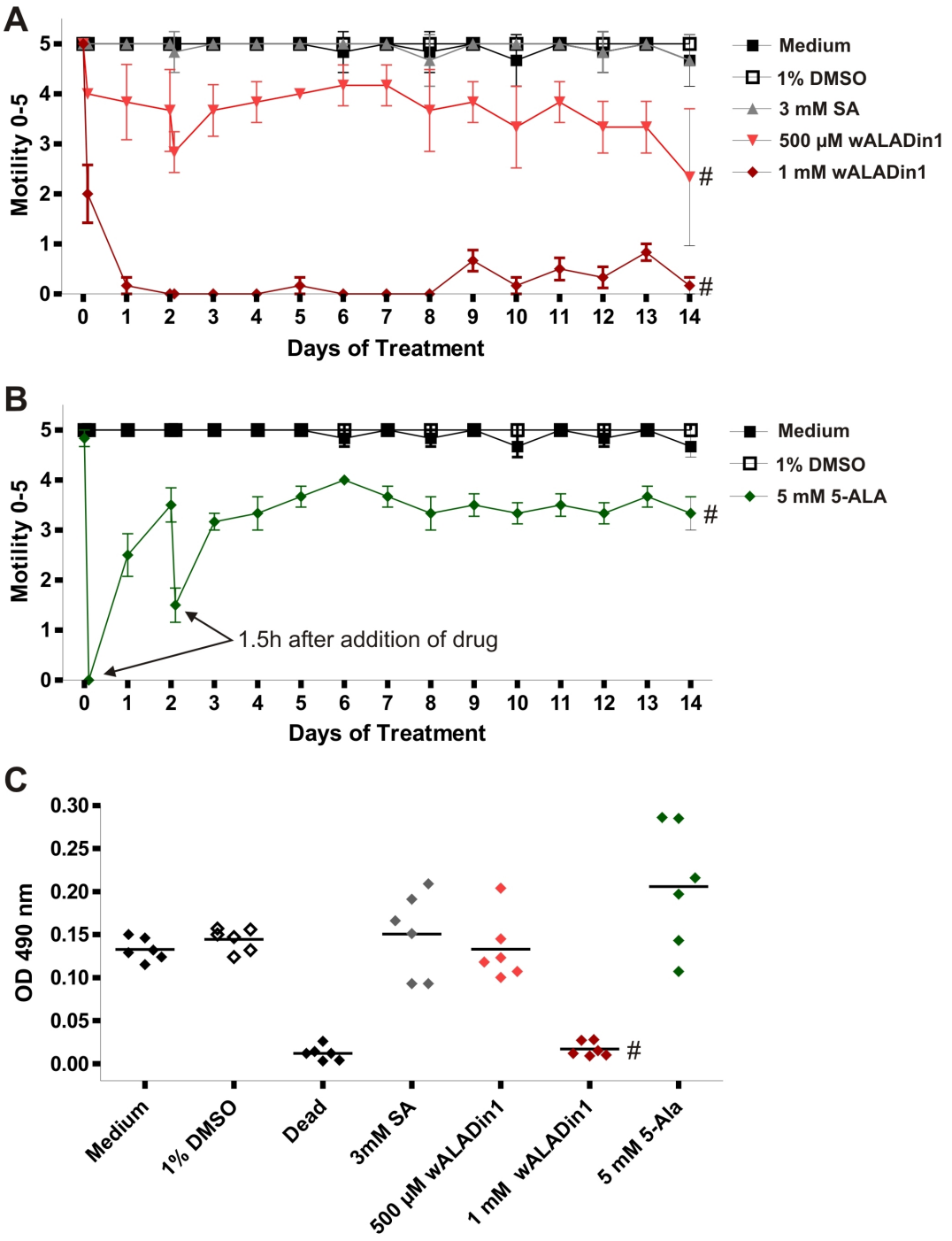

Figure 3.16.: Effect of succinylacetone (SA) and wALADin1 on the viability of *A. viteae ex vivo*. Single female worms were isolated from jirds and cultured on a LLCMK2 cell layer in 3 ml MEM + 10 % FCS + 1 % Penicillin/Streptomycin (control) or in medium containing 3 mM SA, 5-ALA, 500 µM and 1mM wALADin1. Media (except 3 mM SA and medium group) contained 1 % DMSO. Medium was completely exchanged every 2 days. Motility of worms was assessed daily using a score from 0 - 5 with 0 = no motility and 5 = best motility (A and B). Arrows indicate the effect of 5-ALA on the worm's motility at 1.5 h after medium exchange and addition of fresh drug. Enzymatic activity of worms was assessed at day 14 using the MTT viability assay (C). Shown are means of 6 worms. # indicates a significant difference compared to the control, as determined with Mann-Whitney-U test ($p \leq 0.05$).

4. Discussion

4.1. Suitability of the *B. malayi* microarray for hybridisation with *L. sigmodontis* cDNA

4.1.1. Cross-hybridisation

In our study we used the *B. malayi* microarray chip to measure changes in gene expression in *L. sigmodontis* after depletion of *Wolbachia*. Due to cDNA from a different filarial species hybridising to the chip, it is expected that only a limited number of *L. sigmodontis* genes with enough sequence similarity to the corresponding oligos are detected by the array. The oligos on the microarray have a length of 65 nucleotides, which means that binding of *L. sigmodontis* genes is only possible if enough similarity in this restricted part of the sequence is present. The more oligos corresponding to one gene present on the array, the higher the chance that one of the oligos can bind the *L. sigmodontis* cDNA. Here, 20 % of the oligos corresponding to filarial genes showed a signal above background level and were included in the analysis. This number is low compared to percentage of detection seen in experiments using cDNA of *B. malayi* where ~ 70 % of hybridisation signals were above threshold (Li et al., 2005). Experiments using the *B. malayi* microarray chip with *L. sigmodontis* cDNA are therefore not expected to provide a complete picture of the gene expression status. However, we showed that within the genes that have enough homology to the oligos on the chip, a comparison of RNA levels from untreated with treated worms is possible and can serve as tool for identification of differentially regulated genes. Additionally, genes that hybridised in our experiment possibly represent evolutionary conserved genes with greater biologic importance. Compared with differential display, a method previously used to find differentially regulated genes (Heider et al., 2006), the *B. malayi* microarray provided greater speed and more information on gene expression changes in *L. sigmodontis*. The tool box to study the molecular mechanism of the *Wolbachia*-filaria symbiosis is restricted and the establishment of experimental set ups for its study is important. Our microarray experiment showed that the sequence information available for *B. malayi* is of great

use to promote investigations of symbiosis using the well established filarial model organism *L. sigmodontis*.

4.1.2. Reproducibility of microarray data

A subset of differentially expressed genes was ,,cherry picked" from the microarray data to be validated by qPCR with samples from a different experiment. Including the mitochondrial encoded genes, we performed qPCR for 25 genes and confirmed 63 % of the genes regulated in response to the loss of *Wolbachia*. QPCR results of the up-regulated genes better agreed with the microarray data than the down-regulated genes. An increased variability of low-intensity spots has been reported and it has been speculated that this may lead to a worse validation of down-regulated genes compared to up-regulated genes (Morey et al., 2006). Indeed, most of the selected genes with a validated expression change in qPCR had higher fluorescence intensities in the microarray than genes whose differential expression change could not be confirmed. The selected down-regulated genes had a lower fluorescence intensity than most of the selected up-regulated genes. Interestingly, for the spots of the two out of 9 selected down-regulated genes with a confirmed differential expression, higher intensities could be ascertained than for all of the 7 not validated genes (Table 3.4). To achieve a greater reproducibility of the data further studies could use more restricted criteria for the analysis of this microarray with a minimal intensity unit higher than 200.

Our data and the data of Ghedin et al. (2009) show that genes of many distinct pathways are affected by endosymbiont depletion, therefore it cannot be excluded that the gene used for normalisation is also affected by the disruption of symbiosis. Of note, the mitochondrial encoded NADH-dehydrogenase subunit 1 gene used by Ghedin et al. (2009) for normalisation after *Wolbachia* depletion in *B. malayi* was up-regulated in our microarray experiment after 36 days of Tet treatment (Table 3.5). Therefore caution should be used when using this gene for normalising gene expression.

4.2. Differentially expressed genes after *Wolbachia* depletion

4.2.1. General expression patterns after *Wolbachia* depletion

We detected most of the regulated genes at day 36, with *Wolbachia* copies reduced by 99.8 %, fewer genes at day 6 and the fewest genes at day 15. This resembles a bimodal pattern that has been observed before for phosphate permease (Heider et al., 2006) and was explained by an early response due to dying of embryonic stages, which have been shown to be more sensitive to the loss of *Wolbachia* (Langworthy et al., 2000), and the later peak due to the adult worms responding to disruption of symbiosis. A bimodal expression pattern of genes belonging to signalling pathways was also reported by Ghedin et al. (2009), although this was seen at an earlier time point with the first up-regulation at day one of Tet treatment and the second at day 6. As they cultured the worms *ex vivo* in tetracycline containing medium, the earlier gene expression response might be due to a more direct exposure of the worms to tetracycline.

The regulation of genes in this pattern supports that the gene expression changes result from disruption of symbiosis and do not result from a general stress response due to the dying bacteria within the worm. We also showed that most of the *Wolbachia* had already died by day 6 of Tet treatment (Figure 3.1) and were eliminated from the worms by day 36. Further evidence to support that the regulation was not simply a stress response is that *hsp60* was not up-regulated for any time point as measured by qPCR (Figure 3.2). Gene expression changes seen at this time point are therefore more probably the result of lack of supply by *Wolbachia* and attempt of the worm to adapt to this situation than a general stress response.

Although we used oligo-dT primer to reverse transcribe *L. sigmodontis* mRNA, we also detected some hybridisation to *Wolbachia* oligos. These *Wolbachia* genes were strongly down-regulated and reflected successful bacterial depletion in our experiment. If one compares the significantly down-regulated *Wolbachia* genes at the 3 different time points, it can be noticed that the same genes come up at day 6, 15 and 36 (Tables 3.2 and 3.1). Likely, this is not because these are the only genes down-regulated, but because these are the only ones which had A-rich regions (to be reverse transcribed by oligo-dT primers) and because they were expressed high enough to be detected and to exceed the minimal fluorescence intensity to be included in the analysis.

4.2.2. Cytoskeletal proteins

B. malayi has 67 genes which encode several cuticle collagens. They are expressed differentially during development, therefore each larval stage contains a characteristic composition of collagens (Scott and Ghedin, 2009). We detected several cuticle collagens up-regulated at day 36 of Tet treatment and one up- and one down-regulated collagen at day 15. Ghedin et al. (2009) found collagens predominantly down-regulated in *w*Bm depleted *B. malayi*, but these were not the same genes that we found to be differentially expressed. Only collagen *col-34* (Bm1_36555) was both up-regulated in *B. malayi* (day 7) and in our microarray analysis (day 36). Cuticle biosynthesis occurs prior to molting at the end of the embryonic and each larval stage (Page and Johnstone, 2007), thus a change in the expression of cuticle collagens might reflect the impairment of larval development after *Wolbachia* depletion.

Troponin C, troponin T and tropomyosin were up-regulated in the microarray. The globular molecule troponin is, together with actin and tropomyosin, part of the thin filament of the muscle apparatus and responsible for regulation of contraction. Troponin consist of 3 subunits: troponin T, which binds to tropomyosin, troponin C, which binds calcium and thereby produces a conformational change in troponin I and Troponin I, which binds to the actin thin filaments (Hooper et al., 2008). We confirmed the up-regulation of the troponin genes by qPCR (Figure 3.5 C and D). Besides their role in locomotion, troponin and tropomyosin are important regulators for ovarian contraction in *Caenorhabditis elegans* (Ono and Ono, 2004) and differential expression of these genes might result from the block in embryogenesis seen after disruption of symbiosis (Hoerauf et al., 1999, 2003). Furthermore, mutations in several genes for regulatory components of the muscle filaments affect embryonic and larval development in *C. elegans*. Specifically, mutations in the *pat-10* gene, which encodes the up-regulated troponin C, lead to paralysed, arrested embryos late in development (Terami et al., 1999). This coincides with the phenotype observed in filarial worms after *Wolbachia* depletion. Also, the actin binding proteins profilin, gelsolin, coronin, actin-depolymerization factor 1 and calponin were differentially expressed after *Wolbachia* depletion. Together, these observations might either be a result of the disturbed symbiosis or even might reflect an interaction of *Wolbachia* proteins with the host cytoskeleton.

4.2.3. Transcriptional regulation

Our microarray analysis identified a retinoblastoma binding protein to be down-regulated in *L. sigmodontis* at day 6 of *Wolbachia* depletion. A decrease in expression at day 6 has been confirmed by qPCR analysis. This protein is a orthologue to the mammalian protein RbAp48 which plays a role in regulation of chromatin remodelling during transcription. RbAp48 binds the retinoblastoma protein (Rb) and the histone deacetylase 1 (HDAC1) and is thereby involved in the repression of the transcription factor E2F-1. E2F-1 activates the transcription of S phase genes, promoting the progression of cell cycle from G1 to S phase (Nicolas et al., 2000)(Figure 4.1). Consistent with that result, another protein, PurA, which can bind to the transcription factor E2F-1 and thereby inhibits transcription of E2F-1 responsive genes (Darbinian et al., 1999), was down-regulated at day 6 in the microarray. Homologues of Rb and RbAp48 in *C. elegans* are the proteins Lin-35 and Lin-53 and they also seem to function in transcriptional repression and developmental regulation (Harrison et al., 2006). RbAp48 targets the chromatin remodelling complex to nucleosomes by binding histones. Consistent with that, several genes encoding histones were also differentially expressed in our microarray and after *Wolbachia* depletion in *B. malayi* (Ghedin et al., 2009). *Wolbachia* encode several Ank proteins which have been implicated in diverse functions to establish intracellular lifestyle of bacteria within the host. In *Anaplasma phagocytophilum* an Ank protein has been observed in association with condensed chromatin of the host cell and a role in regulation or modification of host cell gene transcription has been suggested (Caturegli et al., 2000). The differential expression of a histone binding protein, which is involved in the deacetylation of chromatin during transcriptional regulation indicates that *Wolbachia* bacteria as well might be able to modify host cell gene expression. Landmann et al. (2009) proposed an impaired histone deposition as the mechanism for *Wolbachia* induced CI in insects, thus *Wolbachia* possibly influence chromatin remodelling for transcriptional regulation of host genes.

It is unknown how *Wolbachia* synchronises its replication with the filarial cell cycle. The differential expression of the proteins RbAp48 and PurA after *Wolbachia* depletion, which regulate an important transcription factor for cell cycle control, might be an indication for an interaction of *Wolbachia* with host cell cycle regulation.

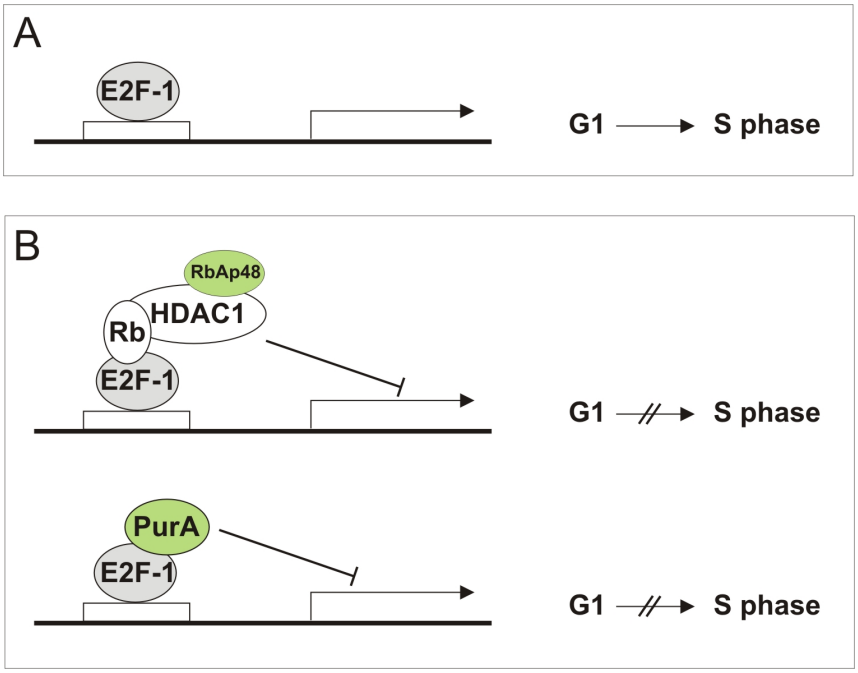

Figure 4.1.: Regulation of transcription of E2F responsive genes is altered after *Wolbachia* depletion. The transcription factor E2F-1 activates the transcription of S-phase genes (A). The complex of Rb, histone deacetylase 1 (HDAC1) and RbAp48 as well as Pur alpha (PurA) are repressors of E2F-1 and inhibit G1/S cell cycle progression. RbAp48 and Pur alpha (green) are down-regulated at day 6 of *Wolbachia* depletion in *L. sigmodontis* (B).

4.2.4. Post-transcriptional processing and protein synthesis

Several genes involved in post-transcriptional processing were differentially expressed in *L. sigmodontis* after *Wolbachia* depletion. One of these genes, an RNA binding protein (Bm1_37780), has been validated by qPCR to be up-regulated at day 36 of Tet treatment (Figure 3.5 B). This gene contains an RRM domain, which are very abundant protein domains in eukaryotes, but are also found in prokaryotes and viruses. The structural motif allows high RNA binding and specific recognition. It has multiple biological functions, mostly associated with post-transcriptional gene regulation (Maris et al., 2005). The gene up-regulated in our experiments has high homology to the subunit 2 of the cleavage stimulation factor (CstF2 tau variant), that is involved in cleavage and polyadenylation of the 3' site of pre-mRNAs (Salisbury et al., 2006). The maturation of the pre-mRNAs ensures stability and function of the transcripts, therefore an expression change in post-transcriptional modification processes might affect the copy numbers of RNA transcripts of many genes. This might in part explain why we and Ghedin et al. (2009) observed differential expression of many different gene classes, especially considering that we used oligo-dT primer to reverse transcribe mature mRNA into cDNA.

We detected a considerable number of genes involved in splicing to be differentially expressed after *Wolbachia* depletion. Cis- and trans-splicing in nematodes requires several small nuclear RNAs (snRNA) which are associated with proteins in a complex called spliceosome (Hannon et al., 1991). One of the hypothetical proteins (Bm1_04280) that we confirmed by qPCR to be up-regulated at day 36 of Tet treatment had BLAST hits to the small nuclear RNA U2-1. Furthermore, our microarary data revealed the DDX5 RNA helicase up-regulated at day 36, whereas 2 splicing factors and the U2 small nuclear ribonucleoprotein A were down-regulated at this point of time. A U6 snRNA-associated protein (Lsm4) was down-regulated at day 6. Results of other studies support an alteration of the splicing process after *Wolbachia* depletion: differential display previously identified the early up-regulation (day 3 to day 15) of the small nuclear RNA U6-3 after *Wolbachia* depletion in *L. sigmodontis* (Klemm, Pfarr and Hoerauf, unpublished data) and in the study of Ghedin et al. (2009) several splicing factors were up-regulated in *B. malayi* at day 14 of *Wolbachia* depletion. The up-regulation and at the same time the down-regulation of splicing factors and spliceosome associated proteins is not necessarily an inconsistent finding, as splicing factors can have repressor and activator functions and can even reverse their effects on a substrate depending on changes in the splicing process during development (Barberan-Soler et al., 2011). A differential expression might reflect an adaption of the worm to the impaired developmental processes after *Wolbachia* depletion. A change in general processes like post-transcriptional regulation might also reflect the disturbed homeostasis after disruption of the mutualistic symbiosis. Another possible explanation of these results is supported by a recent study of Sugimoto et al. (2010) that showed that *Wolbachia* influences the alternative splicing of a sex determination gene and thereby induces sexual alterations in a moth. Thus, the differential expression of splicing related genes seen in *L. sigmodontis* after endosymbiont depletion might indicate an interaction of *Wolbachia* molecules in this process. Whether nematode *Wolbachia* alter the expression of specific genes at the mRNA level to establish its intracellular lifestyle is a topic that needs further research.

Our microarray analysis revealed translation genes to be predominantly down-regulated at day 36 of Tet treatment. Similarly, in the study of Ghedin et al. (2009) differential regulation of genes involved in translation was observed after depleting *w*Bm, although they found them to be up-regulated at days 7 and 14 of Tet treatment. They explained this finding by a general stress response induced due to a shortage of essential nutrients which are otherwise supplied by *Wolbachia*. An

early increase in protein synthesis could reflect the attempt of the worm to provide necessary proteins and thereby counteract the loss of supply from *Wolbachia*. At a later time point, as seen in our results, the protein synthesis machinery might be down-regulated again, reflecting the failure to compensate for the loss of *Wolbachia*.

4.2.5. Immunoregulatory proteins

The major *L. sigmodontis* excretory/secretory protein Juv-p120, produced by juvenile female worms (Hintz et al., 1998), was down-regulated at day 36 of Tet treatment in our experiments (and confirmed by qPCR) as well as at day 14 in *Wolbachia* depleted *B. malayi* (Ghedin et al., 2009). In *B. malayi* an early up-regulation of this protein has been observed, which coincides with the slight increase of expression we observed by qPCR at day 6, before expression decreases 2-fold at day 36. Juv-p120 is highly decorated with dimethylaminoethanol (DMAE) (Houston et al., 2008). The major secretory product of *A. viteae*, ES-62, is conjugated with phosphorylcholine (PC), which inhibits pro-inflammatory responses of the mammalian host. DMAE contains only two methyl groups, whereas PC contains 3. It is hypothesised that the DMAE decorated Juv-p120 may function immunologically in a manner similar to PC (Hewitson et al., 2009). Further, our microarray analysis detected galectin-1 (Bm1_24940) to be down-regulated at day 6 of Tet treatment. This protein is one of the most prominent excretory-secretory products of adult *B. malayi* (Hewitson et al., 2008). Galectin is thought to participate in filarial down-regulation of host immune responses, as it is able to inhibit Th1 and Th2 inflammatory responses in humans and affects regulation of regulatory T-cells (Garn et al., 2007; Toscano et al., 2006). A change in the expression of immunomodulatory molecules suggests a change in the immunological environment of the worm after *Wolbachia* depletion.

4.2.6. Hypothetical proteins

The many hypothetical proteins that were up- and down- regulated after *Wolbachia* depletion are also of interest, because they may represent proteins with important functions for symbiosis and parasitic life style. 20 % of total genes encoded by *B. malayi* and ca. 2000 of the hypothetical genes are only found in *B. malayi* and may encode filarial-specific gene products (Ghedin et al., 2007). Assigning functions to the hypothetical proteins that have a role in symbiosis will be of great interest, because they might have evolved since the establishment of the filaria-*Wolbachia* symbiosis and might have key roles in maintaining the homeostasis. Up-coming

interactome studies by other filarial research groups will surely shed light on this issue by identifying interactions of *Wolbachia* proteins with filarial proteins.

4.3. Heme proteins of the respiratory chain are up-regulated after *Wolbachia* depletion

The most striking result in our study was the up-regulation of nearly all mitochondrial encoded genes of the respiratory chain at day 36 of Tet treatment (Table 3.5, Figure 3.8). Distinct localisation patterns of filarial mitochondria and *Wolbachia* have been reported (Pfarr et al., 2008) which would limit a direct interaction between the mitochondria and the vesicles containing *Wolbachia*. A trend towards up-regulation of these respiratory chain subunits during Tet treatment was also reported in *Wolbachia* depleted *B. malayi* (Ghedin et al., 2009), where increased transcript levels were detected at day 14 of Tet treatment. As tetracycline acts by inhibiting the bacterial 30S ribosomal subunit (Brodersen et al., 2000) and mitochondria have proteobacterial ancestors, an impairment on mitochondrial protein synthesis due to an inhibition by tetracycline is possible and has been reported (McKee et al., 2006). To exclude this possibility, jirds infected with the *Wolbachia*-free filaria *A. viteae* were treated for 6 weeks with tetracycline in drinking water. The treatment time used was the same previously demonstrated to achieve a sustained depletion of *Wolbachia* from *L. sigmodontis* to levels equivalent to 36 days of intraperitoneal treatment in mice (Arumugam et al., 2008). As expression of respiratory chain genes did not change after Tet treatment in *A. viteae* (Figure 3.9), we conclude that the up-regulation of the mitochondrial respiratory chain subunits is specific to *Wolbachia* depletion from worms dependent on this endosymbiont.

One possible reason for the change in the expression of these mitochondrial subunits is their requirement for heme and riboflavin (Figure 3.7), cofactors that may be provided by the *Wolbachia* (Foster et al., 2005). Specifically, the complexes cytochrome c oxidase and cytochrome bc1 need heme as a prosthetic group. Genome analysis revealed that *Wolbachia* possess all but one enzyme required to synthesise this essential cofactor (Figure 4.4). The missing gene is protoporphyrinogen, a gene that is absent in many alpha-proteobacteria, but very likely complemented by another gene (Foster et al., 2005). However, *B. malayi* lack most of the genes needed to produce heme and therefore must take it up from the environment or are dependent on their intracellular *Wolbachia* bacteria. Furthermore, riboflavin, another cofactor that also can be synthesised by *Wolbachia*, is essential in the NADH-dehydrogenase complex (Figure 3.7). No enzymes for riboflavin synthesis have been detected in

the *B. malayi* genome (Foster et al., 2005). We hypothesise that due to a lack of essential cofactors it is not possible to form functional respiratory chain complexes. As a consequence, the nematode cells attempt to correct for their lack by increasing the transcription of respiratory chain subunits (Figure 4.2).

Another heme-binding protein of the globin family (Bm1_50430), the orthologue of the canonical globin 1 of *C. elegans* (ZK637.13), was also up-regulated after *Wolbachia* depletion and validated by qPCR (Figure 3.5 A). *C. elegans* expresses 33 globin genes with high diversity in gene structure, amino acid sequence and expression profiles, and the *B. malayi* genome encodes 13 different globin variants. Nonvertebrate globins are much more heterogeneous than globins from vertebrates and have, besides the conventional oxygen storage and transport, a wealth of diverse functions (Geuens et al., 2010; Hoogewijs et al., 2007). As this protein is encoded by the nucleus, the up-regulation of heme-dependent proteins was not limited to mitochondrial proteins.

Wolbachia-containing filarial nematodes may be dependent on the heme provided by *Wolbachia* and needed for mitochondrial and nuclear encoded heme-requiring proteins. A loss of function of the heme containing enzymes required for ecdysone signalling has been hypothesised to contribute to the developmental defects after *Wolbachia* depletion (Tzertzinis et al., 2010). Furthermore, deficiency of mitochondrial respiratory chain due to loss of heme may also account for the developmental impairments, as seen in *C. elegans* (Tsang et al., 2001).

4.3.1. Tet treatment differentially affects mitochondrial copy number in *L. sigmodontis* and *A. viteae*

The number of mitochondria in a cell can change depending on energy needs during development (Lemire, 2005). We therefore analysed whether a change of mitochondria per cell in *L. sigmodontis* might be a cause for the elevated mRNA levels after *Wolbachia* treatment. Copy number of the mitochondrial encoded genes were elevated at days 15 and 36 of Tet treatment, nevertheless, copies of the nuclear encoded actin showed the same pattern after treatment (Figure 3.10). Therefore, we conclude that the numbers of mitochondria per cell are not increased after Tet treatment and that this is not an explanation for the increased mRNA levels we observed. We also performed the same analysis with untreated and 6 weeks orally Tet treated *A. viteae*. We did not observe a change of mtDNA copies, but we observed an unexpected drop of actin copy numbers to 5-fold under the control level (Figure 3.11). Previous experiments have shown that Tet treatment does not affect development in

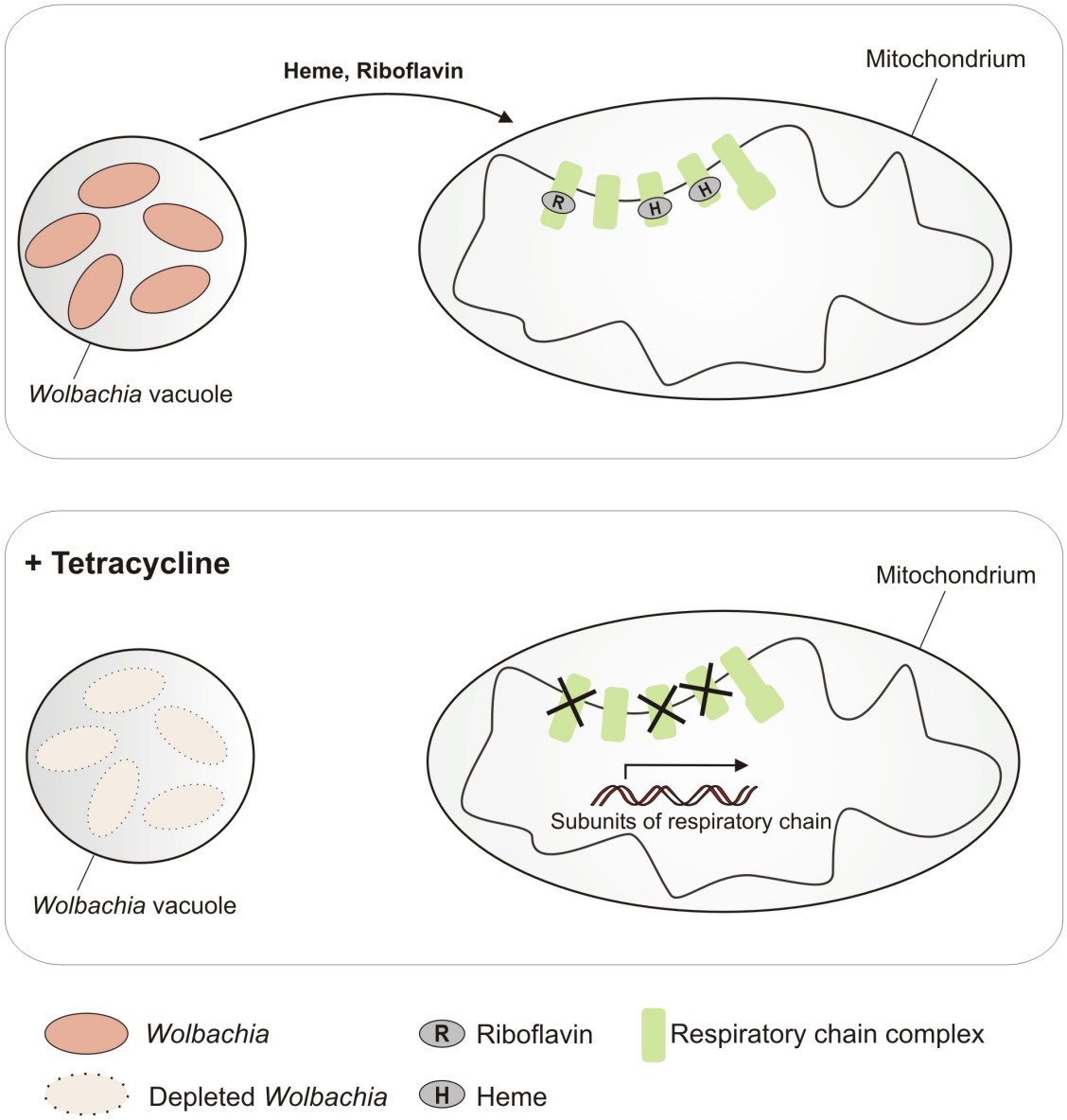

Figure 4.2.: *Wolbachia* depletion leads to up-regulation of mitochondrial encoded heme containing enzymes of the respiratory chain of *L. sigmodontis*. We hypothesise that filarial worms are dependent on heme and riboflavin, provided by *Wolbachia*, to form a functional respiratory chain. After depletion of *Wolbachia* with tetracycline, loss of the cofactors leads to deficiencies in respiratory chain function, which the nematode attempt to correct by increasing transcription of genes for the respiratory chain.

the *Wolbachia*-free filaria *A. viteae*. We also did not see a difference in microfilariae number in blood of untreated and Tet treated *A. viteae*-infected jirds (Figure 3.12). A difference in embryo content within the worms could have led to differences in gDNA amounts extracted from the worms.

In mammalian cells, tetracycline analogues can induce apoptosis, which is demonstrated by growth inhibition and DNA fragmentation, a typical hallmark of apoptosis (Onoda et al., 2006). It could be possible that decreased gDNA copies in *A. viteae* are due to degraded DNA as a consequence of apoptosis induced by tetracycline. To address this question, further experiments could investigate whether DNA is degraded after Tet treatment in *A. viteae* compared to *L. sigmodontis*. Furthermore, determining the amount of cytochrome c would help answer this question, as cytochrome c is released during apoptosis. Regarding our findings, it is advised not to use gDNA copy numbers for normalising gene expression in Tet treatment experiments, as this would lead to misinterpretations.

Clearly, our experiment showed that *L. sigmodontis* and *A. viteae* are differentially affected by tetracycline. One explanation for a different effect of tetracycline on infected versus uninfected species is given by Ballard and Melvin (2007). They showed, that Tet treatment led to an increase in mtDNA density in *Wolbachia*-uninfected *Drosophila*, whereas in *Wolbachia*-containing individuals this was not seen. They hypothesised that tetracycline enters both the mitochondria and the *Wolbachia* bacteria and therefore tetracycline concentration is diluted in the mitochondria. The effects of tetracycline on the mitochondria would therefore be less prominent in *Wolbachia*-infected compared to uninfected individuals. This argument might also explain why *Wolbachia*-infected and uninfected filaria were differentially affected by tetracycline in our study. Tetracycline reaches the *Wolbachia* in our experiments, evident by a 99.3 % reduction of bacterial copy number (Figure 3.1). Nevertheless, there is no knowledge of pumps or ABC transporters that actively transport tetracycline into the bacterium or help getting it out, respectively. Tetracycline might also reach the *Wolbachia* by passive transport. Such possible unspecific effects of tetracycline would be overestimated in uninfected compared to *Wolbachia*-infected species and would not devalue the effects on filaria that are caused by loss of the *Wolbachia* endosymbiont.

4.4. *Ex vivo* cultivation of *L. sigmodontis*

In order to clarify a possible dependency of filarial nematodes on *Wolbachia* heme biosynthesis, we first established appropriate culture conditions for *ex vivo* drug treatment experiments with *L. sigmodontis*. Comparable to the results seen with *O. gutturosa* (Townson et al., 1986) LLCMK2 feeder cells greatly enhanced the survival of worms compared to worms cultured in medium only. That way, it is possible to perform experiments over 14 days without damaging the worms. An established *ex*

vivo cultivation of this well established model organism for filariasis (Hoffmann et al., 2000) has considerable advantages, as pharmacokinetic issues are reduced compared to *in vivo* experiments in mice. Uptake of substances, accumulation within the worm and anti-filarial efficiency can be tested *ex vivo* to preselect substances prior to *in vivo* studies. Furthermore, experiments involving substances which would be toxic for mice are possible.

4.4.1. Inhibition of heme biosynthesis specifically impairs *Wolbachia*-containing filaria

The importance of heme biosynthesis for filarial survival has recently been shown *ex vivo* in a study by Wu et al. (2009). The inhibition of heme biosynthesis led to immobility of *B. malayi* worms. *C. elegans* do not synthesis heme, but are able to take up heme from the environment (Hieb et al., 1970; Rao et al., 2005). Although the *B. malayi* were cultured in the presence of hemin, they were not able to make use of this environmental source of heme. In addition, 10 % FCS was added to the medium in the studies by Wu et al. (2009) as well as in our experiments and might be sufficient as an external source of heme, assuming that filaria could take it up. However, succinylacetone (SA), the inhibitor of aminolevulinic acid dehydratase (ALAD), also slightly affected larval growth of *C. elegans*, therefore one cannot fully exclude that unspecific effects of SA have contributed to the impaired motility of *B. malayi* worms. We addressed this question in our study by treating *L. sigmodontis* as well as the *Wolbachia*-free filaria *A. viteae* with SA. A significant impairment of SA on the feeder cells could be excluded (data not shown), as this would have led to an additional disadvantage of survival of SA treated worms. As seen with *B. malayi* we observed a reduction in motility of *L. sigmodontis* when cultured in the presence of 3 mM SA. However, the effect was not as detrimental as in the study by Wu et al. (2009). Whereas female *B. malayi* were immotile after 8 days of treatment, female *L. sigmodontis* were moving, although more slowly, until the end of the observation period at day 14 (Figure 3.14 A). Differences in permeability of the cuticles of *B. malayi* and *L. sigmodontis* and different sensitivities and ages of worms may account for these distinct observations. Furthermore, the presence of feeder cells in our worm culture very likely not only promotes the survival of the control but also the SA treated worms. Nevertheless, the effect of SA on *L. sigmodontis* was significant, which is also clearly reflected by the biochemical evaluation of viability (Figure 3.15 B). In contrast, the *Wolbachia*-free *A. viteae* worms were not affected by SA treatment, as demonstrated by assessment of motility and enzymatic viability assay (Figure 3.16 A and C). Thus, SA reduces viability in two *Wolbachia*

containing filaria, but not in a *Wolbachia*-free species. We believe this effect is due to inhibition of *Wolbachia* heme biosynthesis, leading to loss of function of essential heme containing proteins.

Several questions remain open, e.g. regarding the function of ferrochelatase (FC), which is the only heme biosynthesis enzyme found in *Wolbachia*-containing filaria as well as in the *Wolbachia*-free filaria *A. viteae*. FC catalyses the last step of heme biosynthesis, the conversion of protoporphyrin IX into heme. Complementation assays in *E. coli* show that this filarial enzyme is functional. Furthermore, the heme auxotroph *C. elegans* transfected with Bm-FC are able to utilise the heme precursor protoporphyrin IX (Slatko et al., 2010). Thus, it is possible that filarial nematodes obtain protoporphyrin IX from the environment and convert it into heme. It may be a second source of heme additional to the provision of heme by *Wolbachia*. As developmental processes require heme dependent functions like ecdysone mediated molting and energy metabolism and because embryos are affected first by *Wolbachia* depletion, filarial nematodes might require additional heme from *Wolbachia* in times of high needs of this cofactor. Inhibiting *Wolbachia* heme biosynthesis in the presence of protopophyrin IX might elucidate whether filaria are able to take up and utilise this heme precursor. Also, further experiments should address the possibility that filarial worms obtain heme or protoporphyrin IX from red blood cells, as haematophagy seems to play a role for maturation of *L. sigmodontis* (Attout et al., 2005). Determining the heme content within the worms (e.g. in *Wolbachia* depletion experiments) could also give more informations about the heme metabolism. Measuring of heme concentration is possible by reconstitution of peroxidase activity with heme and an apoenzyme (Thomas and Weinstein, 1990) or with a colorimetric assay that measures the heme that is converted into an uniform coloured form in an aqueous alkaline solution (QuantiChromTM Heme Assay Kit, BioAssay Systems, Hayward, USA). This would control for an eventual utilisation of heme precursors, decrease of heme after *Wolbachia* depletion or for the efficiency of heme biosynthesis inhibitors.

4.4.2. In search of a *Wolbachia*-specific heme biosynthesis inhibitor

Genome information, previous and our studies showed the potential of the *Wolbachia* heme biosynthesis as a target for drugs against filariasis. Therefore, efforts are being made to find drugs that specifically inhibit *Wolbachia* heme biosynthesis enzymes but not the human enzyme. wALADin1 showed a drastic dose dependent effect on

vitality of *L. sigmodontis*. Lower concentrations than used for SA, which was used as a control, were needed to achieve a greater reduction in motility and in the enzymatic viability assay (Figure 3.15 A and C). An unspecific effect was observed, as evidenced by the impact of the drug on the *Wolbachia*-free *A. viteae*. Nevertheless, comparing the effect of 500 µM wALADin1 on motility of *L. sigmodontis* and *A. viteae* it was clear that the drug acts differently on the both filarial species. Whereas motility of *L. sigmodontis* gradually worsens over time of treatment, motility of *A. viteae* is slightly impaired initially, but then does not worsen until the end of treatment (Figure 3.16 A). Also, viability of *A. viteae* was at control level after 14 days treatment with 500 µM wALADin1 (Figure 3.15 C), but the same concentration strongly reduced the motility of *L. sigmodontis* (Figure 3.15 C). Thus, wALADin1 seems to effectively block heme biosynthesis in *L. sigmodontis*, but a different additional effect on filaria can be observed. Lower concentrations of wALADin1 might still effectively block heme biosynthesis without an additional side effect. Further experiments will also elucidate whether wALADin1 has unspecific effects on mammalian cells.

ALAD inhibitors might have an additional anti-filarial effect by a different mechanism: The substrate of ALAD is 5-aminolevulinic acid (5-ALA), which has structural similarities to the neurotransmitters GABA and glutamic acid (Figure 4.3) and can act as GABA agonist (Meyer et al., 1998).

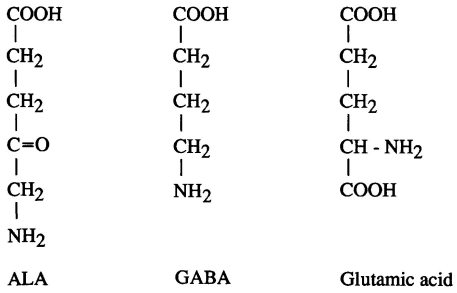

Figure 4.3.: Structural similarity of 5-aminolevulinic acid (ALA) with the neurotransmitters GABA and glutamic acid. Figure taken from Meyer et al. (1998).

Blocking the enzyme would lead to the accumulation of 5-ALA. GABA agonists have been shown to reduce spontaneous contractions of *A. viteae* (Christ et al., 1990). The same observations were made in our experiments when treating *A. viteae* with the GABA agonist 5-ALA. Paralysis of worms occurs directly after adding the substance to the medium, but worms quickly recover from the blockade of contraction (Figure 3.16 B). These results suggest that 5-ALA can function as an GABA agonist in filaria, leading to a blockade of spontaneous contractions of the worms. The mode of action might resemble those of ivermectin. Ivermectin disrupts neurotransmission processes by binding to glutamate-gated chloride channels, which

also control the muscles responsible for the excretory-secretory apparatus (Moreno et al., 2010).

Thus, the anti-filarial effect, exhibited by ALAD inhibitors in *L. sigmodontis* can have two possible causes: 1) Inhibition of *Wolbachia* heme biosynthesis leads to deficiency of essential heme enzymes, eventually leading to death of the worm. 2) Inhibition of ALAD leads to accumulation of 5-ALA, leading to disfunctions of regulation of nerve system and paralysis of worms (Figure 4.4). Further experiments by Christian Lentz are underway to titrate wALADin1 concentrations, testing the efficiency of wALADin1 derivatives and evaluating the potential of the anti-filarial effect *in vivo* using the *L. sigmodontis* BALB/c mouse model.

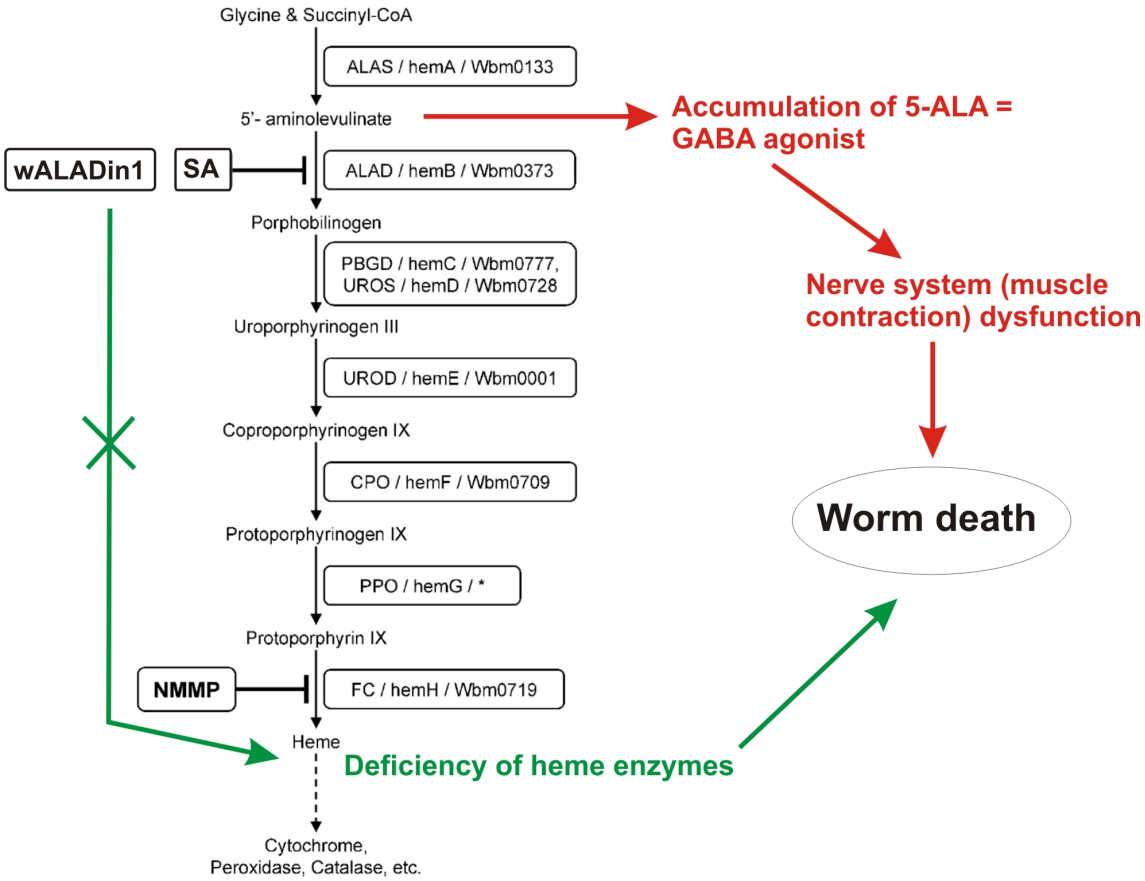

Figure 4.4.: Inhibition of *Wolbachia* heme biosynthesis using succinylacetone (SA) and wALADin1. Inhibition of *Wolbachia* ALAD might lead to death of filarial worms by preventing synthesis of heme, which would lead to deficiency of essential enzymes (green) and also by accumulation of the GABA agonist 5-ALA, thereby leading to disfunctions of neuromuscular regulation (red). Figure adapted from Wu et al. (2009).

4.5. Conclusions

In summary, our microarray analysis of *L. sigmodontis* after *Wolbachia* depletion has shown that:

1. the *B. malayi* microarray can be used to detect changes in gene expression and provided more molecular information about the *L. sigmodontis* genes than differential display,

2. although not a direct match to the results from the *B. malayi* microarray hybridised with cDNA from *B. malayi* worms treated with tetracycline, differential regulation of genes of interest such as cuticular collagens, juvenile protein p120 and energy metabolism were in agreement,

3. processes of transcriptional regulation as well as mRNA processing were altered and might indicate that *Wolbachia* can influence host gene expression,

4. expression of immunosuppressive proteins decreased, thus indicating a change in the immunological environment of the worm,

5. mitochondria were sensitive to the loss of *Wolbachia* resulting in the up-regulation of subunits of the respiratory chain complexes. The latter findings support the hypothesis that filaria are dependent on heme provided by *Wolbachia*,

6. *Wolbachia* heme biosynthesis inhibition experiments in *L. sigmodontis* confirmed the importance of heme provided by *Wolbachia* to filaria and supports targeting heme biosynthesis as antifilarial therapy,

7. the second enzyme of the pathway, ALAD, may be a particularly good target as accumulation of the substrate 5-ALA has an additional anti-filarial effect.

The *ex vivo* culture now allows one to look at the function of interesting genes identified in this study, as successfully shown for ALAD. It also can be extended to perform RNAi experiments (using established dsRNA methods (Pfarr et al., 2006) or siRNA or shRNA) to answer open questions regarding the *Wolbachia*-filaria symbiosis, e.g. a knock-down of the *L. sigmodontis* ferrochochelatase in the presence of the heme precursor protoporphyrin IX could clarify a possible involvement of this filarial gene in heme metabolism. The results of this study can be used for further discovery of drugs that will help to combat filariasis in humans.

Summary

Filarial infections, caused by *Brugia malayi*, *Wuchereria bancrofti* and *Onchocerca volvulus* are a worldwide health problem in developing countries, causing elephantiasis or dermatitis and blindness. 1.3 billion people live at risk of infection. Current mass drug administration programmes with ivermectin, diethylcarbamazine and albendazole prevented many cases of disease, nevertheless, as they are only microfilaricidal they have to be given over many years to stop transmission. Targeting the essential *Wolbachia* endobacteria with doxycycline has been proven to be an effective therapy, as worm development and survival of adult worms is greatly reduced without the endosymbiont. However, doxycycline is contraindicated for a large portion of the at risk population.

My work aimed to analyse the molecular interactions between filaria and their endosymbiotic *Wolbachia* in order to promote target identification for new drugs against filariasis. The *B. malayi* microarray was used in a cross-species hybridisation experiment to identify genes that are differentially expressed in *Litomosoides sigmodontis* after depletion of *Wolbachia* and therefore might have a role in symbiosis. The microarray data were filtered for regulated genes with a false discovery rate $\leq 5\,\%$ and a ≥ 2-fold change. Most of the genes were differentially expressed at day 36 of tetracycline treatment, when 99.8 % of *Wolbachia* were depleted. Several classes of genes were affected, including genes for general processes like translation, transcription, post-transcriptional processing and folding/sorting of proteins and also genes involved in motility, structure and signalling pathways. *L. sigmodontis* specific quantitative PCR validated $\sim 60\,\%$ of the genes found to be regulated in the microarray.

Interestingly, most of the mitochondrial encoded subunits of respiratory chain complexes containing heme and riboflavin were up-regulated. No change in the expression of these genes was seen in tetracycline treated *Wolbachia*-free *Acanthocheilonema viteae*. As *Wolbachia* synthesise heme and filaria do not, we hypothesise that without the endosymbionts no functional heme-containing enzymes can be formed, leading to loss of energy metabolism which then results in up-regulation of the mitochondrial encoded subunits in an attempt to correct the deviation from

homeostasis. A nuclear encoded heme-binding protein of the globin family was also up-regulated, therefore the differential expression of heme proteins after *Wolbachia* depletion was not limited to the mitochondria. Using a filarial *ex vivo* culture, established as part of my thesis work, we confirmed that *Wolbachia*-containing *L. sigmodontis* worms were sensitive to inhibition of the heme biosynthesis pathway, whereas *Wolbachia*-less worms were not affected by the same treatment. The results indicate that filarial nematodes are dependent on the heme provided by their essential *Wolbachia* and support further targeting the *Wolbachia* heme synthesis pathway for the discovery of new anti-filarial drugs.

Zusammenfassung

Die durch die Filarien *Brugia malayi*, *Wuchereria bancrofti* und *Onchocerca volvulus* verursachte Onchozerkose und Lymphatische Filariose stellt ein weltweites Gesundheitsproblem in den Entwicklungsländern dar und kann zu Dermatitis, Erblindung oder Elephantiasis führen. Weltweit sind 1.3 Milliarden Menschen dem Risiko einer Infektion ausgesetzt. Derzeitige Massenbehandlungen mit Ivermectin, Diethylcarbamazin und Albendazol haben bereits viele Krankheitsfälle verhindern können, jedoch wirken sie nur auf die Mikrofilarien, so dass diese Medikamente über viele Jahre verabreicht werden müssen, um eine Transmission zu stoppen. Eine neue Behandlungsstrategie mit Doxyzyklin hat sich als sehr effektiv erwiesen, da es das endosymbiontische Bakterium *Wolbachia* angreift, welches für die Wurmentwicklung und das Überleben der adulten Filarien essenziell ist. Doxyzyklin ist jedoch für einen großen Anteil der Bevölkerung kontraindiziert.

Ziel der vorliegenden Arbeit war es, die molekularen Interaktionen zwischen Filarien und ihrem Endosymbionten *Wolbachia* zu analysieren, um symbiotische Mechanismen und damit Angriffspunkte für die Entwicklung von neuen Medikamenten gegen Filariosen zu identifizieren. Der *B. malayi* Microarray wurde für die Detektion von Genen genutzt, die in der nahe verwandten Nagetier-Filarie *L. sigmodontis* nach Depletion der Wolbachien eine veränderte Expression aufweisen. Diese Gene könnten auf symbiotische Abhängigkeiten zwischen Filarien und *Wolbachia*-Bakterien hinweisen. Die Microarray-Daten wurden nach Genen mit einem ≥ 2-fachen Unterschied in der Expression und einer falsch-positiven Rate von $\leq 5\,\%$ gefiltert. Nach 36 Tagen Tetrazyklinbehandlung, ein Zeitpunkt an dem die Wolbachien-Zahl zu über 99 % reduziert war, konnten die meisten regulierten Gene nachgewiesen werden. Viele verschiedene Genklassen waren betroffen, unter anderem Gene für allgemeine Prozesse wie Translation, Transkription, posttranskriptionale Prozessierung und Faltung/Sortieren von Proteinen sowie Gene für Motilität, Struktur und Signalwege. *L. sigmodontis* spezifische quantitative PCR bestätigte $\sim 60\,\%$ der im Microarray regulierten Gene.

Interessanterweise wiesen fast alle mitochondrial kodierten Untereinheiten der Atmungskettenkomplexe, welche Häm und Riboflavin enthalten, eine hochregulierte

Genexpression auf. Bei der *Wolbachia*-freien Filarie *Acanthocheilonema viteae* konnte nach Tetrazyklinbehandlung keine Expressionsänderung dieser Gene nachgewiesen werden. Da Wolbachien im Gegensatz zu den Filarien Häm synthetisieren können, vermuten wir, dass ohne das Endobakterium keine funktionellen Komplexe für die Atmungskette gebildet werden können. Dies würde zu einem Defekt im Energiemetabolismus und dadurch zu einer Hochregulierung der Untereinheiten der Atmungskette führen, um die Abweichung der Homeostase auszugleichen. Die Expressionsänderung nach Depletion der Wolbachien beschränkte sich nicht auf mitochondrial kodierte Hämproteine, da auch für ein nuklear kodiertes Hämprotein aus der Globin-Familie eine Hochregulierung des Transkripts nachgewiesen werden konnte. Mittels einer *ex vivo* Filarienkultur, die im Rahmen dieser Arbeit etabliert wurde, konnte bestätigt werden, dass *Wolbachia*-enthaltende Filarien sensitiv auf eine Inhibition der Häm-Synthese reagieren, wohingegen *Wolbachia*-freie Filarien von der gleichen Behandlung nicht beeinträchtigt waren. Die Ergebnisse deuten darauf hin, dass Filarien von dem von ihren essenziellen Wolbachien zur Verfügung gestelltem Häm abhängig sind und unterstreichen die Bedeutung des *Wolbachia* Häm-Synthesewegs als effektiven Angriffspunkt für die Entwicklung neuer Medikamente gegen Filariosen.

Bibliography

Addiss, D. G. and Brady, M. A. (2007). Morbidity management in the Global Programme to Eliminate Lymphatic Filariasis: a review of the scientific literature. Filaria J *6*, 2.

Allen, J. E., Adjei, O., Bain, O., Hoerauf, A., Hoffmann, W. H., Makepeace, B. L., Schulz-Key, H., Tanya, V. N., Trees, A. J., Wanji, S. and Taylor, D. W. (2008). Of mice, cattle, and humans: the immunology and treatment of river blindness. PLoS Negl Trop Dis *2*, e217.

Allen, J. E., Daub, J., Guiliano, D., McDonnell, A., Lizotte-Waniewski, M., Taylor, D. W. and Blaxter, M. (2000). Analysis of genes expressed at the infective larval stage validates utility of *Litomosoides sigmodontis* as a murine model for filarial vaccine development. Infect Immun *68*, 5454–5458.

Arumugam, S., Pfarr, K. M. and Hoerauf, A. (2008). Infection of the intermediate mite host with *Wolbachia*-depleted *Litomosoides sigmodontis* microfilariae: impaired L1 to L3 development and subsequent sex-ratio distortion in adult worms. Int J Parasitol *38*, 981–987.

Asano-Kato, N., Fukagawa, K., Okada, N., Kawakita, T., Takano, Y., Dogru, M., Tsubota, K. and Fujishima, H. (2005). TGF-beta1, IL-1beta, and Th2 cytokines stimulate vascular endothelial growth factor production from conjunctival fibroblasts. Exp Eye Res *80*, 555–560.

Attout, T., Babayan, S., Hoerauf, A., Taylor, D. W., Kozek, W. J., Martin, C. and Bain, O. (2005). Blood-feeding in the young adult filarial worms *Litomosoides sigmodontis*. Parasitology *130*, 421–428.

Baldo, L., Prendini, L., Corthals, A. and Werren, J. H. (2007). *Wolbachia* are present in southern african scorpions and cluster with supergroup F. Curr Microbiol *55*, 367–373.

Ballard, J. W. O. and Melvin, R. G. (2007). Tetracycline treatment influences mitochondrial metabolism and mtDNA density two generations after treatment in *Drosophila*. Insect Mol Biol *16*, 799–802.

Bandi, C., Anderson, T. J., Genchi, C. and Blaxter, M. L. (1998). Phylogeny of *Wolbachia* in filarial nematodes. Proc Biol Sci *265*, 2407–2413.

Bandi, C., McCall, J. W., Genchi, C., Corona, S., Venco, L. and Sacchi, L. (1999). Effects of tetracycline on the filarial worms *Brugia pahangi* and *Dirofilaria immitis* and their bacterial endosymbionts *Wolbachia*. Int J Parasitol *29*, 357–364.

Barberan-Soler, S., Medina, P., Estella, J., Williams, J. and Zahler, A. M. (2011). Co-regulation of alternative splicing by diverse splicing factors in *Caenorhabditis elegans*. Nucleic Acids Res *39*, 666–674.

Basanez, M.-G., Pion, S. D. S., Churcher, T. S., Breitling, L. P., Little, M. P. and Boussinesq, M. (2006). River blindness: a success story under threat? PLoS Med *3*, e371.

Bennuru, S., Meng, Z., Ribeiro, J. M. C., Semnani, R. T., Ghedin, E., Chan, K., Lucas, D. A., Veenstra, T. D. and Nutman, T. B. (2011). Stage-specific proteomic expression patterns of the human filarial parasite *Brugia malayi* and its endosymbiont *Wolbachia*. Proc Natl Acad Sci U S A *108*, 9649–9654.

Boatin, B. A. and Richards, F. O. (2006). Control of onchocerciasis. Adv Parasitol *61*, 349–394.

Bordenstein, S. and Rosengaus, R. B. (2005). Discovery of a novel *Wolbachia* super group in Isoptera. Curr Microbiol *51*, 393–398.

Bordenstein, S. R., Paraskevopoulos, C., Hotopp, J. C. D., Sapountzis, P., Lo, N., Bandi, C., Tettelin, H., Werren, J. H. and Bourtzis, K. (2009). Parasitism and mutualism in *Wolbachia*: what the phylogenomic trees can and cannot say. Mol Biol Evol *26*, 231–241.

Bourguinat, C., Ardelli, B. F., Pion, S. D. S., Kamgno, J., Gardon, J., Duke, B. O. L., Boussinesq, M. and Prichard, R. K. (2008). P-glycoprotein-like protein, a possible genetic marker for ivermectin resistance selection in *Onchocerca volvulus*. Mol Biochem Parasitol *158*, 101–111.

Bourguinat, C., Pion, S. D. S., Kamgno, J., Gardon, J., Duke, B. O. L., Boussinesq, M. and Prichard, R. K. (2007). Genetic selection of low fertile *Onchocerca volvulus* by ivermectin treatment. PLoS Negl Trop Dis *1*, e72.

Brattig, N. W., Bazzocchi, C., Kirschning, C. J., Reiling, N., Büttner, D. W., Ceciliani, F., Geisinger, F., Hochrein, H., Ernst, M., Wagner, H., Bandi, C. and Hoerauf, A. (2004). The major surface protein of *Wolbachia* endosymbionts in filarial nematodes elicits immune responses through TLR2 and TLR4. J Immunol *173*, 437–445.

Brennan, L. J., Keddie, B. A., Braig, H. R. and Harris, H. L. (2008). The endosymbiont *Wolbachia pipientis* induces the expression of host antioxidant proteins in an *Aedes albopictus* cell line. PLoS One *3*, e2083.

Brodersen, D. E., Clemons, W. M., Carter, A. P., Morgan-Warren, R. J., Wimberly, B. T. and Ramakrishnan, V. (2000). The structural basis for the action of the antibiotics tetracycline, pactamycin, and hygromycin B on the 30S ribosomal subunit. Cell *103*, 1143–1154.

Brownlie, J. C., Adamski, M., Slatko, B. and McGraw, E. A. (2007). Diversifying selection and host adaptation in two endosymbiont genomes. BMC Evol Biol *7*, 68.

Brownlie, J. C., Cass, B. N., Riegler, M., Witsenburg, J. J., Iturbe-Ormaetxe, I., McGraw, E. A. and O'Neill, S. L. (2009). Evidence for metabolic provisioning by a common invertebrate endosymbiont, *Wolbachia pipientis*, during periods of nutritional stress. PLoS Pathog *5*, e1000368.

Brownlie, J. C. and O'Neill, S. L. (2005). *Wolbachia* genomes: insights into an intracellular lifestyle. Curr Biol *15*, R507–R509.

Büttner, D. W., Wanji, S., Bazzocchi, C., Bain, O. and Fischer, P. (2003). Obligatory symbiotic *Wolbachia* endobacteria are absent from *Loa loa*. Filaria J *2*, 10.

Casiraghi, M., Bordenstein, S. R., Baldo, L., Lo, N., Beninati, T., Wernegreen, J. J., Werren, J. H. and Bandi, C. (2005). Phylogeny of *Wolbachia pipientis* based on *gltA*, *groEL* and *ftsZ* gene sequences: clustering of arthropod and nematode symbionts in the F supergroup, and evidence for further diversity in the *Wolbachia* tree. Microbiology *151*, 4015–4022.

Caturegli, P., Asanovich, K. M., Walls, J. J., Bakken, J. S., Madigan, J. E., Popov, V. L. and Dumler, J. S. (2000). ankA: an *Ehrlichia phagocytophila* group gene encoding a cytoplasmic protein antigen with ankyrin repeats. Infect Immun *68*, 5277–5283.

Christ, D., Goebel, M. and Saz, H. J. (1990). Actions of acetylcholine and GABA on spontaneous contractions of the filariid, *Dipetalonema viteae*. Br J Pharmacol *101*, 971–977.

Daehnel, K., Gillette-Ferguson, I., Hise, A. G., Diaconu, E., Harling, M. J., Heinzel, F. P. and Pearlman, E. (2007). Filaria/*Wolbachia* activation of dendritic cells and development of Th1-associated responses is dependent on Toll-like receptor 2 in a mouse model of ocular onchocerciasis (river blindness). Parasite Immunol *29*, 455–465.

Darbinian, N., Gallia, G. L., Kundu, M., Shcherbik, N., Tretiakova, A., Giordano, A. and Khalili, K. (1999). Association of Pur alpha and E2F-1 suppresses transcriptional activity of E2F-1. Oncogene *18*, 6398–6402.

Debrah, A. Y., Mand, S., Marfo-Debrekyei, Y., Batsa, L., Albers, A., Specht, S., Klarmann, U., Pfarr, K., Adjei, O. and Hoerauf, A. (2011). Macrofilaricidal Activity in *Wuchereria bancrofti* after 2 Weeks Treatment with a Combination of Rifampicin plus Doxycycline. J Parasitol Res *2011*, 201617.

Debrah, A. Y., Mand, S., Specht, S., Marfo-Debrekyei, Y., Batsa, L., Pfarr, K., Larbi, J., Lawson, B., Taylor, M., Adjei, O. and Hoerauf, A. (2006). Doxycycline reduces plasma VEGF-C/sVEGFR-3 and improves pathology in lymphatic filariasis. PLoS Pathog *2*, e92.

Falcone, F. H., Zahner, H., Schlaak, M. and Haas, H. (1995). *In vitro* cultivation of third-stage larvae of *Brugia malayi* to the young adult stage. Trop Med Parasitol *46*, 230–234.

Fenn, K. and Blaxter, M. (2006). *Wolbachia* genomes: revealing the biology of parasitism and mutualism. Trends Parasitol *22*, 60–65.

Fenollar, F., Maurin, M. and Raoult, D. (2003). *Wolbachia pipientis* growth kinetics and susceptibilities to 13 antibiotics determined by immunofluorescence staining and real-time PCR. Antimicrob Agents Chemother *47*, 1665–1671.

Ferree, P. M., Frydman, H. M., Li, J. M., Cao, J., Wieschaus, E. and Sullivan, W. (2005). *Wolbachia* utilizes host microtubules and Dynein for anterior localization in the *Drosophila* oocyte. PLoS Pathog *1*, e14.

Fischer, K., Beatty, W. L., Jiang, D., Weil, G. J. and Fischer, P. U. (2011). Tissue and Stage-Specific Distribution of *Wolbachia* in *Brugia malayi*. PLoS Negl Trop Dis *5*, e1174.

Fleige, S. and Pfaffl, M. W. (2006). RNA integrity and the effect on the real-time qRT-PCR performance. Mol Aspects Med *27*, 126–139.

Foster, J., Ganatra, M., Kamal, I., Ware, J., Makarova, K., Ivanova, N., Bhattacharyya, A., Kapatral, V., Kumar, S., Posfai, J., Vincze, T., Ingram, J., Moran, L., Lapidus, A., Omelchenko, M., Kyrpides, N., Ghedin, E., Wang, S., Goltsman, E., Joukov, V., Ostrovskaya, O., Tsukerman, K., Mazur, M., Comb, D., Koonin, E. and Slatko, B. (2005). The *Wolbachia* genome of *Brugia malayi*: endosymbiont evolution within a human pathogenic nematode. PLoS Biol *3*, e121.

Frentiu, F. D., Robinson, J., Young, P. R., McGraw, E. A. and O'Neill, S. L. (2010). *Wolbachia*-mediated resistance to dengue virus infection and death at the cellular level. PLoS One *5*, e13398.

Garn, M. I., Chu, C.-C., Golshayan, D., Cernuda-Morolln, E., Wait, R. and Lechler, R. I. (2007). Galectin-1: a key effector of regulation mediated by CD4+CD25+ T cells. Blood *109*, 2058–2065.

Geuens, E., Hoogewijs, D., Nardini, M., Vinck, E., Pesce, A., Kiger, L., Fago, A., Tilleman, L., Henau, S. D., Marden, M. C., Weber, R. E., Doorslaer, S. V., Vanfleteren, J., Moens, L., Bolognesi, M. and Dewilde, S. (2010). Globin-like proteins in *Caenorhabditis elegans*: *in vivo* localization, ligand binding and structural properties. BMC Biochem *11*, 17.

Ghedin, E., Hailemariam, T., DePasse, J. V., Zhang, X., Oksov, Y., Unnasch, T. R. and Lustigman, S. (2009). *Brugia malayi* gene expression in response to the targeting of the *Wolbachia* endosymbiont by tetracycline treatment. PLoS Negl Trop Dis *3*, e525.

Ghedin, E., Wang, S., Foster, J. M. and Slatko, B. E. (2004). First sequenced genome of a parasitic nematode. Trends Parasitol *20*, 151–153.

Ghedin, E., Wang, S., Spiro, D., Caler, E., Zhao, Q., Crabtree, J., Allen, J. E., Delcher, A. L., Guiliano, D. B., Miranda-Saavedra, D., Angiuoli, S. V., Creasy, T., Amedeo, P., Haas, B., El-Sayed, N. M., Wortman, J. R., Feldblyum, T., Tallon, L., Schatz, M., Shumway, M., Koo, H., Salzberg, S. L., Schobel, S., Pertea, M., Pop, M., White, O., Barton, G. J., Carlow, C. K. S., Crawford, M. J., Daub, J., Dimmic, M. W., Estes, C. F., Foster, J. M., Ganatra, M., Gregory, W. F., Johnson, N. M., Jin, J., Komuniecki, R., Korf, I., Kumar, S., Laney, S., Li, B.-W., Li, W., Lindblom, T. H., Lustigman, S., Ma, D., Maina, C. V., Martin, D. M. A., McCarter, J. P., McReynolds, L., Mitreva, M., Nutman, T. B., Parkinson, J., Peregrn-Alvarez, J. M., Poole, C., Ren, Q., Saunders, L., Sluder, A. E., Smith, K., Stanke, M., Unnasch, T. R., Ware, J., Wei, A. D., Weil, G., Williams, D. J., Zhang, Y., Williams, S. A., Fraser-Liggett, C., Slatko, B., Blaxter, M. L. and Scott, A. L. (2007). Draft genome of the filarial nematode parasite *Brugia malayi*. Science *317*, 1756–1760.

Gillette-Ferguson, I., Hise, A. G., McGarry, H. F., Turner, J., Esposito, A., Sun, Y., Diaconu, E., Taylor, M. J. and Pearlman, E. (2004). *Wolbachia*-induced neutrophil activation in a mouse model of ocular onchocerciasis (river blindness). Infect Immun *72*, 5687–5692.

Hannon, G. J., Maroney, P. A. and Nilsen, T. W. (1991). U small nuclear ribonucleoprotein requirements for nematode *cis*- and *trans*-splicing *in vitro*. J Biol Chem *266*, 22792–22795.

Harrison, M. M., Ceol, C. J., Lu, X. and Horvitz, H. R. (2006). Some *C. elegans* class B synthetic multivulva proteins encode a conserved LIN-35 Rb-containing complex distinct from a NuRD-like complex. Proc Natl Acad Sci U S A *103*, 16782–16787.

Hedges, L. M., Brownlie, J. C., O'Neill, S. L. and Johnson, K. N. (2008). *Wolbachia* and virus protection in insects. Science *322*, 702.

Heider, U., Blaxter, M., Hoerauf, A. and Pfarr, K. M. (2006). Differential display of genes expressed in the filarial nematode *Litomosoides sigmodontis* reveals a putative phosphate permease up-regulated after depletion of *Wolbachia* endobacteria. Int J Med Microbiol *296*, 287–299.

Henrichfreise, B., Schiefer, A., Schneider, T., Nzukou, E., Poellinger, C., Hoffmann, T.-J., Johnston, K. L., Moelleken, K., Wiedemann, I., Pfarr, K., Hoerauf, A. and Sahl, H. G. (2009). Functional conservation of the lipid II biosynthesis pathway in the cell wall-less bacteria *Chlamydia* and *Wolbachia*: why is lipid II needed? Mol Microbiol *73*, 913–923.

Hertig, M. (1936). The Rickettsia, *Wolbachia pipientis* (Gen. et Sp. Nov) and associated inclusions of the mosquito, *Culex pipiens*. Parasitology *28*, 453–486.

Hertig, M. and Wolbach, S. B. (1924). Studies on *Rickettsia*-Like Micro-Organisms in Insects. J Med Res *44*, 329–374.

Hewitson, J. P., Grainger, J. R. and Maizels, R. M. (2009). Helminth immunoregulation: the role of parasite secreted proteins in modulating host immunity. Mol Biochem Parasitol *167*, 1–11.

Hewitson, J. P., Harcus, Y. M., Curwen, R. S., Dowle, A. A., Atmadja, A. K., Ashton, P. D., Wilson, A. and Maizels, R. M. (2008). The secretome of the filarial parasite, *Brugia malayi*: proteomic profile of adult excretory-secretory products. Mol Biochem Parasitol *160*, 8–21.

Hieb, W. F., Stokstad, E. L. and Rothstein, M. (1970). Heme requirement for reproduction of a free-living nematode. Science *168*, 143–144.

Hiepe, T., Lucius, R. and Gottstein, B. (2006). Allgemeine Parasitologie. Parey in MVS Medizinverlage Stuttgart GmbH & Co. KG.

Hilgenboecker, K., Hammerstein, P., Schlattmann, P., Telschow, A. and Werren, J. H. (2008). How many species are infected with *Wolbachia*?–A statistical analysis of current data. FEMS Microbiol Lett *281*, 215–220.

Hintz, M., Schares, G., Taubert, A., Geyer, R., Zahner, H., Stirm, S. and Conraths, F. J. (1998). Juvenile female *Litomosoides sigmodontis* produce an excretory/secretory antigen (Juv-p120) highly modified with dimethylaminoethanol. Parasitology *117 (Pt 3)*, 265–271.

Hiroki, M., Tagami, Y., Miura, K. and Kato, Y. (2004). Multiple infection with *Wolbachia* inducing different reproductive manipulations in the butterfly *Eurema hecabe*. Proc Biol Sci *271*, 1751–1755.

Hise, A. G., Daehnel, K., Gillette-Ferguson, I., Cho, E., McGarry, H. F., Taylor, M. J., Golenbock, D. T., Fitzgerald, K. A., Kazura, J. W. and Pearlman, E. (2007). Innate immune responses to endosymbiotic *Wolbachia* bacteria in *Brugia malayi* and *Onchocerca volvulus* are dependent on TLR2, TLR6, MyD88, and Mal, but not TLR4, TRIF, or TRAM. J Immunol *178*, 1068–1076.

Hoerauf, A. (2008). Filariasis: new drugs and new opportunities for lymphatic filariasis and onchocerciasis. Curr Opin Infect Dis *21*, 673–681.

Hoerauf, A. (2011). Tropical Infectious Diseases: Principles, Pathogens and Practice. Chapter 106: Onchocerciasis. Richard L. Guerrant, David H. Walker and Peter F. Weller.

Hoerauf, A., Fleischer, B. and Walter, R. D. (2001a). Of filariasis, mice and men. Trends Parasitol *17*, 4–5.

Hoerauf, A., Mand, S., Adjei, O., Fleischer, B. and Büttner, D. W. (2001b). Depletion of *Wolbachia* endobacteria in *Onchocerca volvulus* by doxycycline and microfilaridermia after ivermectin treatment. Lancet *357*, 1415–1416.

Hoerauf, A., Mand, S., Volkmann, L., Büttner, M., Marfo-Debrekyei, Y., Taylor, M., Adjei, O. and Büttner, D. W. (2003). Doxycycline in the treatment of human onchocerciasis: Kinetics of *Wolbachia* endobacteria reduction and of inhibition of embryogenesis in female *Onchocerca* worms. Microbes Infect *5*, 261–273.

Hoerauf, A., Nissen-Pähle, K., Schmetz, C., Henkle-Dührsen, K., Blaxter, M. L., Büttner, D. W., Gallin, M. Y., Al-Qaoud, K. M., Lucius, R. and Fleischer, B. (1999). Tetracycline therapy targets intracellular bacteria in the filarial nematode *Litomosoides sigmodontis* and results in filarial infertility. J Clin Invest *103*, 11–18.

Hoerauf, A., Satoguina, J., Saeftel, M. and Specht, S. (2005). Immunomodulation by filarial nematodes. Parasite Immunol *27*, 417–429.

Hoerauf, A., Specht, S., Büttner, M., Pfarr, K., Mand, S., Fimmers, R., Marfo-Debrekyei, Y., Konadu, P., Debrah, A. Y., Bandi, C., Brattig, N., Albers, A., Larbi, J., Batsa, L., Taylor, M. J., Adjei, O. and Büttner, D. W. (2008). *Wolbachia* endobacteria depletion by doxycycline as antifilarial therapy has macrofilaricidal activity in onchocerciasis: a randomized placebo-controlled study. Med Microbiol Immunol *197*, 295–311.

Hoerauf, A., Volkmann, L., Hamelmann, C., Adjei, O., Autenrieth, I. B., Fleischer, B. and Büttner, D. W. (2000). Endosymbiotic bacteria in worms as targets for a novel chemotherapy in filariasis. Lancet *355*, 1242–1243.

Hoerauf, A. M. (2010). Onchocerciasis. Book, Guerrant *Chapter 106*.

Hoffmann, W., Petit, G., Schulz-Key, H., Taylor, D., Bain, O. and Goff, L. L. (2000). *Litomosoides sigmodontis* in mice: reappraisal of an old model for filarial research. Parasitol Today *16*, 387–389.

Hoogewijs, D., Geuens, E., Dewilde, S., Vierstraete, A., Moens, L., Vinogradov, S. and Vanfleteren, J. R. (2007). Wide diversity in structure and expression profiles among members of the *Caenorhabditis elegans* globin protein family. BMC Genomics *8*, 356.

Hoogewijs, D., Henau, S. D., Dewilde, S., Moens, L., Couvreur, M., Borgonie, G., Vinogradov, S. N., Roy, S. W. and Vanfleteren, J. R. (2008). The *Caenorhabditis* globin gene family reveals extensive nematode-specific radiation and diversification. BMC Evol Biol *8*, 279.

Hooper, S. L., Hobbs, K. H. and Thuma, J. B. (2008). Invertebrate muscles: thin and thick filament structure; molecular basis of contraction and its regulation, catch and asynchronous muscle. Prog Neurobiol *86*, 72–127.

Houston, K. M., Babayan, S. A., Allen, J. E. and Harnett, W. (2008). Does *Litomosoides sigmodontis* synthesize dimethylethanolamine from choline? Parasitology *135*, 55–61.

Iturbe-Ormaetxe, I., Burke, G. R., Riegler, M. and O'Neill, S. L. (2005). Distribution, expression, and motif variability of ankyrin domain genes in *Wolbachia pipientis*. J Bacteriol *187*, 5136–5145.

Johnston, K. L., Wu, B., Guimares, A., Ford, L., Slatko, B. E. and Taylor, M. J. (2010). Lipoprotein biosynthesis as a target for anti-*Wolbachia* treatment of filarial nematodes. Parasit Vectors *3*, 99.

Kanehisa, M. and Goto, S. (2000). KEGG: kyoto encyclopedia of genes and genomes. Nucleic Acids Res *28*, 27–30.

Keiser, P. B., Coulibaly, Y., Kubofcik, J., Diallo, A. A., Klion, A. D., Traor, S. F. and Nutman, T. B. (2008). Molecular identification of *Wolbachia* from the filarial nematode *Mansonella perstans*. Mol Biochem Parasitol *160*, 123–128.

Klasson, L., Walker, T., Sebaihia, M., Sanders, M. J., Quail, M. A., Lord, A., Sanders, S., Earl, J., O'Neill, S. L., Thomson, N., Sinkins, S. P. and Parkhill, J. (2008). Genome evolution of *Wolbachia* strain *w*Pip from the *Culex pipiens* group. Mol Biol Evol *25*, 1877–1887.

Kozek, W. J. (1977). Transovarially-transmitted intracellular microorganisms in adult and larval stages of *Brugia malayi*. J Parasitol *63*, 992–1000.

Kozek, W. J. and Marroquin, H. F. (1977). Intracytoplasmic bacteria in *Onchocerca volvulus*. Am J Trop Med Hyg *26*, 663–678.

Kremer, N., Voronin, D., Charif, D., Mavingui, P., Mollereau, B. and Vavre, F. (2009). *Wolbachia* interferes with ferritin expression and iron metabolism in insects. PLoS Pathog *5*, e1000630.

Landmann, F., Foster, J. M., Slatko, B. and Sullivan, W. (2010). Asymmetric *Wolbachia* Segregation during Early *Brugia malayi* Embryogenesis Determines Its Distribution in Adult Host Tissues. PLoS Negl Trop Dis *4*, e758.

Landmann, F., Orsi, G. A., Loppin, B. and Sullivan, W. (2009). *Wolbachia*-mediated cytoplasmic incompatibility is associated with impaired histone deposition in the male pronucleus. PLoS Pathog *5*, e1000343.

Langworthy, N. G., Renz, A., Mackenstedt, U., Henkle-Dührsen, K., de Bronsvoort, M. B., Tanya, V. N., Donnelly, M. J. and Trees, A. J. (2000). Macrofilaricidal activity of tetracycline against the filarial nematode *Onchocerca ochengi*: elimination of *Wolbachia* precedes worm death and suggests a dependent relationship. Proc Biol Sci *267*, 1063–1069.

Lemire, B. (2005). Mitochondrial genetics. WormBook, 1–10.

Li, B.-W., Rush, A. C., Crosby, S. D., Warren, W. C., Williams, S. A., Mitreva, M. and Weil, G. J. (2005). Profiling of gender-regulated gene transcripts in the filarial nematode *Brugia malayi* by cDNA oligonucleotide array analysis. Mol Biochem Parasitol *143*, 49–57.

Li, B.-W., Rush, A. C., Mitreva, M., Yin, Y., Spiro, D., Ghedin, E. and Weil, G. J. (2009). Transcriptomes and pathways associated with infectivity, survival and immunogenicity in *Brugia malayi* L3. BMC Genomics *10*, 267.

Lo, N., Paraskevopoulos, C., Bourtzis, K., O'Neill, S. L., Werren, J. H., Bordenstein, S. R. and Bandi, C. (2007). Taxonomic status of the intracellular bacterium *Wolbachia pipientis*. Int J Syst Evol Microbiol *57*, 654–657.

Lucius, R. and Textor, G. (1995). *Acanthocheilonema viteae*: rational design of the life cycle to increase production of parasite material using less experimental animals. Appl Parasitol *36*, 22–33.

Mand, S., Pfarr, K., Sahoo, P. K., Satapathy, A. K., Specht, S., Klarmann, U., Debrah, A. Y., Ravindran, B. and Hoerauf, A. (2009). Macrofilaricidal activity and amelioration of lymphatic pathology in bancroftian filariasis after 3 weeks of doxycycline followed by single-dose diethylcarbamazine. Am J Trop Med Hyg *81*, 702–711.

Maris, C., Dominguez, C. and Allain, F. H.-T. (2005). The RNA recognition motif, a plastic RNA-binding platform to regulate post-transcriptional gene expression. FEBS J *272*, 2118–2131.

Masui, S., Sasaki, T. and Ishikawa, H. (2000). Genes for the type IV secretion system in an intracellular symbiont, *Wolbachia*, a causative agent of various sexual alterations in arthropods. J Bacteriol *182*, 6529–6531.

McKee, E. E., Ferguson, M., Bentley, A. T. and Marks, T. A. (2006). Inhibition of mammalian mitochondrial protein synthesis by oxazolidinones. Antimicrob Agents Chemother *50*, 2042–2049.

McLaren, D. J., Worms, M. J., Laurence, B. R. and Simpson, M. G. (1975). Micro-organisms in filarial larvae (Nematoda). Trans R Soc Trop Med Hyg *69*, 509–514.

McMeniman, C. J., Lane, R. V., Cass, B. N., Fong, A. W. C., Sidhu, M., Wang, Y.-F. and O'Neill, S. L. (2009). Stable introduction of a life-shortening *Wolbachia* infection into the mosquito *Aedes aegypti*. Science *323*, 141–144.

McNulty, S. N., Foster, J. M., Mitreva, M., Hotopp, J. C. D., Martin, J., Fischer, K., Wu, B., Davis, P. J., Kumar, S., Brattig, N. W., Slatko, B. E., Weil, G. J. and Fischer, P. U. (2010). Endosymbiont DNA in endobacteria-free filarial nematodes indicates ancient horizontal genetic transfer. PLoS One *5*, e11029.

Meyer, U. A., Schuurmans, M. M. and Lindberg, R. L. (1998). Acute porphyrias: pathogenesis of neurological manifestations. Semin Liver Dis *18*, 43–52.

Moran, N. A. (2003). Tracing the evolution of gene loss in obligate bacterial symbionts. Curr Opin Microbiol *6*, 512–518.

Moreno, Y., Nabhan, J. F., Solomon, J., Mackenzie, C. D. and Geary, T. G. (2010). Ivermectin disrupts the function of the excretory-secretory apparatus in microfilariae of *Brugia malayi*. Proc Natl Acad Sci U S A *107*, 20120–20125.

Morey, J. S., Ryan, J. C. and Dolah, F. M. V. (2006). Microarray validation: factors influencing correlation between oligonucleotide microarrays and real-time PCR. Biol Proced Online *8*, 175–193.

Mosavi, L. K., Cammett, T. J., Desrosiers, D. C. and Peng, Z.-Y. (2004). The ankyrin repeat as molecular architecture for protein recognition. Protein Sci *13*, 1435–1448.

Narita, S., Taketani, S. and Inokuchi, H. (1999). Oxidation of protoporphyrinogen IX in Escherichia coli is mediated by the aerobic coproporphyrinogen oxidase. Mol Gen Genet *261*, 1012–1020.

Negri, I., Pellecchia, M., Grve, P., Daffonchio, D., Bandi, C. and Alma, A. (2010). Sex and stripping: The key to the intimate relationship between *Wolbachia* and host? Commun Integr Biol *3*, 110–115.

Nicolas, E., Morales, V., Magnaghi-Jaulin, L., Harel-Bellan, A., Richard-Foy, H. and Trouche, D. (2000). RbAp48 belongs to the histone deacetylase complex that associates with the retinoblastoma protein. J Biol Chem *275*, 9797–9804.

O'Neill, S. L., Giordano, R., Colbert, A. M., Karr, T. L. and Robertson, H. M. (1992). 16S rRNA phylogenetic analysis of the bacterial endosymbionts associated with cytoplasmic incompatibility in insects. Proc Natl Acad Sci U S A *89*, 2699–2702.

Ono, K. and Ono, S. (2004). Tropomyosin and troponin are required for ovarian contraction in the *Caenorhabditis elegans* reproductive system. Mol Biol Cell *15*, 2782–2793.

Onoda, T., Ono, T., Dhar, D. K., Yamanoi, A. and Nagasue, N. (2006). Tetracycline analogues (doxycycline and COL-3) induce caspase-dependent and -independent apoptosis in human colon cancer cells. Int J Cancer *118*, 1309–1315.

Osei-Atweneboana, M. Y., Eng, J. K. L., Boakye, D. A., Gyapong, J. O. and Prichard, R. K. (2007). Prevalence and intensity of *Onchocerca volvulus* infection and efficacy of ivermectin in endemic communities in Ghana: a two-phase epidemiological study. Lancet *369*, 2021–2029.

Ottesen, E. A., Hooper, P. J., Bradley, M. and Biswas, G. (2008). The global programme to eliminate lymphatic filariasis: health impact after 8 years. PLoS Negl Trop Dis *2*, e317.

Page, A. P. and Johnstone, I. L. (2007). The cuticle. WormBook, 1–15.

Petit, G., Diagne, M., Marchal, P., Owen, D., Taylor, D. and Bain, O. (1992). Maturation of the filaria *Litomosoides sigmodontis* in BALB/c mice; comparative susceptibility of nine other inbred strains. Ann Parasitol Hum Comp *67*, 144–150.

Petryk, A., Warren, J. T., Marqus, G., Jarcho, M. P., Gilbert, L. I., Kahler, J., Parvy, J.-P., Li, Y., Dauphin-Villemant, C. and O'Connor, M. B. (2003). Shade is the *Drosophila* P450 enzyme that mediates the hydroxylation of ecdysone to the steroid insect molting hormone 20-hydroxyecdysone. Proc Natl Acad Sci U S A *100*, 13773–13778.

Pfarr, K., Heider, U. and Hoerauf, A. (2006). RNAi mediated silencing of actin expression in adult *Litomosoides sigmodontis* is specific, persistent and results in a phenotype. Int J Parasitol *36*, 661–669.

Pfarr, K. M., Debrah, A. Y., Specht, S. and Hoerauf, A. (2009). Filariasis and lymphoedema. Parasite Immunol *31*, 664–672.

Pfarr, K. M., Heider, U., Schmetz, C., Büttner, D. W. and Hoerauf, A. (2008). The mitochondrial heat shock protein 60 (HSP60) is up-regulated in *Onchocerca volvulus* after the depletion of *Wolbachia*. Parasitology *135*, 529–538.

Pichon, S., Bouchon, D., Cordaux, R., Chen, L., Garrett, R. A. and Grve, P. (2009). Conservation of the Type IV secretion system throughout *Wolbachia* evolution. Biochem Biophys Res Commun *385*, 557–562.

Rao, A. U., Carta, L. K., Lesuisse, E. and Hamza, I. (2005). Lack of heme synthesis in a free-living eukaryote. Proc Natl Acad Sci U S A *102*, 4270–4275.

Rasgon, J. L., Gamston, C. E. and Ren, X. (2006). Survival of *Wolbachia pipientis* in cell-free medium. Appl Environ Microbiol *72*, 6934–6937.

Rikihisa, Y. and Lin, M. (2010). *Anaplasma phagocytophilum* and *Ehrlichia chaffeensis* type IV secretion and Ank proteins. Curr Opin Microbiol *13*, 59–66.

Ristimäki, A., Narko, K., Enholm, B., Joukov, V. and Alitalo, K. (1998). Proinflammatory cytokines regulate expression of the lymphatic endothelial mitogen vascular endothelial growth factor-C. J Biol Chem *273*, 8413–8418.

Rowley, S. M., Raven, R. J. and McGraw, E. A. (2004). *Wolbachia pipientis* in Australian spiders. Curr Microbiol *49*, 208–214.

Saeftel, M., Arndt, M., Specht, S., Volkmann, L. and Hoerauf, A. (2003). Synergism of gamma interferon and interleukin-5 in the control of murine filariasis. Infect Immun *71*, 6978–6985.

Salisbury, J., Hutchison, K. W. and Graber, J. H. (2006). A multispecies comparison of the metazoan 3'-processing downstream elements and the CstF-64 RNA recognition motif. BMC Genomics *7*, 55.

Salzberg, S. L., Hotopp, J. C. D., Delcher, A. L., Pop, M., Smith, D. R., Eisen, M. B. and Nelson, W. C. (2005). Serendipitous discovery of *Wolbachia* genomes in multiple *Drosophila* species. Genome Biol *6*, R23.

Scott, A. L. and Ghedin, E. (2009). The genome of *Brugia malayi* - all worms are not created equal. Parasitol Int *58*, 6–11.

Scott, A. L., Ghedin, E., Nutman, T. B., McReynolds, L. A., Poole, C. B., Slatko, B. E. and Foster, J. M. (2011). Filarial and *Wolbachia* Genomics. Parasite Immunol *Epub ahead of print.*

Serbus, L. R., Casper-Lindley, C., Landmann, F. and Sullivan, W. (2008). The genetics and cell biology of *Wolbachia*-host interactions. Annu Rev Genet *42*, 683–707.

Serbus, L. R. and Sullivan, W. (2007). A cellular basis for *Wolbachia* recruitment to the host germline. PLoS Pathog *3*, e190.

Sironi, M., Bandi, C., Sacchi, L., Sacco, B. D., Damiani, G. and Genchi, C. (1995). Molecular evidence for a close relative of the arthropod endosymbiont *Wolbachia* in a filarial worm. Mol Biochem Parasitol *74*, 223–227.

Slatko, B. E., Taylor, M. J. and Foster, J. M. (2010). The *Wolbachia* endosymbiont as an anti-filarial nematode target. Symbiosis *51*, 55–65.

Sugimoto, T. N., Fujii, T., Kayukawa, T., Sakamoto, H. and Ishikawa, Y. (2010). Expression of a doublesex homologue is altered in sexual mosaics of *Ostrinia scapulalis* moths infected with *Wolbachia*. Insect Biochem Mol Biol *40*, 847–854.

Sun, L. V., Foster, J. M., Tzertzinis, G., Ono, M., Bandi, C., Slatko, B. E. and O'Neill, S. L. (2001). Determination of *Wolbachia* genome size by pulsed-field gel electrophoresis. J Bacteriol *183*, 2219–2225.

Supali, T., Djuardi, Y., Pfarr, K. M., Wibowo, H., Taylor, M. J., Hoerauf, A., Houwing-Duistermaat, J. J., Yazdanbakhsh, M. and Sartono, E. (2008). Doxycycline treatment of *Brugia malayi*-infected persons reduces microfilaremia and adverse reactions after diethylcarbamazine and albendazole treatment. Clin Infect Dis *46*, 1385–1393.

Taylor, M. J., Bilo, K., Cross, H. F., Archer, J. P. and Underwood, A. P. (1999). 16S rDNA phylogeny and ultrastructural characterization of *Wolbachia* intracellular bacteria of the filarial nematodes *Brugia malayi*, *B. pahangi*, and *Wuchereria bancrofti*. Exp Parasitol *91*, 356–361.

Taylor, M. J., Cross, H. F. and Bilo, K. (2000). Inflammatory responses induced by the filarial nematode *Brugia malayi* are mediated by lipopolysaccharide-like activity from endosymbiotic *Wolbachia* bacteria. J Exp Med *191*, 1429–1436.

Taylor, M. J. and Hoerauf, A. (1999). *Wolbachia* bacteria of filarial nematodes. Parasitol Today *15*, 437–442.

Taylor, M. J., Hoerauf, A. and Bockarie, M. (2010). Lymphatic filariasis and onchocerciasis. Lancet *376*, 1175–1185.

Taylor, M. J., Makunde, W. H., McGarry, H. F., Turner, J. D., Mand, S. and Hoerauf, A. (2005). Macrofilaricidal activity after doxycycline treatment of *Wuchereria bancrofti*: a double-blind, randomised placebo-controlled trial. Lancet *365*, 2116–2121.

Teixeira, L., Ferreira, A. and Ashburner, M. (2008). The bacterial symbiont *Wolbachia* induces resistance to RNA viral infections in *Drosophila melanogaster*. PLoS Biol *6*, e2.

Terami, H., Williams, B. D., Kitamura, S., Sakube, Y., Matsumoto, S., Doi, S., Obinata, T. and Kagawa, H. (1999). Genomic organization, expression, and analysis of the troponin C gene *pat-10* of *Caenorhabditis elegans*. J Cell Biol *146*, 193–202.

Thomas, J. and Weinstein, J. D. (1990). Measurement of heme efflux and heme content in isolated developing chloroplasts. Plant Physiol *94*, 1414–1423.

Toscano, M. A., Commodaro, A. G., Ilarregui, J. M., Bianco, G. A., Liberman, A., Serra, H. M., Hirabayashi, J., Rizzo, L. V. and Rabinovich, G. A. (2006). Galectin-1 suppresses autoimmune retinal disease by promoting concomitant Th2- and T regulatory-mediated anti-inflammatory responses. J Immunol *176*, 6323–6332.

Townson, S., Connelly, C. and Muller, R. (1986). Optimization of culture conditions for the maintenance of *Onchocerca gutturosa* adult worms *in vitro*. J Helminthol *60*, 323–330.

Townson, S., Tagboto, S., McGarry, H. F., Egerton, G. L. and Taylor, M. J. (2006). *Onchocerca* parasites and *Wolbachia* endosymbionts: evaluation of a spectrum of antibiotic types for activity against *Onchocerca gutturosa* in vitro. Filaria J *5*, 4.

Tsang, W. Y., Sayles, L. C., Grad, L. I., Pilgrim, D. B. and Lemire, B. D. (2001). Mitochondrial respiratory chain deficiency in *Caenorhabditis elegans* results in developmental arrest and increased life span. J Biol Chem *276*, 32240–32246.

Turner, J. D., Langley, R. S., Johnston, K. L., Gentil, K., Ford, L., Wu, B., Graham, M., Sharpley, F., Slatko, B., Pearlman, E. and Taylor, M. J. (2009). *Wolbachia* lipoprotein stimulates innate and adaptive immunity through Toll-like receptors 2 and 6 to induce disease manifestations of filariasis. J Biol Chem *284*, 22364–22378.

Tusher, V. G., Tibshirani, R. and Chu, G. (2001). Significance analysis of microarrays applied to the ionizing radiation response. Proc Natl Acad Sci U S A *98*, 5116–5121.

Tzertzinis, G., Egaa, A. L., Palli, S. R., Robinson-Rechavi, M., Gissendanner, C. R., Liu, C., Unnasch, T. R. and Maina, C. V. (2010). Molecular evidence for a functional ecdysone signaling system in *Brugia malayi*. PLoS Negl Trop Dis *4*, e625.

Udall, D. N. (2007). Recent updates on onchocerciasis: diagnosis and treatment. Clin Infect Dis *44*, 53–60.

v Saint Andre, A., Blackwell, N. M., Hall, L. R., Hoerauf, A., Brattig, N. W., Volkmann, L., Taylor, M. J., Ford, L., Hise, A. G., Lass, J. H., Diaconu, E. and Pearlman, E. (2002). The role of endosymbiotic *Wolbachia* bacteria in the pathogenesis of river blindness. Science *295*, 1892–1895.

Volkmann, L., Bain, O., Saeftel, M., Specht, S., Fischer, K., Brombacher, F., Matthaei, K. I. and Hoerauf, A. (2003). Murine filariasis: interleukin 4 and interleukin 5 lead to containment of different worm developmental stages. Med Microbiol Immunol *192*, 23–31.

Voronin, D. A., Dudkina, N. V. and Kiseleva, E. V. (2004). A new form of symbiotic bacteria *Wolbachia* found in the endoplasmic reticulum of early embryos of *Drosophila melanogaster*. Dokl Biol Sci *396*, 227–229.

Walker, T., Klasson, L., Sebaihia, M., Sanders, M. J., Thomson, N. R., Parkhill, J. and Sinkins, S. P. (2007). Ankyrin repeat domain-encoding genes in the *w*Pip strain of *Wolbachia* from the *Culex pipiens* group. BMC Biol *5*, 39.

Werren, J. H., Baldo, L. and Clark, M. E. (2008). *Wolbachia*: master manipulators of invertebrate biology. Nat Rev Microbiol *6*, 741–751.

Werren, J. H. and Windsor, D. M. (2000). *Wolbachia* infection frequencies in insects: evidence of a global equilibrium? Proc Biol Sci *267*, 1277–1285.

WHO (2008). Global programme to eliminate lymphatic filariasis. Wkly Epidemiol Rec *83*, 333348.

WHO (2010a). African Programme for Onchocerciasis Control - report of the sixth meeting of national task forces, October 2009. Wkly Epidemiol Rec *85*, 23–28.

WHO (2010b). Progress report 2000-2010 and strategic plan 2010-2020 of the Global Programme to Eliminate Lymphatic Filariasis: halfway towards eliminating lymphatic filariasis.

Wu, B., Novelli, J., Foster, J., Vaisvila, R., Conway, L., Ingram, J., Ganatra, M., Rao, A. U., Hamza, I. and Slatko, B. (2009). The heme biosynthetic pathway of the obligate *Wolbachia* endosymbiont of *Brugia malayi* as a potential anti-filarial drug target. PLoS Negl Trop Dis *3*, e475.

Wu, M., Sun, L. V., Vamathevan, J., Riegler, M., Deboy, R., Brownlie, J. C., McGraw, E. A., Martin, W., Esser, C., Ahmadinejad, N., Wiegand, C., Madupu, R., Beanan, M. J., Brinkac, L. M., Daugherty, S. C., Durkin, A. S., Kolonay, J. F., Nelson, W. C., Mohamoud, Y., Lee, P., Berry, K., Young, M. B., Utterback, T., Weidman, J., Nierman, W. C., Paulsen, I. T., Nelson, K. E., Tettelin, H., O'Neill, S. L. and Eisen, J. A. (2004). Phylogenomics of the reproductive parasite *Wolbachia pipientis* *w*Mel: a streamlined genome overrun by mobile genetic elements. PLoS Biol *2*, E69.

A. Appendix

Table A.1.: List of videos of *L. sigmodontis* and *A. viteae ex vivo* culture experiments. Videos are available on enclosed DVD.

Video No.	**Description of contents**
	Motility scoring
1	Examples of *L. sigmodontis* motility scoring 0 - 5
2	Examples of *A. viteae* motility scoring 0 - 5
	L. sigmodontis ex vivo culture: control, 500 µM/1 mM wALADin1, 3 mM SA
3	Day 0
4	Day 3
5	Day 9
6	Day 14
	A. viteae ex vivo culture: control, 500 µM/1 mM wALADin1, 3 mM SA
7	Day 0, before treatment
8	Day 0, 1.5 h after addition of drug
9	Day 3
10	Day 9
11	Day 14
	A. viteae ex vivo culture: control and 5 mM 5-ALA
12	Day 0 (before treatment and 1.5 h after addition of drug), day 3 and 14

B. Appendix

Table B.1.: Up- and down-regulated filarial genes at day 6 of tetracycline treatment

Oligo ID	FDR %	Fold change	Model Name or EST	*B. malayi* locus	Annotation or blast match
Up-regulated genes					
bm.00032	2,79	2,38	BMC00075	Bm1_55000	troponin-T
Down-regulated genes					
bm.01065	2,79	0,49	BMC04361	Bm1_46680	26S proteasome subunit P45 family protein
BMX577	1,76	0,44	12902.m00230	Bm1_03910	40S ribosomal protein S27, putative
BMX3571	4,15	0,47	14652.m00402	Bm1_22990	actin-depolymerizing factor 1, putative
BMX9144	1,76	0,37	15470.m00007	Bm1_57025	ADP-ribosylation factor 1, putative
BMX3068	3,35	0,48	14469.m00103	Bm1_19880	Autoantigen NGP-1, putative
BMX6459	4,94	0,39	14972.m07843	Bm1_40640	conserved hypothetical protein
BMX4090	1,76	0,44	14782.m00009	Bm1_19520	conserved hypothetical protein
BMX10446	3,35	0,40	AW191516	Bm1_13830	eukaryotic initiation factor 4A
BMX6796	4,15	0,39	14975.m04474	Bm1_42660	fizzy-related protein, putative
BMX7493	1,76	0,49	14981.m02382	Bm1_46715	Gaba, putative
bm.02929	2,79	0,32	BMC07434	Bm1_24940	galectin, putative
BMX4949	4,61	0,45	14954.m01743	Bm1_31380	glycogen synthase kinase 3 alpha, putative
BMX6316	4,15	0,49	14972.m07666	Bm1_39805	GMC oxidoreductase family protein
BMX2838	0,00	0,23	14361.m00189	Bm1_18395	Hepatic leukemia factor, putative
BMX7231	4,61	0,49	14979.m04549	Bm1_45200	High mobility group protein 1.2, putative
bm.00432	1,76	0,50	BMC01644	Bm1_25620	high mobility group protein, putative
bm.01720	1,76	0,33	BMC11925	Bm1_45075	HMG box family protein
BMX5096	4,61	0,47	14961.m04954	Bm1_32310	Innexin family protein
BMX5537	4,15	0,44	14967.m01540	Bm1_35075	Innexin inx-3, putative
BMX5161	2,53	0,46	14961.m05031	Bm1_32700	Leucine carboxyl methyltransferase family protein
BMX3761	4,15	0,36	14704.m00452	Bm1_24150	mbt repeat family protein
BMX2325	4,15	0,45	14157.m00017	Bm1_03265	N-terminal acetyltransferase complex ARD1 subunit homolog, putative
BMX8645	3,35	0,48	15081.m00161	Bm1_53755	NADH-ubiquinone oxidoreductase subunit B14.5b, putative
BMX5408	0,00	0,30	14961.m05354	Bm1_34295	Neurotransmitter-gated ion-channel ligand binding domain containing protein
BMX8754	4,15	0,45	15161.m00148	Bm1_54505	oxidoreductase, zinc-binding dehydrogenase family protein
BMX9886	4,15	0,44	AA841464	Bm1_14590	Probable U6 snRNA-associated Sm-like protein LSm4, putative
BMX3351	3,35	0,49	14590.m00346	Bm1_21620	Profilin family protein
BMX2627	4,15	0,50	14276.m00250	Bm1_17085	proteasome subunit alpha type 4, putative
BMX136	1,76	0,50	12512.m00025	Bm1_00955	Protein kinase domain containing protein
BMX16	2,79	0,47	12417.m00015	Bm1_00130	Protein kinase domain containing protein
BMX7409	4,94	0,37	14980.m02764	Bm1_46210	Protein kinase domain containing protein
bm.02416	2,79	0,40	BMC11777	Bm1_14145	protein phosphatase PP2A regulatory subunit, putative
BMX6123	1,76	0,47	14972.m07434	Bm1_38675	PurA ssDNA and RNA-binding protein
bm.01810	1,76	0,38	BMC03608	Bm1_32095	Ras-related protein Rab-6B, putative
BMX9089	2,79	0,35	15424.m00007	Bm1_56635	RE63138p, putative
bm.02415	1,76	0,31	BMC08875	Bm1_15930	retinoblastoma-binding protein, putative
BMX2440	1,76	0,32	14224.m00309	Bm1_15930	retinoblastoma-binding protein, putative
bm.02856	1,76	0,45	BMC11307	Bm1_57630	retinoblastoma-binding protein., putative

BMX2977	3,35	0,38	14412.m00158	Bm1_19325	RNA and export factor binding protein 2, putative
bm.00326	2,53	0,46	BMC01082	Bm1_24070	RNA recognition motif domain containing protein
bm.01654	1,76	0,28	BMC11108	Bm1_46695	RNA recognition motif.
bm.02941	2,53	0,44	BMC00658	Bm1_17780	signal recognition particle 54 kDa protein (SRP54), putative
BMX3352	2,01	0,43	14590.m00348	Bm1_21630	transcription elongation factor B polypeptide 1, putative
BMX4463	4,15	0,44	14930.m00346	Bm1_28480	translation elongation factor aEF-2, putative
BMX1320	4,94	0,44	13409.m00048	Bm1_08695	trehalose-6-phosphate synthase, putative
BMX7233	2,79	0,50	14979.m04551	Bm1_45210	Ubiquitin-like protein SMT3, putative
BMX6196	4,15	0,35	14972.m07521	Bm1_39100	V-ATPase subunit C family protein
bm.02489	2,79	0,48	BMC06799	Bm1_39100	V-ATPase subunit C family protein
BMX8923	2,53	0,48	15268.m00008	Bm1_55505	hypothetical protein
BMX2358	3,35	0,39	14181.m00071	Bm1_15420	hypothetical protein
BMX6102	4,94	0,37	14972.m07406	Bm1_38535	hypothetical protein
BMX3239	4,15	0,45	14542.m00051	Bm1_20915	hypothetical protein
BMX3136	1,76	0,47	14500.m00155	Bm1_20270	hypothetical protein
BMX3270	1,76	0,38	14559.m00034	Bm1_21110	hypothetical protein
BMX2107	4,15	0,41	14038.m00030	Bm1_13865	hypothetical protein
BMX9338	4,15	0,28	AA110565		hypothetical protein W02A2.9
BMX7420	3,35	0,36	14980.m02778	Bm1_46275	Hypothetical UPF0185 protein ZK652.3 in chromosome III, putative

Table B.2.: Up- and down-regulated filarial genes at day 15 of tetracycline treatment

Oligo ID	**FDR** %	**Fold change**	**Model Name or EST**	***B. malayi* locus**	**Annotation or blast match**
Up-regulated genes					
BMX208	4,95	2,00	12577.m00007	Bm1_01465	cuticular collagen Bmcol-2
BMX12229	4,36	2,73	BMC00075	Bm1_30045	hypothetical protein
bm.01661	4,36	2,91	BMC11473		no match
Down-regulated genes					
BMX6517	0,00	0,15	14973.m02591	Bm1_40960	Chymotrypsin/elastase isoinhibitors 2 to 5, putative
BMX13295	0,00	0,47	TC3302	Bm1_17480	cuticle collagen
BMX2838	0,00	0,47	14361.m00189	Bm1_18395	Hepatic leukemia factor, putative
BMX1993	0,00	0,06	13945.m00125	Bm1_13070	conserved hypothetical protein
BMX12963	0,00	0,20	TC2959		no_match

Table B.3.: Up- and down-regulated filarial genes at day 36 of tetracycline treatment

Oligo ID	**FDR** %	**Fold change**	**Model Name or EST**	***B. malayi* locus**	**Annotation or blast match**
Up-regulated genes					
bm.00007	0,84	2,30	BMC00011		40S ribosomal protein S6
bm.00532	0,00	5,96	BMC02077		5S ribosomal RNA gene
BMX4795	2,48	2,02	14952.m01388	Bm1_30435	ABC transporter, putative
BMX6847	4,28	2,12	14975.m04536	Bm1_42975	Acetyl-CoA hydrolase/transferase family protein
bm.02799	2,79	2,05	BMC09181	Bm1_28250	amidase, putative
BMX12198	1,84	6,15	WB-contig_1369		Ascaris lumbricoides small nuclear RNA (snRNA) U1-1, U1-2, U1-3, U1-4 genes
BMX12816	1,84	2,51	TC2809	AF538716	ATP synthase F0 subunit 6
BMX11446	2,48	2,21	BMW00445.38	Bm1_52675	ATP-dependent RNA helicase DDX5/DBP2
bm.00104	1,34	2,31	BMC00238	Bm1_28435	Bm-Mif-1, identical
BMX7866	3,13	2,49	14990.m07940	Bm1_49080	Calponin homolog OV9M., putative
bm.03088	1,34	2,22	BMC06828	Bm1_36555	collagen col-34, putative
bm.03416	4,28	2,18	BMC11971	Bm1_13245	Cuticle collagen C09G5.5, putative
bm.03300	2,48	2,03	BMC04762	Bm1_13245	Cuticle collagen C09G5.5, putative
BMX12481	0,00	2,93	WB-contig_187	AF538716	cytochrome b
BMX12492	3,59	2,00	WB-contig_207	AF538716	cytochrome b

bm.03368	2,48	2,22	BMC11632	AF538716	cytochrome b
BMX12792	2,79	3,50	TC2778	AF538716	cytochrome c oxidase subunit I
BMX10990	0,84	2,89	TC7739	AF538716	cytochrome c oxidase subunit I
BMX12477	0,84	2,72	WB-contig_182	AF538716	cytochrome c oxidase subunit I
bm.03325	1,34	2,47	BMC06165	AF538716	cytochrome c oxidase subunit I
BMX12794	3,13	2,32	TC2780	AF538716	cytochrome c oxidase subunit I
BMX11370	0,84	2,70	BMW00283.860	AF538716	cytochrome c oxidase subunit I
bm.03436	2,48	2,22	BMC12111	AF538716	cytochrome c oxidase subunit I
bm.01757	0,84	2,70	BMC12170	AF538716	cytochrome c oxidase subunit I
bm.03171	1,34	2,81	BMC00030	AF538716	cytochrome c oxidase subunit II
bm.03082	2,79	2,31	BMC06256	AF538716	cytochrome c oxidase subunit II
bm.03174	1,34	2,40	BMC00071	AF538716	cytochrome c oxidase subunit II
bm.03438	0,00	2,82	BMC12116	AF538716	cytochrome c oxidase subunit II
bm.03045	0,00	3,05	BMC00359	AF538716	cytochrome c oxidase subunit III
bm.00380	0,00	27,36	BMC01393	AF538716	cytochrome c oxidase subunit III
BMX12806	0,84	2,48	TC2796	Bm1_48810	EF hand family protein, Troponin C (tnc-1)
BMX11372	0,52	2,60	BMW00285.523	Bm1_48810	EF hand family protein, Troponin C (tnc-1)
bm.03443	1,34	2,26	BMC12124	Bm1_48810	EF hand family protein, Troponin C (tnc-1)
BMX11740	1,24	2,25	BMW01217.101	Bm1_48810	EF hand family protein, Troponin C (tnc-1)
BMX5583	2,79	2,86	14968.m01464	Bm1_35360	EGF-like domain containing protein
BMX12421	1,34	2,10	WB-contig_1637	Bm1_33155	gelsolin, putative
BMX8086	0,00	4,78	14992.m10859	Bm1_50430	Globin family protein
bm.01805	2,48	2,03	BMC02156	Bm1_26160	Ground-like domain containing protein
bm.00432	1,34	2,26	BMC01644	Bm1_25620	high mobility group protein, putative
bm.01434	3,13	2,08	BMC06812	Bm1_32130	Hsp20/alpha crystallin family protein
bm.03350	3,59	2,01	BMC09956	Bm1_15210	conserved hypothetical protein
bm.03546	0,00	2,99	BMC00600	AF538716	large subunit ribosomal RNA, mitochondrial
BMX12812	1,34	2,36	TC2803	AF538716	NADH dehydrogenase subunit 1
bm.03545	1,84	2,54	BMC00485	AF538716	NADH dehydrogenase subunit 1
BMX11795	3,59	2,20	BMW01358.408	AF538716	NADH dehydrogenase subunit 2
BMX12282	1,34	2,43	WB-contig_1474	AF538716	NADH dehydrogenase subunit 2
BMX13241	2,48	2,64	TC3244	AF538716	NADH dehydrogenase subunit 3
BMX13096	3,13	2,15	TC3096	AF538716	NADH dehydrogenase subunit 5
BMX11838	1,34	2,28	BMW01496.504	Bm1_17485	Nematode cuticle collagen N-terminal domain containing protein
BMX11969	2,79	2,00	WB-contig_1102	Bm1_27595	nematode cuticle collagen, N-terminal domain
bm.03038	2,48	2,33	gi|443682|gb|L27686.1| ONGIGGORF		Onchocerca volvulus retinoid binding protein precursor, mRNA
BMX12596	3,59	2,14	WB-contig_369	Bm1_41305	phosphatidylserine decarboxylase proenzyme, putative
BMX9936	3,13	2,07	AA841929	Bm1_18520	Protein kinase domain containing protein, CDK family
bm.02455	1,84	2,09	BMC00090	Bm1_37575	Protein kinase domain containing protein, similar to c-met
BMX10922	3,59	2,28	N89547		putative RNA binding protein (bm-rbp-1)
bm.03194	0,84	3,63	BMC00185	Bm1_37780	RNA binding protein
BMX5979	3,59	2,41	14972.m07250	Bm1_37780	RNA binding protein, identical
bm.00761	1,84	2,32	BMC03055	Bm1_37185	Saposin-like type B, region 1 family protein
BMX8848	3,13	2,30	15217.m00022	Bm1_55060	SET domain containing protein
bm.02729	3,59	2,08	BMC06625		similar to RNA helicase p68 (DDX5)
BMX11224	1,34	2,79	BMW00034.265	AF538716	small subunit ribosomal RNA, mitochondrial
BMX634	0,00	7,02	12962.m00049	Bm1_04280	snRNA U2-1 gene, snRNA U2-2 pseudogenes, and snRNA U2-1
BMX13116	0,00	7,32	TC3117	Bm1_04280	snRNA U2-1 gene, snRNA U2-2 pseudogenes, and snRNA U2-1
BMX12521	0,00	6,22	WB-contig_256	Bm1_04280	snRNA U2-1 gene, snRNA U2-2 pseudogenes, and snRNA U2-1
BMX120	1,84	4,64	12498.m00044	Bm1_00840	succinyl-CoA ligase [ADP-forming] beta-chain, mitochondrial, putative
BMX5661	3,13	2,12	14971.m02813	Bm1_35865	TGF-beta induced apoptosis protein 2, putative
BMX11378	1,34	2,85	BMW00296.538	Bm1_09630	Transcription factor

BMX13174	1,84	2,27	TC3177	Bm1_06445	Transthyretin-like family protein
BMX12574	2,79	2,01	WB-contig_339	Bm1_01235	Tropomyosin, putative
bm.00032	0,84	2,78	BMC00075	Bm1_55000	Troponin T
BMX12801	1,84	2,07	TC2790	Bm1_55000	Troponin T
bm.00553	0,00	6,16	BMC02185		no match
BMX4544	2,48	3,43	14938.m00329	Bm1_13985	Zinc finger, C2H2 type family protein
bm.03154	1,34	2,06	BMC12254		no match
BMX5835	1,84	2,11	14972.m07082	Bm1_36960	conserved hypothetical protein
BMX1246	3,13	2,04	13367.m00045	Bm1_08200	conserved hypothetical protein
BMX5031	2,48	2,28	14958.m00358	Bm1_31905	Conserved hypothetical protein, putative
bm.00738	0,00	9,52	BMC02980	Bm1_30045	hypothetical protein
BMX4726	0,00	7,56	14950.m01825	Bm1_30045	hypothetical protein
BMX6509	2,48	2,15	14973.m02582	Bm1_40920	hypothetical protein
BMX977	1,84	2,07	13253.m00068	Bm1_06495	hypothetical protein
BMX12074	3,13	2,01	WB-contig_1229		hypothetical protein
bm.03139	1,34	2,39	BMC00307		hypothetical protein
BMX12229	0,00	7,19	WB-contig_1411	Bm1_30045	hypothetical protein
BMX663	3,59	2,23	13016.m00022	Bm1_04515	hypothetical protein
BMX176	1,34	2,95	12548.m00028	Bm1_01160	hypothetical protein
BMX6250	4,28	3,12	14972.m07589	Bm1_39435	hypothetical protein
BMX11863	3,13	3,21	BMW01588.491		hypothetical protein
BMX2148	2,48	2,46	14052.m00190	Bm1_14110	hypothetical protein
BMX11622	0,00	2,54	BMW00915.413		hypothetical protein
BMX13363	0,52	2,61	TC3370		hypothetical protein
bm.01661	0,00	3,50	BMC11473		hypothetical protein
bm.03409	3,59	4,82	BMC11908	Bm1_15895	hypothetical protein
BMX12514	0,00	5,47	WB-contig_247	Bm1_03790	hypothetical protein
BMX860	1,34	2,22	13186.m00013	Bm1_05750	hypothetical protein
BMX664	4,28	3,64	13022.m00018	Bm1_04540	hypothetical protein
BMX5153	2,48	3,83	14961.m05023	Bm1_32660	hypothetical protein
BMX1916	0,00	4,77	13891.m00014	Bm1_12555	hypothetical protein
BMX7604	1,84	2,31	14982.m02250	Bm1_47370	hypothetical protein
BMX12188	1,84	2,59	WB-contig_136	Bm1_11040	hypothetical protein
bm.00050	1,34	2,07	BMC00114	Bm1_47225	hypothetical protein, putative
bm.02312	1,34	2,40	BMC07204	Bm1_04980	Hypothetical RING finger protein F54G8.4 in chromosome III, putative
BMX730	1,84	2,27	13081.m00126	Bm1_04980	Hypothetical RING finger protein F54G8.4 in chromosome III, putative
BMX4160	3,13	2,01	14830.m00076	Bm1_26585	Hypothetical UPF0205 protein C40H1.5 in chromosome III precursor, putative
bm.01554	2,48	2,45	BMC07907		no match
BMX11823	2,48	2,79	BMW01444.86		no match
bm.03330	1,34	2,92	BMC06439		no match
bm.03432	0,84	2,83	BMC12091		no match
bm.03316	0,00	2,83	BMC05768		no match
bm.03233	0,84	2,53	BMC01489		no match
bm.01474	2,48	2,59	BMC07089		no match
bm.00248	2,79	2,57	BMC00802		no match
BMX10049	1,34	2,76	AI043369		no match
BMX11412	0,52	2,74	BMW00374.174		no match
BMX11927	2,79	2,12	WB-contig_1051		no match
bm.03269	2,48	2,30	BMC02796		no match
BMX12848	1,34	2,30	TC2843		no match
BMX10707	3,59	2,01	CD570734		no match
BMX11787	1,34	2,02	BMW01339.1		no match
BMX11857	2,48	2,05	BMW01563.274		no match
BMX11405	2,79	2,06	BMW00355.11		no match
BMX11194	3,59	2,06	BMBC_gene_64.1319		no match
bm.03424	1,34	2,58	BMC12074		no match
BMX11862	2,48	2,38	BMW01584.43		no match
BMX11569	3,59	2,23	BMW00757.255		no match

bm.00760	1,34	2,09	BMC03051		no match
BMX11687	1,84	2,10	BMW01104.236		no match
bm.03147	1,34	2,11	BMC07069		no match
bm.01018	0,00	9,57	BMC04151		no match
BMX11926	0,00	7,65	WB-contig_1050		no match
BMX11761	1,34	2,24	BMW01276.443		no match
BMX12927	0,00	4,12	TC2922		no match
BMX11067	4,28	2,12	W00314		no match
BMX12251	1,34	2,31	WB-contig_1438		no match
BMX12274	1,34	3,35	WB-contig_1466		no match
BMX10628	2,48	2,08	CB328940		no match
bm.00033	0,00	3,60	BMC00077		no match
bm.01634	0,00	3,42	BMC10048		no match
BMX10005	0,00	2,93	AA842849		no match
BMX11510	2,48	2,16	BMW00613.288		no match
BMX11537	1,34	2,04	BMW00684.508		no match
bm.03351	0,00	3,22	BMC09976		no match
Down-regulated genes					
BMX9813	1,52	0,18	AA840846		16S rRNA gene, bacterial
bm.03452	2,48	0,47	BMC12165	Bm1_09900	40S ribosomal protein S7, putative
BMX13179	1,52	0,31	TC3182	Bm1_46405	50S ribosomal protein L21, mitochondrial precursor
bm.03243	4,28	0,36	BMC01716	Bm1_07030	60S ribosomal protein L12
bm.00263	2,48	0,43	BMC00864	Bm1_23030	60S ribosomal protein L18a
bm.00397	1,52	0,34	BMC01506	Bm1_47445	60S ribosomal protein L21, putative
BMX4542	2,79	0,45	14937.m00494	Bm1_28975	60S ribosomal protein L27, putative
BMX2112	1,52	0,37	14039.m00115	Bm1_13895	60S ribosomal protein L3, putative
BMX12710	2,79	0,39	WB-contig_530	Bm1_13895	60S ribosomal protein L3, putative
BMX12573	3,13	0,50	WB-contig_338	Bm1_24260	6330505F04Rik protein, putative
BMX1007	2,79	0,48	13261.m00257	Bm1_06670	Acid phosphatase F26C11.1, putative
BMX3428	1,52	0,43	14610.m00102	Bm1_22105	acyl-CoA desaturase, putative
BMX856	2,79	0,33	13183.m00075	Bm1_05725	Acyltransferase family protein
bm.00853	3,59	0,48	BMC03403	Bm1_19050	ADIPOR-like receptor C43G2.1, putative
BMX2534	1,52	0,42	14246.m00079	Bm1_16495	ADP-sugar pyrophosphatase , putative
BMX8610	2,48	0,37	15062.m00043	Bm1_53535	alanyl-tRNA synthetase family protein
BMX196	4,28	0,48	12568.m00015	Bm1_01370	alpha-1,3-mannosyltransferase, putative
BMX3477	2,48	0,46	14623.m00077	Bm1_22410	ATP-dependent RNA helicase DDX18
bm.02069	3,59	0,50	BMC05925	Bm1_46895	Autophagocytosis associated protein, C-terminal domain containing protein
bm.02386	0,00	0,23	BMC10217		bacterial adhesin
BMX4479	1,52	0,41	14931.m00329	Bm1_28580	bifunctional aminoacyl-tRNA synthetase, putative
BMX7517	0,00	0,13	14981.m02410	Bm1_46865	Biopterin-dependent aromatic amino acid hydroxylase family protein
bm.01896	1,52	0,10	BMC09332	Bm1_51990	BRM protein, putative
BMX3794	3,59	0,49	14710.m00262	Bm1_24355	calcium ATPase, putative
BMX7234	4,28	0,46	14979.m04553	Bm1_45220	CG7038-PA, putative
BMX2989	4,28	0,38	14417.m00066	Bm1_19385	CG7192-PB, ESCRT-I complex subunit MVB12
BMX13366	1,52	0,44	TC3373	Bm1_52920	Chain B, Crystal Structure Of The D1d2 Sub-Complex From The Human Snrnp Core Domain
BMX8276	3,13	0,48	14992.m11086	Bm1_51525	chromosome 14 open reading frame 153, putative
BMX3771	2,48	0,39	14705.m00192	Bm1_24215	CHY zinc finger family protein
BMX723	3,13	0,31	13074.m00011	Bm1_03260	coronin 2A, putative
BMX5114	2,48	0,49	14961.m04976	Bm1_32425	CRAL/TRIO domain containing protein
bm.01302	2,79	0,49	BMC06039	Bm1_13860	Cyclin, N-terminal domain containing protein
BMX13369	1,84	0,50	TC3376	Bm1_52100	cyclophilin-type peptidyl-prolyl cis-trans isomerase-13, Bmcyp-13
BMX11137	3,59	0,47	BMB_gene_13.435	Bm1_21700	cyclophilin-type peptidyl-prolyl cis-trans isomerase-4, Bmcyp-4
BMX13028	1,84	0,37	TC3026	Bm1_02045	cysteine-rich protein 1, putative
BMX301	0,84	0,35	12628.m00036	Bm1_02045	cysteine-rich protein 1, putative

BMX7969	4,28	0,50	14990.m08067		Cytochrome c oxidase assembly protein CtaG / Cox11 containing protein
BMX12230	1,52	0,29	WB-contig_1412	Bm1_31675	Death domain containing protein
BMX6842	2,48	0,28	14975.m04530	Bm1_42945	diphosphomevalonate decarboxylase family protein
BMX7438	1,52	0,46	14980.m02798	Bm1_46365	DIRP family protein
bm.02690	2,48	0,48	BMC03590	Bm1_45070	DNA / pantothenate metabolism flavoprotein
bm.02962	2,79	0,43	BMC07387	Bm1_27955	EF-1 guanine nucleotide exchange domain containing protein
BMX8031	4,28	0,45	14990.m08149	Bm1_50100	EST embl—AI107989—AI107989 comes from the 3' UTR, putative
BMX13481	2,48	0,47	TC3493	Bm1_32915	Eukaryotic translation initiation factor 4E type 3, putative
BMX3080	1,52	0,42	14478.m00108	Bm1_19955	excretory/secretory protein Juv-p120 precursor, putative
BMX3081	3,59	0,44	14478.m00109	Bm1_00865	excretory/secretory protein Juv-p120 precursor, putative
BMX3809	2,79	0,36	14712.m00229	Bm1_24435	exodeoxyribonuclease III family protein
bm.01844	2,79	0,49	BMC02897	Bm1_38160	Fatty acid desaturase family protein
BMX7078	0,84	0,27	14977.m05104	Bm1_44270	GATA zinc finger family protein
bm.01994	1,84	0,43	BMC11004	Bm1_39355	GDP-fucose protein O-fucosyltransferase 2 precursor, putative
BMX11652	2,79	0,48	BMW01009.534	Bm1_31280	Gex interacting protein protein 10, isoform a, putative
BMX6596	1,52	0,34	14973.m02692	Bm1_41495	Gex interacting protein protein 4, isoform c, putative
BMX7403	1,52	0,35	14980.m02757	Bm1_46175	Glutamate receptor 2 precursor.-related
bm.02518	3,13	0,45	BMC04064	Bm1_25005	Glutamate-rich WD-repeat protein 1, putative
BMX7383	1,52	0,40	14980.m02727	Bm1_46035	Gro-1 operon protein 2, putative
BMX2449	3,59	0,30	14227.m00028	Bm1_15980	guanine nucleotide-binding protein G(o), alpha subunit, putative
BMX6627	4,28	0,19	14974.m00799	Bm1_41670	Haemolysin-III related family protein
bm.02396	1,84	0,50	BMC07369	Bm1_10400	haloacid dehalogenase-like hydrolase domain containing 2, putative
bm.00164	3,13	0,48	BMC00470	Bm1_43675	heat shock 70 kDa protein, putative
BMX12036	0,52	0,31	WB-contig_1184	Bm1_43675	heat shock 70 kDa protein, putative
BMX671	1,52	0,43	13032.m00029	Bm1_04585	Hepatocellular carcinoma-associated antigen 59 family protein
bm.01606	1,52	0,37	BMC08827	Bm1_20285	histone H2A
BMX4000	3,13	0,47	14768.m00181	Bm1_25575	hrp36.1, putative
BMX6519	2,48	0,39	14973.m02593	Bm1_40970	Hsp20/alpha crystallin family protein
BMX5997	4,28	0,49	14972.m07280	Bm1_37925	initiation factor 2-associated protein., putative
BMX11365	3,13	0,50	BMW00275.499	Bm1_38165	Lanthionine synthetase C-like protein
bm.03203	3,59	0,35	BMC00271	AAN62757.1	larval allergen
BMX6540	1,84	0,38	14973.m02621	Bm1_41125	LBP / BPI / CETP family, N-terminal domain containing protein
BMX3718	2,79	0,44	14696.m00211	Bm1_23910	lipoic acid synthetase, mitochondrial precursor, putative
BMX13070	1,52	0,47	TC3070	Bm1_17915	Mak16 protein
BMX13288	0,84	0,23	TC3295	Bm1_23975	MED7 protein
BMX13319	3,13	0,50	TC3326	Bm1_23975	MED7 protein
bm.00413	3,13	0,50	BMC01584	Bm1_54980	Mediator protein 18, putative
BMX5430	1,52	0,41	14962.m00668	Bm1_34420	MGC52693 protein, putative
BMX7873	1,84	0,45	14990.m07948	Bm1_49110	MGC86306 protein
bm.01727	4,28	0,44	BMC11946	Bm1_41590	Mitochondrial import inner membrane translocase subunit Tim17 family protein
BMX12258	1,52	0,23	WB-contig_1447		NADH:ubiquinone dehydrogenase, putative
BMX334	3,59	0,23	12665.m00135	Bm1_02270	OTU-like cysteine protease family protein
BMX1400	3,59	0,31	13458.m00087	Bm1_09210	Partner of SLD five, PSF1 family protein
BMX1224	3,13	0,41	13358.m00040	Bm1_08075	Paxneb protein, putative

bm.01734	3,59	0,45	BMC11983	Bm1_54480	Peptidyl-tRNA hydrolase domain containing protein
BMX7134	1,84	0,50	14979.m04429	Bm1_44615	Phosphatidylcholine:ceramide cholinephosphotransferase 3, putative
BMX13266	3,13	0,49	TC3271	Bm1_22915	Phospholipase/Carboxylesterase family protein
BMX4461	2,79	0,45	14930.m00344	Bm1_28470	Probable DNA replication complex GINS protein PSF2, putative
bm.02654	2,48	0,32	BMC07408	Bm1_40665	probable homocysteine S-methyltransferase, putative
BMX6492	2,79	0,40	14972.m07881	Bm1_40820	Probable inner membrane protein OXA1L2, putative
bm.03394	2,79	0,33	BMC11783	Bm1_38970	Probable nucleolar GTP-binding protein 1
bm.02841	1,84	0,43	BMC09283	Bm1_30555	Proteasome A-type and B-type family protein
BMX8873	2,79	0,44	15233.m00030	Bm1_55200	Proteasome A-type and B-type family protein
BMX12704	1,84	0,38	WB-contig_523	Bm1_50865	Protein KIAA0174, putative
BMX6027	3,13	0,41	14972.m07316	Bm1_38095	Protein kinase domain containing protein
BMX11817	3,59	0,36	BMW01427.519	Bm1_51830	Protein kinase domain containing protein
BMX13426	3,59	0,50	TC3435	Bm1_56705	protein x 0004, putative
BMX5139	3,59	0,48	14961.m05007	Bm1_32580	Protein-tyrosine phosphatase containing protein
BMX7218	3,13	0,50	14979.m04531	Bm1_45110	PX domain containing protein
BMX4706	0,00	0,31	14950.m01801	Bm1_29925	Rab5 GDP/GTP exchange factor, putative
bm.03070	3,13	0,41	BMC04800		radical SAM domain protein
BMX6503	2,48	0,47	14972.m07894	Bm1_40885	Ras family protein
BMX3765	1,84	0,33	14704.m00458	Bm1_24180	Ras-related protein Rap-2c, putative
bm.00500	2,79	0,46	BMC01914	Bm1_38100	Rhodanese-like domain containing protein
BMX9069	3,13	0,41	15398.m00011	Bm1_56480	RhoGAP domain containing protein
bm.01962	1,52	0,29	BMC11877	Bm1_52810	Ribosome biogenesis protein BMS1 homolog, putative
bm.00181	3,59	0,47	BMC00539	Bm1_47790	RNA polymerase Rpc34 subunit family protein
bm.02854	3,13	0,50	BMC06741	Bm1_56655	RNA-binding protein., putative
BMX95	1,52	0,36	12481.m00076	Bm1_00700	RNA, U transporter 1, putative
BMX2219	4,28	0,46	14089.m00011	Bm1_14575	Salivary glue protein Sgs-4 precursor, putative
bm.03019	2,48	0,47	BMC03755	Bm1_49815	SCAMP family protein
BMX9465	1,84	0,36	AA241571	Bm1_23870	SEC14-like protein 4
bm.02497	2,48	0,39	BMC04147	Bm1_32220	Serine/threonine protein phosphatase PP1-alpha catalytic subunit, putative
BMX1673	1,52	0,44	13663.m00019	Bm1_11010	Serologically defined colon cancer antigen 1, putative
BMX7340	3,59	0,41	14980.m02677	Bm1_45785	SF2, putative, splicing factor
BMX7372	3,59	0,39	14980.m02713	Bm1_45965	Skb1 methyltransferase family protein
bm.02997	3,13	0,50	BMC02742	Bm1_12960	SMC family, C-terminal domain containing protein
BMX13360	3,13	0,40	TC3367	Bm1_47485	T-complex protein 1, epsilon subunit, putative
BMX6820	2,48	0,42	14975.m04505	Bm1_42820	TAR-binding protein, putative
BMX8733	2,79	0,49	15150.m00062	Bm1_54355	TPR Domain containing protein
bm.02843	3,59	0,49	BMC06557	Bm1_44395	translation elongation factor eEF-2 homolog eft-1, putative
BMX6995	3,59	0,48	14977.m05008	Bm1_43805	Trehalase family protein
BMX4707	1,84	0,24	14950.m01802	Bm1_29930	tRNA-specific adenosine deaminase 2, putative
BMX12651	3,13	0,38	WB-contig_445	Bm1_02060	Tropomyosin family protein (tmy-1)
BMX6907	2,48	0,34	14977.m04907	Bm1_43315	Troponin C, isoform 2, putative
BMX12520	2,48	0,47	WB-contig_255	Bm1_43315	Troponin C, isoform 2, putative
BMX9052	2,79	0,47	15378.m00019	Bm1_56355	Tubulin-tyrosine ligase family protein
BMX13242	2,79	0,42	TC3245	Bm1_15860	U2 small nuclear ribonucleoprotein A
BMX1337	1,52	0,43	13415.m00440	Bm1_08805	ubiquinone biosynthesis O-methyltransferase family protein
bm.02261	3,59	0,48	BMC09009	Bm1_56725	Ubiquitin carboxyl-terminal hydrolase family protein
BMX4535	3,13	0,49	14937.m00485	Bm1_28920	Ubqln2 (Ubiquilin-2) protein, putative
BMX5760	3,13	0,29	14972.m06992	Bm1_36515	UBX domain containing protein
BMX7735	2,79	0,44	14990.m07764	Bm1_48215	Vacuolar h atpase protein 16, putative
BMX12381	3,59	0,49	WB-contig_1591	Bm1_32805	Vacuolar protein sorting-associated protein 45, putative
bm.03336	1,52	0,43	BMC06819	Bm1_14040	venom allergen antigen-like protein 1, putative

bm.02180	2,79	0,44	BMC00560	Bm1_45520	Vps53-like, N-terminal family protein
BMX3281	4,28	0,49	14563.m00109	Bm1_21170	WD domain containing protein
BMX7654	2,79	0,49	14990.m07660	Bm1_47705	WD40 associated region in TFIID subunit family protein
bm.02264	2,48	0,42	BMC00091	Bm1_55855	Zinc finger, C2H2 type family protein
BMX6570	0,00	0,25	14973.m02657	Bm1_41325	Zinc finger, C2H2 type family protein
BMX6860	4,28	0,44	14975.m04552	Bm1_43055	Zinc finger, C2H2 type family protein
bm.02710	2,79	0,33	BMC02626	Bm1_55855	Zinc finger, C2H2 type family protein
BMX1113	1,84	0,49	13313.m00085	Bm1_07340	zinc metalloproteinase toh-2 precursor , putative
BMX4758	2,48	0,46	14950.m01863	Bm1_30230	Hypothetical 19.4 kDa protein ZC395.10 in chromosome III, putative
BMX1056	2,79	0,46	13281.m00013	Bm1_06970	Hypothetical 28.7 kDa protein in RNR3-ARC15 intergenic region, putative
bm.02648	3,59	0,38	BMC09182	Bm1_45770	Hypothetical 31.4 kDa protein T19C3.2 in chromosome III, putative
bm.00360	1,52	0,45	BMC01287	Bm1_13740	Hypothetical 37.7 kDa protein ZK686.3 in chromosome III, putative
BMX8602	3,59	0,41	15053.m00051	Bm1_53480	Hypothetical 45.1 kDa protein C16C10.6 in chromosome III, putative
BMX102	0,00	0,32	12485.m00052	Bm1_00740	hypothetical protein
BMX5927	0,00	0,31	14972.m07192	Bm1_37490	hypothetical protein
BMX8980	4,28	0,49	15315.m00009	Bm1_55900	hypothetical protein
BMX3235	0,52	0,29	14541.m00148	Bm1_20895	hypothetical protein
BMX1475	4,28	0,17	13499.m00138	Bm1_09715	hypothetical protein
BMX2912	3,59	0,25	14387.m00357	Bm1_18885	hypothetical protein
BMX6477	4,28	0,47	14972.m07865	Bm1_40740	hypothetical protein
BMX4150	1,52	0,25	14824.m00119	Bm1_26530	hypothetical protein
BMX2530	4,28	0,50	14245.m00086	Bm1_16475	hypothetical protein
BMX4294	2,48	0,23	14907.m00579	Bm1_27405	hypothetical protein
BMX6730	3,13	0,40	14975.m04393	Bm1_42280	hypothetical protein
BMX1421	1,84	0,42	13466.m00197	Bm1_09370	hypothetical protein
BMX8293	1,52	0,40	14992.m11105	Bm1_51615	hypothetical protein
BMX1985	2,48	0,46	13939.m00060	Bm1_13005	hypothetical protein
BMX12969	3,59	0,44	TC2966	Bm1_24320	hypothetical protein
bm.01122	3,59	0,41	BMC04958	Bm1_03285	hypothetical protein
BMX4396	4,28	0,41	14921.m00197	Bm1_28045	hypothetical protein
BMX2994	1,52	0,42	14419.m00094	Bm1_19415	hypothetical protein
BMX8270	3,13	0,40	14992.m11075	Bm1_51480	hypothetical protein
BMX3256	3,13	0,33	14553.m00038	Bm1_21020	hypothetical protein
BMX2312	2,79	0,34	14146.m00015	Bm1_15130	hypothetical protein
BMX766	1,84	0,49	13130.m00010	Bm1_05200	hypothetical protein
BMX7856	2,48	0,49	14990.m07928	Bm1_49020	hypothetical protein
BMX2479	1,52	0,48	14232.m00275	Bm1_16160	hypothetical protein
BMX3608	3,59	0,47	14658.m00022	Bm1_23225	hypothetical protein
BMX4004	2,48	0,34	14768.m00186	Bm1_25600	hypothetical protein
BMX12748	4,28	0,46	WB-contig_989	Bm1_55905	hypothetical protein
BMX8367	2,79	0,34	14992.m11195	Bm1_52065	hypothetical protein
BMX376	1,52	0,33	12698.m00332	Bm1_02525	hypothetical protein
BMX1990	4,28	0,49	13943.m00028	Bm1_13045	hypothetical protein
BMX5467	1,52	0,35	14963.m01802	Bm1_34660	Hypothetical UPF0054 protein TTE0972, putative
BMX9784	1,52	0,35	AA661405		no match
BMX12288	3,59	0,42	WB-contig_1482		no match
BMX12963	1,52	0,16	TC2959		no match
BMX12270	2,79	0,26	WB-contig_1461		no match
BMX12155	4,28	0,50	WB-contig_1325		no match
BMX11586	1,52	0,24	BMW00827.474		no match

Erklärung

Hiermit versichere ich, dass ich diese Arbeit selbständig und ohne jede unerlaubte Hilfe angefertigt habe und zur Anfertigung der Arbeit ausschliesslich die angegebenen Quellen und Hilfsmittel verwendet habe. Desweiteren versichere ich, dass ich diese oder eine ähnliche Arbeit noch keiner anderen Stelle als Dissertation vorgelegt habe, um ein Promotionsverfahren zu eröffnen.

Bonn, Februar 2012